APPLICATIONS OF MICROBIAL DESALINATION AND PHOTOCATALYTIC DISINFECTION FOR THE REMOVAL OF CONTAMINANTS IN DRINKING WATER

by

Kristen S. Brastad

A Dissertation Submitted in

Partial Fulfilment of the

Requirements for the Degree of

Doctor of Philosophy

in Engineering

at

The University of Wisconsin-Milwaukee

May 2015

ABSTRACT

APPLICATIONS OF MICROBIAL DESALINATION AND PHOTOCATALYTIC DISINFECTION FOR THE REMOVAL OF CONTAMINANTS IN DRINKING WATER

by

Kristen S. Brastad

The University of Wisconsin – Milwaukee, 2015
Under the Supervision of Professor Jason (Zhen) He and Professor Ying Li

Trends in drinking water treatment in recent years have been moving toward the use of membrane separation in order to reduce contaminants in water. There are many forms of membrane separation technology such as ultrafiltration, nanofiltration, microfiltration, reverse osmosis, and extruded ion exchange membranes. These membranes have many different applications and may be used to remove many materials from water such as salts, viruses and bacteria, selectively remove cations or anions, or remove organics.

Microbial desalination cells (MDCs) are an emerging concept which use bioelectric potential produced from organics via microbial metabolism to accomplish desalination. MDCs consist of three compartments, the anode, the cathode, and a salt compartment, which is between the anode membrane and the cathode membrane. This study reported a bench-scale laboratory experiment for evaluating the effectiveness of using MDC technology to remove hardness from several different hard water samples collected from across the United States, ranging in concentrations from 220 to 2080 mg/L as $CaCO_3$. It was found that the MDC generally removed more than 90% of the hardness

from the tested water samples driven by electron movement in batch operation. Electricity production was highly related to the conductivity of the hard water samples. It was also found that the MDC could remove 89% of arsenic, 97% of copper, 99% of mercury, and 95% of nickel at the testing concentration in a synthetic solution. These results provided a proof-of-concept that MDCs can be used to soften hard water that is driven by an electric current.

Photocatalysis is an attractive technology for the disinfection of microorganisms in drinking water. Titanium dioxide (TiO_2) is widely recognized for its disinfecting capabilities under the irradiation of ultraviolet (UV) light. Metal ions such as silver and copper serve as good dopants for TiO_2 in order to increase the photoactive yield and are also known for their bactericidal properties. This report details a method for the combination of silver and copper ions onto TiO_2 and the evaluation of its disinfection efficiency. TiO_2, Ag-TiO_2, Cu-TiO_2, and Ag-Cu-TiO_2 were applied onto a glass-fiber membrane substrate and irradiated with a UV light taken from an existing point-of-use UV disinfection filter. When activated with UV light, the Ag-Cu-TiO_2 membranes exhibited stronger bactericidal and virucidal activity than UV alone, TiO_2, Ag-TiO_2, or Cu-TiO_2. For experiments conducted in the dark, bactericidal activity of the Ag-Cu-TiO_2 membranes was greater than that of Ag-TiO_2 or Cu-TiO_2 suggesting that the silver and copper worked in a synergistic antibacterial effect unrelated to photoactivity. These results have shown that a silver-copper doped titanium dioxide membrane can be effective for removing bacteria and viruses from drinking water.

to
my parents, my cat
and coffee

TABLE OF CONTENTS

LIST OF FIGURES

LIST OF TABLES

LIST OF ABBREVIATIONS

AEM	Anion Exchange Membrane
Ag	Silver
ANSI	American National Standards Institute
AOP	Advanced Oxidation Process
CB	Conduction Band
CEM	Cation Exchange Membrane
CO_2	Carbon Dioxide
Cu	Copper
DBP	Disinfection by-Products
DOE	Design of Experiments
EDS	Energy Dispersive Spectroscopy
EPA	Environmental Protection Agency
FIC	Fractional Inhibitory Concentration
g	Gram
H_2O	Water
HO^-	Hydroxyl Radical
HRT	Hydraulic Retention Time
ICP-MS	Inductively Coupled Plasma-Mass Spectrometry
IX	Ion Exchange
L	Liter
mA	Milliamp
MCL	Maximum Contaminant Level
MDC	Microbial Desalination Cell
MFC	Microbial Fuel Cell

mg	Milligram
mL	Milliliter
MGD	Million-Gallons-per-Day
mm	Millimeter
mM	Millimolar
M	Molarity
NaCl	Sodium Chloride
NF	Nanofiltration
NSF	National Sanitation Foundation
PBS	Phosphate Buffer Saline
POE	Point-of-Entry
POU	Point-of-Use
PPCPs	Pharmaceuticals and Personal Care Products
ROS	Reactive Oxygen Species
RO	Reverse Osmosis
RPM	Revolutions per Minute
SEM	Scanning Electron Microscopy
TiO_2	Titanium Dioxide
TDS	Total Dissolved Solids
TOC	Total Organic Carbon
TSS	Total Suspended Solids
UV	Ultraviolet
VB	Valence Band
XRD	X-Ray Diffraction

LIST OF SYMBOLS

n = sample size

N_{in} = concentration of microbes in feed water

N_{out} = concentration of microbes in treated water

s = sample standard deviation

$\bar{X}$ = sample mean

μ = hypothesized population mean

Ω = ohms

ACKNOWLEDGMENTS

I would like to acknowledge and express my gratitude for the assistance and feedback given in completing this report to the following people:

- Dr. Zhen He, for assistance in all aspects of the project and dissertation.
- Dr. Ying Li, for assistance in all aspects of project considerations as well as dissertation draft feedback.
- Dr. Hector Bravo, for assistance with various project considerations as well as dissertation draft feedback.
- Dr. Jin Li, for assistance with various project considerations as well as dissertation draft feedback.
- Dr. Yin Wang, for assistance with various project considerations as well as dissertation draft feedback.
- Dr. Ernie (Eunkyu) Lee, Water Treatment Research Engineering of A.O. Smith Corporate Technology Center, for assistance with various project considerations as well as for providing dissertation draft feedback.
- George W. Kennedy III, for his support and encouragement throughout this dissertation.
- Rebecca Robinson, Jeff West, and Qianyi Zhang for their support and assistance throughout this dissertation.
- Frankie Caswell, Candice Buchanan, Jessica Beswick, Hailey McDowell, Nikki Voss, Liz Navarrete, Amanda Jessup, Amber Haire, Yvonne Vidaurre, Yezenia Hernandez, Lailaa Ragins, and Carrie Sasville for their support and encouragement throughout this dissertation.

These individuals all contributed in various ways to this dissertation and deserve recognition for their work.

CHAPTER 1: INTRODUCTION AND BACKGROUND

1.1 Introduction

Water is one of the most fundamental, essential components of life. When it is pure, it is very simple: H_2O. However, almost all of the available freshwater is no longer pure. It contains different physical, chemical, and microbiological contaminants which include bacteria, viruses, and toxic material such as heavy metals. This makes good water difficult to categorize and describe. In order to define the quality of water, especially drinking water, researchers or experts have developed many parameters to categorize the water and the various contamination levels within. By doing so, people can now determine what water is clean and safe for drinking. There are some general parameters such as temperature, color, total suspended solids (TSS), and turbidity to describe the physical appearance of water but this does not tell the whole story. There are many biological characteristics and chemical characteristics, such as hardness, total dissolved solids (TDS), and pH that help to complete the picture. Once these characteristics are known, it is possible to determine what water treatment options can be employed to make the water more drinkable.

Trends in drinking water treatment in recent years have been moving toward the use of membrane separation in order to reduce contaminants in water. Membranes have the advantage of being able to produce water with a constant and well-adjusted quality [1]. Since the development of synthetic asymmetric membranes in 1960, interest in membrane processes for water and wastewater treatment has grown steadily and these technologies are now the subject of substantial international research, development,

commercial activity, and full-scale application [2]. The growth in the use of membrane technology is experiencing an exponential increase as many municipal facilities ranging in capacity from 25 to 100 million-gallons-per-day (mgd) are either planned, in design, or in operation. The desirability of membrane separation technology can be linked to regulatory mandates, their broad applicability, cost, and operational flexibility [3].

There are many forms of membrane separation technology such as ultrafiltration, nanofiltration, microfiltration, reverse osmosis, osmosis (also termed forward osmosis to more clearly distinguish it from reverse osmosis), and extruded ion exchange membranes. The water filtration spectrum shown in Figure 1 illustrates the relationship between contaminants and the different technologies for removing them.

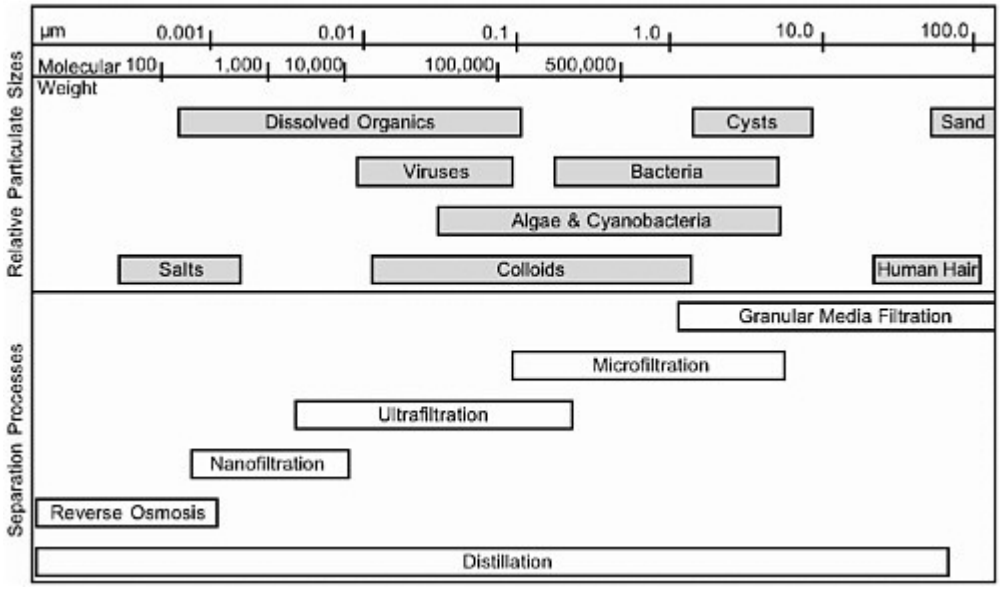

Figure 1: Water filtration spectrum.

From the water filtration spectrum, it is not difficult to determine that different technologies could be better applied to remove different contaminants so that the most optimal performance can be achieved economically. These membranes have many different applications and may be used to remove many materials from water such as salts, viruses and bacteria, selectively remove cations or anions, or remove organics.

1.1.1 Hardness and Heavy Metal Removal

One application for membranes is the removal of minerals such as calcium and magnesium from drinking water. The removal of these ions is done primarily from an aesthetic standpoint as they do not pose a significant health risk.

Ion exchange (IX) is the traditional process used to soften water. In this process, charged polymer resin beads act as the structure on which ion exchange can happen. Resins are made from different plastics and can have a variety of functions. Resin designed to remove cations from water, such as in water softening, would have opposing (negative) exchange sites introduced into the matrix of the resin bead. Once the exchange sites exist on the polymer beads, they can be loaded with positive ions, such as potassium or sodium. Those ions are exchanged into the water while stronger, positively charged ions such as calcium or magnesium are retained at the exchange sites [4].

After the resin exchange sites have become saturated with calcium and magnesium cations, the resin bed must be regenerated. The regeneration process is simply a recharge of the exchange ions. In the case of weak acid resins used in residential water softeners, concentrated brine is drawn slowly into the resin bed where it displaces the hardness ions from the exchange sites [4]. This regeneration process

introduces high concentrations of salt into the sewer system where it travels into the environment.

Ion exchange is the most popular form of water softening because of its high performing resin. Typical ion exchange resin can reject up to 99% of hardness ions in exchange for some salt and energy. Softeners are becoming increasingly energy efficient as rejection capacity increases and electrical consumption decreases, but the problem of adding salt into the environment remains.

In addition to ion exchange, chemical precipitation has been frequently used to soften water on a municipal level. This type of softening, usually known as lime softening, adds lime to hard water to precipitate calcium ions as calcium carbonate and magnesium ions as magnesium hydroxide [5]. Lime softening is also recognized by the U.S. Environmental Protection Agency (EPA) as the best applied technique for arsenic, barium, beryllium, chromium, copper, fluoride, lead, mercury, cadmium, nickel, and radionuclides [6]. However, the drawbacks to lime softening include the production of a high-volume lime sludge stream and the required use of chemicals such as quick lime, coagulants (iron or aluminum based), soda ash, and acids for adjusting the pH [6]. Other methods of water softening include nanofiltration, electrodialysis, carbon nanotubes, capacitive deionization, and reverse osmosis; though these processes consume high amounts of energy, and operation and maintenance of the equipment can be costly, primarily due to fouling [7–12]. Therefore, there is a significant need to develop an environmentally friendly, cost-effective, and low energy consuming process, which would be an ideal addition to the water softening market.

Microbial desalination cells (MDCs) are an attractive and environmentally friendly technology for removing ions from water with relatively little energy consumption (by pumping the system at normal pressures). MDCs are derived from microbial fuel cells (MFCs), which are bioelectrochemical devices that use microorganisms as biocatalysts to convert chemical energy into electrical energy [13]. The main principle behind the operation of an MFC is the generation of electrons from the catabolic action of microorganisms, which can be transferred through the cell membrane to the anode electrode [13,14]. The anode is connected to the cathode via an external circuit through which electrons flow based upon the difference in redox potential that exists between their dissimilar liquid solutions [15]. By installing an additional chamber between the anode and the cathode, an MFC is converted to an MDC with a function of desalination (Figure 2).

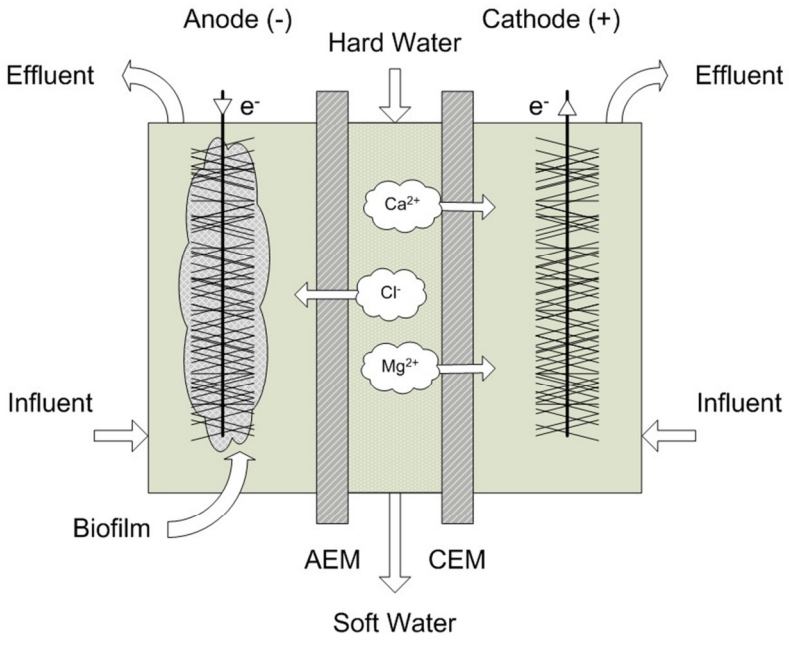

Figure 2: Schematic of a microbial desalination cell modified for hardness removal.

The concept of the MDC was first introduced in 2009 by Cao *et al.* in a small-scale (3 mL salt water capacity) and later scaled up by Zhang *et al.* to create a large-scale MDC (105 L salt water capacity) [16–19]. Bacteria growing on an electrode in the anode chamber will oxidize organic substrates and result in the transfer of electrons, which intrigues the movement of cations from the middle chamber to the cathode chamber, and the migration of anions from the middle chamber to the anode chamber, while at the same time generating electric current [16,17,20–22]. Researchers have found that the removal rate for salts in MDCs varies between 90% and 99% [16,17]. MDC development has focused on the desalination of saline water or seawater with the removal of sodium chloride; however, no studies had investigated this technology for water softening.

1.1.2 Disinfection of Drinking Water

While different membranes (such as ultrafiltration and reverse osmosis) can achieve removal of viruses and bacteria from drinking water, it is not their primary goal. The occurrence of microbial contaminants in drinking water is frequently due to fecal matter from sewage discharges, leaking septic tanks, and runoff from animal feedlots into bodies of water. In order to protect drinking water from these microorganisms, suppliers of water often add a disinfectant to the drinking water such as chlorine or ozone. However, depending on the water chemistry and the types of microorganisms present, traditional disinfectants have some limitation. For example, the microorganism *Cryptosporidium* is highly resistant to traditional disinfection practices [23]. When water has high concentrations of total organic compounds (TOC) or other naturally-occurring matter in the water, the disinfectants themselves can react to form by-products which may pose health risks [24]. It is widely understood that chlorination and ozonation especially

will produce chlorinated and brominated disinfection by-products (DBPs) with potential carcinogenic effects on humans [25]. Therefore, the use of alternate disinfection technologies for the removal and inactivation of microorganisms is of considerable interest.

In order for a system to be considered a microbiological water purifier, it must meet specific performance requirements which are set by the U.S. EPA. A microbiological water purifier is one which removes, kills, or inactivates all types of disease-causing microorganisms from the water, including bacteria, viruses, and protozoan cysts so as to make the processed water safe for drinking. Purifiers which meet this standard are certified under National Sanitation Foundation (NSF)/American National Standards Institute (ANSI) standard P231 and are able to remove 6 logs of bacteria, 4 logs of viruses, and 3 logs of protozoan cysts.

Alternate technologies, such as advanced oxidation processes (AOPs), offer chemical treatment methods that have the potential to surpass conventional treatment processes due to their generation of highly reactive hydroxyl radicals ($HO^{\cdot}$), or reactive oxygen species (ROS). Oxidation itself is defined as the transfer of one or more electrons from an electron donor (reductant) to an electron acceptor (oxidant). The electron transfer results in the chemical transformation of both the oxidant and the reductant, creating species known as radicals, which tend to be highly unstable and therefore highly reactive. The most powerful oxidants are fluorine, hydroxyl radicals, ozone, and chlorine. These oxidants are all capable of disinfection but possess limitations. Ozonation, for example, can also cause DBPs such as bromate to form and has a short residence time [26–28]. Another oxidant, hydrogen peroxide, is a much weaker

disinfectant than chlorine or ozone and is subsequently a less favorable option [28]. One category of AOPs consist of photoactivated processes which have been shown to have enhanced disinfection capabilities. In photoactivated processes the free radicals are initiated by the interaction of photons with a catalyst. A popular photocatalyst for this process is titanium dioxide (TiO_2) and its disinfection prowess has been noted since 1988 [29].

After the discovery of photocatalytic splitting of water in 1972 by Fujishima and Honda, enormous efforts have been devoted towards the research of TiO_2 materials [30]. TiO_2 has the benefit of being inexpensive, abundant, and corrosion-resistant. When activated using a UV light, TiO_2 is widely recognized to provide disinfecting capabilities on a diverse range of microorganisms [31–34]. This is due to the movement of electrons across the band gap from the valence band to the conductance band. As a result of this motion, energy-rich electron hole pairs are formed, which can react with water molecules to form the strong oxidant ROS. The ROS generation can cause oxidative stress damage to cell membranes, effectively inactivating microorganisms. TiO_2 photocatalysts have been proposed to be one of the best disinfection technologies as it produces no dangerous DBPs. Traditional methods of using particulate and colloidal TiO_2 catalyst suspensions are not suitable for drinking water treatment due to their separation and reuse difficulties. Thin films of TiO_2, a relatively new form of the catalyst, have gained much attention due to their ability to attach to substrates which allows reuse of the material [31,35].

Despite the numerous advantages, several limitations of TiO_2 exist, mostly in the relatively large band gap and the low mobility of charge carriers, which can result in the recombination of electron-hole pairs before the ROS can form [36]. A commonly used

strategy for increasing the amount of electron-hole pairs generated is to modify the TiO_2 matrix through selective metal-ion loading or doping. Metal ions such as silver and copper serve as good dopants for TiO_2 as they will increase the yield of the photocatalyst and are also recognized for their antimicrobial effects [37]. Previous research regarding copper and silver ions found that the use of these metals in combination could result in an increased synergistic effect against bacteria [38]. Experiments with silver and copper co-impregnated onto TiO_2-P25 nanoparticles showed an increase in photocatalytic activity, though their effects on disinfection have yet to be studied [39].

The development of new, improved methods of disinfection is the best method to ensure that no hazardous by-products are allowed into water sources. Silver and copper modified titanium dioxide membranes show promising results indicating that adequate disinfection is possible, without the potential for hazardous side effects from disinfection by-products. Titanium dioxide, when activated by UV light, will release hydroxyl radicals which will destroy harmful microorganisms and pollutants. The resulting products of this reaction are carbon dioxide (CO_2) gas and water. Any silver or copper ions that leach into the water from the membranes also have antimicrobial properties and will provide disinfection separate from the photocatalytic process. Although it is necessary to monitor the concentration of the silver and copper ions that leach off of the membranes into the product water to ensure they stay below the EPA maximum contaminant levels, there are no inherent hazardous by-products forming after the disinfection process.

1.2 Dissertation Overview

This dissertation includes discussion on the applications of microbial desalination and photocatalytic disinfection for the removal of contaminants from drinking water. One major finding from this work is the discovery of a new method for achieving residential point of use (POU) purification through the immobilization of silver and copper doped titanium dioxide (Ag-Cu-TiO_2) onto a fiberglass membrane. These Ag-Cu-TiO_2 membranes have the potential to be used as a means to increase water security against contamination of water distribution systems. A characterization of the mechanism behind Ag-Cu-TiO_2 membranes is summarized in Chapter 2. An application of Ag-Cu-TiO_2 membranes is described in Chapter 4.

In Chapter 2, a brief introduction on titanium dioxide and metal-ion doping is discussed. A review of the current literature was conducted in order to determine the role that silver and copper can play in terms of reducing the band-gap of titanium dioxide and disinfecting microorganisms. Reviews of the current literature for free heavy metal ion disinfection and technologies for TiO_2 immobilization were also conducted.

In Chapter 3, a method of removing aesthetic contaminates from drinking water, calcium and magnesium, as well as heavy metals such as arsenic, copper, and nickel, was demonstrated using a microbial desalination cell (MDC). It was discovered that the MDC was able to remove more than 90% of the hardness naturally found in several locations across the United States. It was also found that MDCs were able to achieve a high rate of heavy metal removal: 89% reduction in arsenic, 97% reduction in copper, 99% reduction in mercury, and 95% reduction in nickel.

In Chapter 4, a method for combining a microbial desalination cell with photocatalytic disinfection was explored for water softening and microbial disinfection. The conjoined system was able to remove 60% of hardness ion and remove 3.9 logs of *E. coli*.

In Chapter 5, the use of individual and combined applications of silver and copper doped titanium dioxide immobilized on a fiberglass membrane substrate was investigated for its ability to inactivate microorganisms in water. The membrane which used a combined doping effect for silver and copper with titanium dioxide yielded a 7.6-log reduction of bacteria and a 3.5-log reduction in viruses. These results demonstrate the first combined application of Ag-Cu-TiO_2 membranes in bacteria and virus reduction, and confirm the viability of this approach for moving to scale up the technology.

In Chapter 6, the future challenges to be addressed for creating safe drinking water are examined. Specific research problems that seek to address emerging contaminates along with their potential solutions are outlined.

CHAPTER 2: LITERATURE REVIEW

2.1 Metal-ion Doping on TiO_2

In order to address one of the main drawbacks of TiO_2, electron-hole pair recombination time, modification of the TiO_2 matrix with metal-ions is of considerable interest. The act of doping metal ions into the TiO_2 matrix introduces new energy levels into the band gap. Depending on what metal ion is being used and its concentration, the band gap of TiO_2 can be designed to extend the photoresponsiveness into the visible light region [40,41]. Additionally, the introduction of metal ions to TiO_2 can change the photocatalytic properties by changing the distribution of electrons on the TiO_2 surface. This in turn causes the metal ions to work as charge carrier traps, essentially enhancing charge separation of the electrons and holes. With the enhanced charge separation, an increase in the quantum yield of surface photoreactions is possible [40–43].

In order to understand the benefits of metal doping, it necessary to first understand the mechanism of the TiO_2 photocatalysis. When a particle of light such as photon hv_1 with energy equal to or greater than the band gap energy is absorbed by the TiO_2, electron-hole pairs are generated (Figure 3) [41,44]. These pairs are formed in the space charge region and are separated by the electric field. The holes which are in the valence band (VB) move to the surface and the electrons in the conduction band (CB) move into the bulk TiO_2 [44]. Excited-state electrons and holes can recombine and dissipate the input energy as heat, get trapped in metastable surface states, or react with electron donors and electron acceptors adsorbed on the semiconductor surface or within the surrounding electrical double layer of the charged particles [41]. When water is

introduced, the electron-hole pairs react to form hydroxyl radicals with high redox oxidizing potential by the following reactions [39,45,46].

$$TiO_2 + hv \rightarrow e^- + h^+$$

At the reduction site:

$$O_2 + e^- \rightarrow {O_2}^-$$

$${O_2}^- + H^+ \rightarrow {HO_2}^\bullet$$

$${HO_2}^\bullet + {HO_2}^\bullet \rightarrow H_2O_2 + O_2$$

$$H_2O_2 + e^- \rightarrow OH^- + {}^\bullet OH$$

At the oxidation site:

$$H_2O + h^+ \rightarrow {}^\bullet OH$$

$${}^\bullet OH + {}^\bullet OH \rightarrow H_2O_2$$

$$H_2O_2 + 2h^+ \rightarrow 2H^+ + O_2$$

The reactive oxygen species generated by UV illumination of TiO2 can decompose organic compounds and inactivate cellular activity [39,47].

When metals are added onto the TiO_2 matrix, a new energy level is produced in the band gap of TiO_2. Electrons are excited from the defect state to the TiO_2 conduction band though a new energy level: hv_2 (Figure 3) [41]. The added metals also improve the trapping of electrons, which in turn inhibits the electron-hole recombination during irradiation.

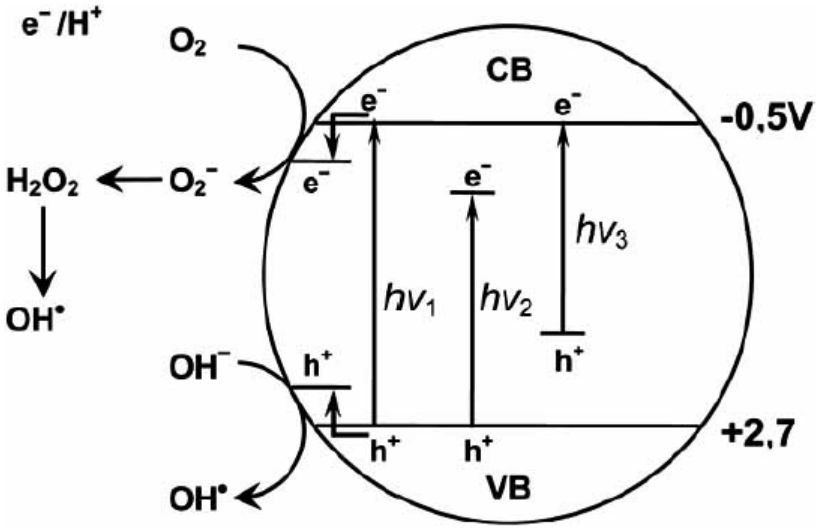

Figure 3: Mechanism of TiO_2 photocatalysis: hv_1: pure TiO_2; hv_2: metal doped TiO_2; and hv_3: non-metal doped TiO_2 [41]**.**

Many methods can be used to introduce metal ions onto TiO_2 such as wet-impregnation, UV photodeposition, sol-gel, template free synthesis, and plasma immersion ion implantation [47–52]. However, TiO_2 doped by a single element may not be as practical for meeting various applications as co-doping with different elements has shown to lead to higher photoactivity [39]. The catalyst may possess better photocatalytic activity if two different transition metals are co-impregnated into the TiO_2. For example, Behnajady *et. al.* found that co-impregnating silver and copper onto TiO_2-P25 nanoparticles yielded a higher photocatalytic activity for the removal of C.I. Acid Orange 7 as compared to Ag-TiO_2-P25 or Cu-TiO_2-P25 [39].

2.2 Disinfection of Metal-ion Doped TiO_2

While many have researched the various activity levels of metal-ion doped TiO_2, researchers are still in the early stages of exploring the best doping arrangement for

disinfection and not as much research has been done to explore and quantify the antimicrobial properties. Two different mechanisms have been theorized to be responsible for the increased antimicrobial properties of metal ion-doped TiO_2: (1) enhanced photoactivity of TiO_2 by removing electrons from TiO_2 particles and (2) blocking electron-hole recombination time [47,51,52].

Li *et. al.* found that Ag-TiO_2 nanoparticles prepared with wet-impregnation the percentage of viable cells decreased to 1% after 180 minutes compared to a reduction of viable cells down to 12% with commercially available DuPont R902 TiO_2 nanoparticles [47]. Li *et. al.* also looked at UV photoreduction, though the results were not as promising: both Ag-TiO_2 and commercially available DuPont R902 TiO_2 nanoparticles achieved a 12% reduction in viable cells [47]. When Li *et. al.* repeated the experiments using UV photoreduction and Degussa P25 TiO_2 nanoparticles, the Ag-TiO_2 nanoparticles preformed much better and the percentage of viable cells decreased to 1% after 180 minutes [47].

Cao *et. al.* used a silver plasma immersion ion implantation process to attach silver onto the surface of plasma-sprayed titanium oxide coatings. Instead of finding that more silver was better, Cao *et. al.* discovered that the further spaced apart the silver ions were, the better the microbial reduction [51]. Ag-TiO_2 samples sprayed with silver for 60 minutes achieved a 70% reduction in microorganisms, while Ag-TiO_2 samples sprayed with silver for 30 minutes achieved a 90% reduction in microorganisms [51].

Tobaldi *et. al.* synthesized Ag-TiO_2 using sol-gel and found that it was possible to achieve a 4-log reduction in *E. coli* under light conditions and a 2-log reduction of *E. coli*

under dark conditions, indicating that the silver ion concentration plays a significant role in the disinfection capability [52]. When the silver concentration was increased to 1 mg/mL a 5-log reduction of *E. coli* in both light and dark conditions was achieved [52].

The bactericidal activity of copper deposited onto a thin film of TiO_2 was explored by Sunada *et. al.* under very weak UV (350 nm and 1 $\mu W/cm^2$) illumination. Sunada proposed that the addition of copper into the TiO_2 caused a two-step inactivation process: TiO_2 would partially decompose the outer membrane in the cell envelope, then the Cu ions would permeate into the cytoplasmic membrane causing a loss of the cell's integrity [46]. The addition of copper onto TiO_2 was achieved via a hydrophilic treatment in order to attain a uniform coating of copper photodeposited onto TiO_2 thin films [46]. Through the use of weak UV illumination, a 0.8 log removal of *E. coli* was observed [46].

A novel Cu_2O/TiO_2 composite photocatalyst was created by Liu *et. al.* using a facile hydrolyzation reaction followed by a solvent-thermal process. Under illumination with visible light, a 3-log reduction was achieved in 80 minutes and under dark conditions a 64% reduction in *E. coli* was achieved in 80 minutes [53].

A water-dispersible Cu-TiO_2 colloidal dispersion was proposed by Chen *et. al.* and created through a photocatalytic reduction process from cupric chloride and TiO_2 [54]. The Cu-TiO_2 colloidal dispersion was investigated in the absence of light for its antimicrobial properties by measuring the optical density at 600 nm using an ultra-violet-visible spectrophotometer [54]. Through this, Chen *et. al.* found that a 99.96% (or about a 3.5 log) inactivation of *E. coli* was possible [54].

Pham *et. al.* investigated the bactericidal properties of several different weight fractions of copper (0, 1, 2.5, 5, 7.5, and 10%) to Cu-TiO_2 coated on glassfibers [45]. Through this, Pham discovered that copper dopants increased the electron-hole pair separation efficiency, inhibited their recombination, and improved the photocatalytic activity. The optimal copper content for disinfection of *E. coli* was found to be 5% copper [45].

The antibacterial capabilities of Ag-TiO_2 and Cu-TiO_2 due to destructive reactive oxygen species under UV illumination have been studied previously. However, based on the primary knowledge and research done for this dissertation, the combination of silver and copper together with titanium dioxide remains largely unexplored for its bacterial properties. In addition, the virucidal properties of metal-ion doped TiO_2 have not been examined, hampering the development of commercializable applications of photocatalysts, such as for drinking water treatment.

2.3 Disinfection with Free Metal Ions

Transition metals such as silver, copper, and zinc have well-documented antimicrobial properties, yet the complete bactericidal mode of action has remained unclear. There are currently three theories which seek to explain the toxicity of metals towards microorganisms. The first is that microorganisms, when overloaded with metals, fall prey to oxidative stress. However, most of the metals on their own are not redox active [55]. The second theory is that divalent metals may compete for the metal binding sites of proteins that normally contain divalent cations [56,57]. Finally, the third theory is that transition metals are potential inhibitors of enzymes that require active-site thiols for activity [58].

Recent research has suggested that the second theory is the most likely; transition metals are inhibiting enzyme clusters of dehydratase-family enzymes [59,60]. Specifically silver, copper, and zinc will interfere with intracellular iron-sulfur (Fe-S) protein clusters by attaching to the sulfur. This prevents the protein from folding correctly and leaves the iron as unattached within the cell, thereby weakening the bacteria [60]. The excess iron inside the bacteria begin to produce more ROS, inadvertently further damaging the cell wall of the bacteria until it dies [60].

With the antimicrobial benefit of heavy metals clear, research has shown that together silver and copper have a combined synergistic effect for inactivating microorganisms [38]. Lin *et. al.* explored the use of copper and silver ions together for their ability to inactivate *Legionella pneumophila*. By calculating the Fractional Inhibitory Concentration Index (FIC Index), which is a quantitative measure of the efficiency of the combination of two antimicrobial agents, Lin was able to determine that copper and silver had a synergistic effect on each other. The primary idea behind synergy is that the combined effect of two antimicrobial agents is significantly greater than the sum of the effects of two agents independently. Batch disinfection studies were used to verify that the effects of copper and silver ions together were indeed greater than that of either ion operating by itself [38].

2.4 Immobilization of Photocatalysts onto Membranes

Titanium dioxide has a large surface area-to-volume ratio which makes fine particles of TiO_2 in a slurry form the preferred application of photocatalysis. It follows that the main technical barrier for the commercialization of photocatalysts hinges on the development of recovery techniques for the catalyst particles after water treatment.

Photocatalyst reactors which use a slurry of catalyst particles require time consuming and expensive post-treatment processes in order to separate and recycle the colloidal catalyst particles from the reactor effluent due to the nano-size of the TiO_2 [61]. A slurry of catalysts can also inhibit UV light penetration due to the absorption by both catalytic particles and dissolved organics present in the slurry [62]. Recovery of TiO_2 can be achieved through membrane filtration, but immobilization of the photocatalyst onto various substrates is also a technique which can be employed.

A number of studies have utilized micron-size immobilizer substrates for catalyst fixation which enhance surface contact with contaminants. Substrates such as mesoporous clays, fiberglass membranes, nanofibers, and membranes have been explored for their ability to immobilize titanium dioxide [35,61]. Fiberglass membranes as a substrate are of particular interest due to their low cost and large pore size. The large pore size of glass fibers is beneficial as it is able to achieve a high pollutant removal rate at low transmembrane pressure (<300 kPa) when coated with a photocatalyst [63,64].

Photocatalytic membrane reactors, or the combination of photocatalytic oxidation with membrane filtration, are in the early stages of development. Currently, four different configurations are under study as shown in Figure 4. The different configurations are: (a) a slurry photocatalytic reactor paired with a membrane filtration unit, (b) an inorganic or polymeric membrane submerged in a slurry photocatalytic reactor, (c) a membrane integrated inside of a photoreactor whose internal walls are coated by a photocatalyst, and (d) a photocatalytic membrane such as a pure TiO_2 membrane or a TiO_2 composite membrane [61].

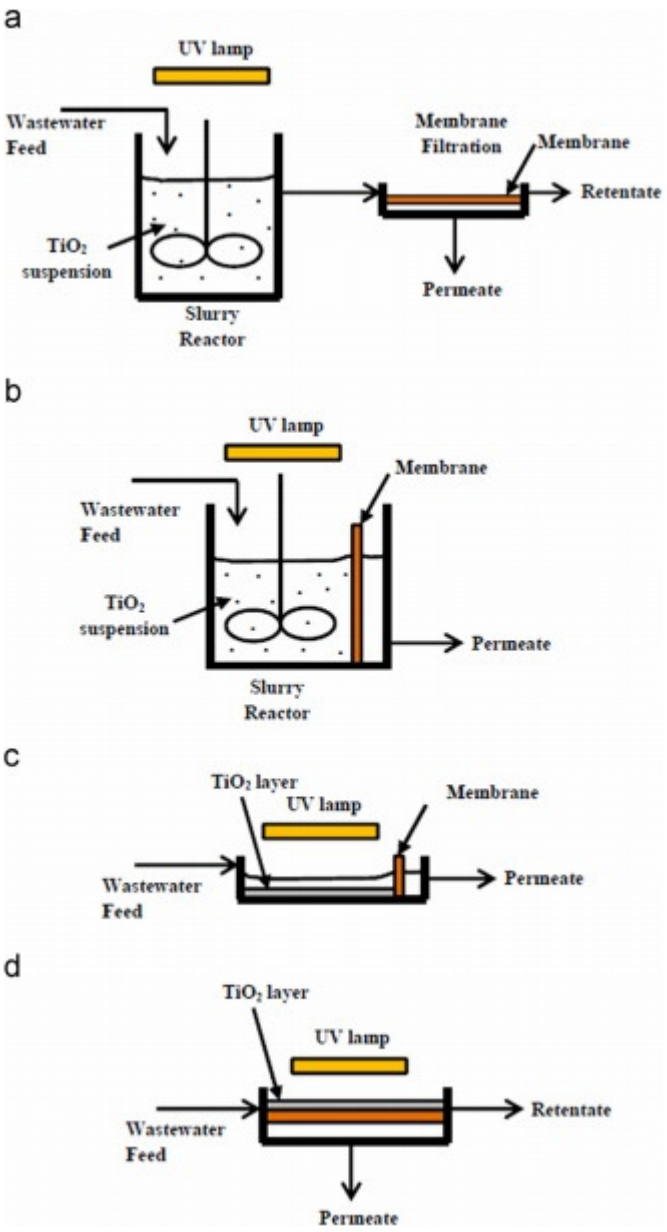

Figure 4: Different configurations of photocatalytic membrane reactors. (a) slurry reactor paired with a membrane filtration unit; (b) submerged membrane in a slurry reactor; (c) submerged membrane in a TiO2 coated reactor; and (d) a photocatalytic membrane [61]**.**

Of these four different configurations, the photocatalytic membrane has an advantage over the other three configurations as it combines the photocatalysis

mechanism for organic degradation and microbial inactivation with the physical separation of membrane filtration into a single reactor.

CHAPTER 3: MICROBIAL DESALINATION CELLS FOR SALTLESS WATER SOFTENING AND HEAVY METAL REMOVAL[1]

This study experimentally demonstrated an MDC for water softening. During batch operation, actual hard water samples collected from seven locations across the U.S. were examined for hardness removal and electricity production in the MDC. The current generation at different concentrations of hardness was investigated and the perspective of MDC technology for water softening is discussed. The results of removing heavy metals in the MDC were also reported.

3.1 Materials and Methods

3.1.1 MDC Setup

The MDC used in this study was a three-chamber bioelectrochemical reactor (Fig. 2). The three chambers were separated with heterogeneous ion-exchange membranes: an anion-exchange membrane (AMI-7001, Membrane International, Inc., Glen Rock, NJ, USA) between the anode chamber and the middle chamber, and a cation-exchange membrane (CMI-7000, Membrane International, Inc.) between the cathode chamber and the middle chamber. A carbon fiber brush with a titanium core (Gordon Brush, Commerce, CA, USA) was inserted into the anode chamber as the anode electrode; a second, identical carbon brush was inserted into the cathode chamber as the cathode

---

[1] This chapter has been published as: Brastad, K.S. and He, Z. (2013) Water softening using microbial desalination cell technology. *Desalination*. Vol 309, pp 32-77.

electrode. Prior to use for water softening, the MDC was pre-operated using NaCl solution (in the middle chamber) to establish a well-functioning biofilm in the anode. Both the anode and cathode chamber held a liquid volume of approximately 60 mL each and the middle chamber contained a volume of approximately 9 mL. The external resistance was set at 1 Ω to achieve a high current generation. During water softening, the calcium and magnesium ions moved into the cathode chamber through the cation-exchange membrane, and the chloride ions plus other anions moved into the anode chamber through the anion-exchange membrane.

3.1.2 Operating Conditions

A synthetic anode solution using acetate as a carbon source was fed into the anode chamber at a rate of 0.042 mL/min (hydraulic retention time, HRT, of one day) with a syringe pump (KD Scientific, Inc., Holliston, MA, USA). The anode solution was prepared using (per L of nanopure water): sodium acetate, 3 g; yeast extract, 0.1 g; NaCl, 0.5 g; $MgSO_4$, 0.015 g; $NaHCO_3$, 0.1 g; $CaCl_2$, 0.02 g; NH_4Cl, 0.15 g; K_2HPO_4, 1.07 g; KH_2PO_4, 0.53 g; and trace elements, 1 mL [65]. In this study, organics were oversupplied to ensure the anode reaction was not a limiting factor in the softening process. The anode was inoculated with a mixture of aerobic and anaerobic sludge from South Shore Wastewater Treatment Plant (Milwaukee, WI, USA). Potassium ferricyanide was used as a terminal electron acceptor in the catholyte and was prepared using (per L of nanopure water): $K_3[Fe(CN)_6]$, 3 g. The catholyte also contained 10 mM phosphate buffer (K_2HPO_4, 1.07 g/L; and KH_2PO_4, 0.53 g/L). The hard waters were collected from seven locations across the U.S. (tested individually) and fed into the middle chamber in batch mode operation (Table 1). The hard water was replaced

completely once the current generation was below 0.2 mA. The heavy metal water was prepared as (per L of nanopure water): $HAsNa_2O_4$, 0.017 g; $CuCl_2$, 0.847 g; $HgSO_4$, 0.029 g; and $NiCl_2$, 0.773 g. The heavy-metal water was replaced once the current generation was below 0.2 mA.

Table 1: Characteristics of the hard water samples from different locations in the United States, and the removal efficiency and electricity generation in the MDC.

Location	pH	Conductivity [µS/cm]	Hardness [mg/L as $CaCO_3$]	% Hardness Removal	Peak Current [mA]	Total Charge [C]
Burnsville, MN	8.06	759	350	84% ± 6%	1.77 ± 0.00	0.32 ± 0.03
Lincoln, NE	8.65	501	300	91% ± 4%	1.52 ± 0.25	0.27 ± 0.07
Roswell, NM	7.48	1902	625	97% ± 0%	5.30 ± 0.43	0.95 ± 0.10
Tipp City, OH	7.32	537	220	94% ± 3%	1.20 ± 0.01	0.22 ± 0.01
Mt. Joy, PA	7.83	586	450	96% ± 2%	2.20 ± 0.33	0.35 ± 0.03
El Paso, TX	7.59	863	475	94% ± 1%	2.15 ± 0.10	0.38 ± 0.05
Chilton, WI	7.68	9310	2080	95% ± 1%	13.16 ± 2.01	2.36 ± 0.36

3.1.3 Measurements and Analyses

The cell voltage was recorded every three minutes by a digital multimeter (2700, Keithley Instruments, Inc., Cleveland, OH, USA). The conductivity of the solutions was measured with a benchtop conductivity meter (Mettler-Toledo, Columbus, OH, USA). The pH was measured with a benchtop pH meter (Oakton Instruments, Vernon Hills, IL, USA). The total hardness was measured with a digital titrator (Hach Company, Loveland, OH, USA). Heavy metal ion concentration was measured using Inductively Coupled Plasma Spectroscopy (ICP; Profile Plus, Teledyne Leeman Labs, NH, USA). The total electric charge produced in one feeding cycle was calculated as an integration of electric current over time. Surface imagery of the scale buildup on the cation exchange membrane was captured using a Topcon ABT Scanning Electron Microscope

(SEM; Paramus, NJ, USA), and its crystal structure was characterized by X-ray diffraction (XRD; Scintag, Inc, CA, USA).

3.2 Results and Discussion

3.2.1 Removal of Total Hardness

The proof-of-concept of the MDC for water softening was demonstrated initially by comparing the open- and the closed-circuit operation to determine if the electricity generation resulted in water softening and to understand the effect of diffusion (Figure 5). The water sample from Chilton, WI (Table 1), was used for both open- and closed-circuit operations, and completely replaced every twenty-four hours. During the closed-circuit operation, the electric current spiked when the water was replaced, and then gradually decreased over a period of ten hours.

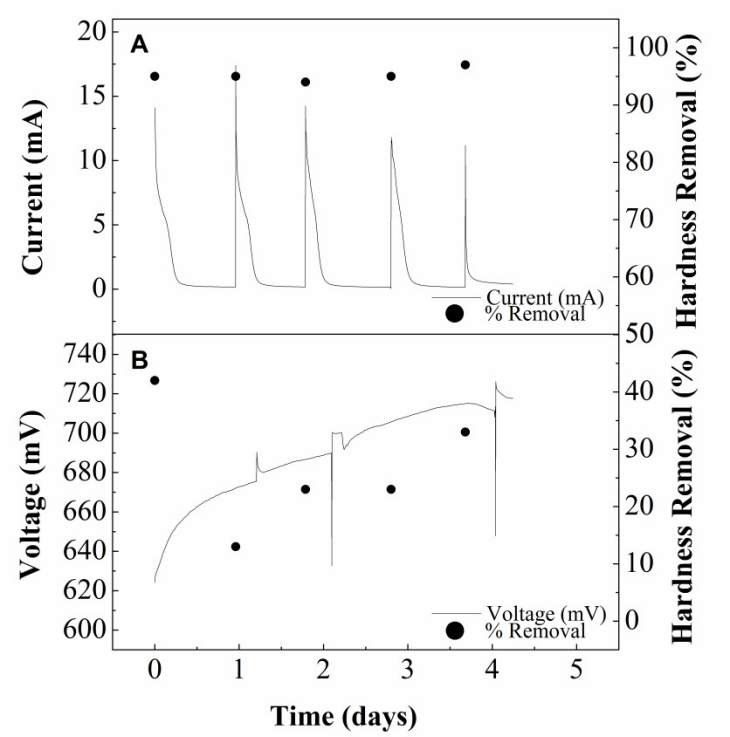

Figure 5: Current (or voltage) variation and hardness removal efficiency under (A) closed circuit and (B) open-circuit operation.

An average peak current of 13.16 mA and an average hardness removal of 95% were obtained under the closed circuit condition (Fig. 5A). On the other hand, the open-circuit condition, under which no current was generated, produced a voltage greater than 700 mV and removed only 27% of hardness (Fig. 5B), which was likely due to diffusion or ion exchange. Previous studies of using MDCs to treat saline water also found salt loss under the open-circuit potential [22]. By comparing both electricity generation and hardness removal between the open-and closed-circuit operations, we can conclude hardness removal was primarily due to current generation, and that natural diffusion/ion exchange made a minor contribution.

To further establish the relationship between current generation and hardness removal, the water sample from Chilton, WI, with an average hardness of 2,080 mg/L as $CaCO_3$ (Table 1) was prepared with dilution to 10% (0.1X), 25% (0.25X), 50% (0.5X) of its original concentration, and no dilution (1X). At the lowest concentration of hard water, approximately 200 mg/L as $CaCO_3$, the peak current was 0.87 mA; increasing the concentration to 520 mg/L as $CaCO_3$ yielded a peak of 3.70 mA; at a dilution of 0.5X, the concentration of 1,050 mg/L as $CaCO_3$ produced a peak current of 7.30 mA; and at full-strength the peak current was 14.11 mA (Fig. 6A). This suggests an almost-linear relationship between the hard water concentration and the peak current (Fig. 6B). To demonstrate an overall production of electrons at a hardness concentration, the total charge was calculated and a similar linear relationship between the hard water concentration and the total charge was identified (Fig. 6B), and the results confirmed that electricity generation led to hardness removal in the MDC.

The MDC performance significantly decreased after 17 months in operation to the point where the peak current for a sample of water (at 1X concentration) was 2 mA. After the MDC was dissembled, it was observed that the CEM had a significant amount of scale build-up on the surface of the membrane facing the cathode chamber.

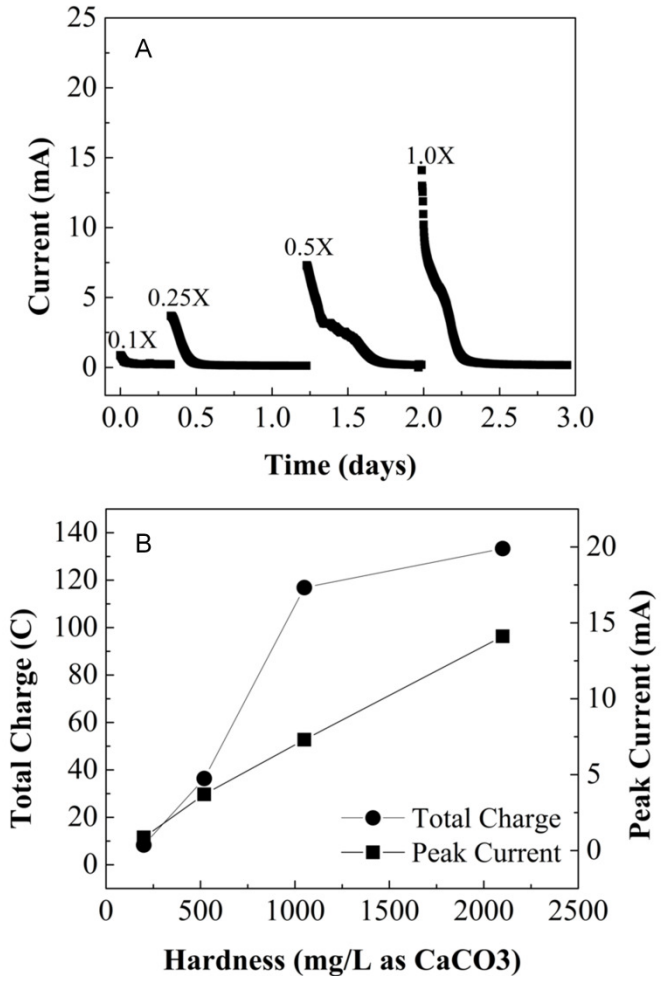

Figure 6: (A) Current variation from different dilutions of the hard water prior to the replacement of both the AEM and CEM and (B) the relationship between hardness concentration and total charge/peak current.

Analyzing the membrane with a scanning electron microscope (SEM) found that the surface of the membrane scaling appeared to have two distinct forms: 1) a cracked mud structure for a majority of the membrane scaling (Fig. 7A), and 2) a crystalline structure (Fig. 7B). The energy dispersive spectrometer (EDS) analysis showed the scaling ranged in thickness from 1.2 mm to 2.1 mm; the mud structure consisted mainly of calcium and phosphorus, and the crystalline structure made primarily of sodium,

calcium and chloride (Fig. 7C). The XRD spectrum peaks of the membrane scaling correspond with calcium hydrogen phosphate hydrate ($CaHPO_4 \bullet 2(H_2O)$), suggesting the scaling occurred when the calcium migrated across the CEM and bonded to the phosphate (Fig. 7D). The presence of chloride ions on the cathode side of the CEM was not expected and the exact reason is not clear at this time.

After both the CEM and AEM membranes were replaced, the performance of the cell increased by 140% as detailed below. At the lowest concentration of hard water, the peak current was 4.34 mA; increasing the concentration to 520 mg/L as $CaCO_3$ yielded a peak of 9.67 mA; the dilution of 0.5X produced a peak current of 13.90 mA; and at full-strength the peak current was 19.50 mA (Fig. 8A). Likewise, an almost-linear relationship is displayed between the hard water concentration, the peak current and, consequently, the amount of electrons generated (Fig. 8B). The results demonstrated the effect of membrane scaling on hardness removal and the necessity of replacing or cleaning the membranes for maintaining a satisfactory performance. A complete prevention of membrane scaling is impossible, but we can certainly reduce the scaling by modifying the MDC operation.

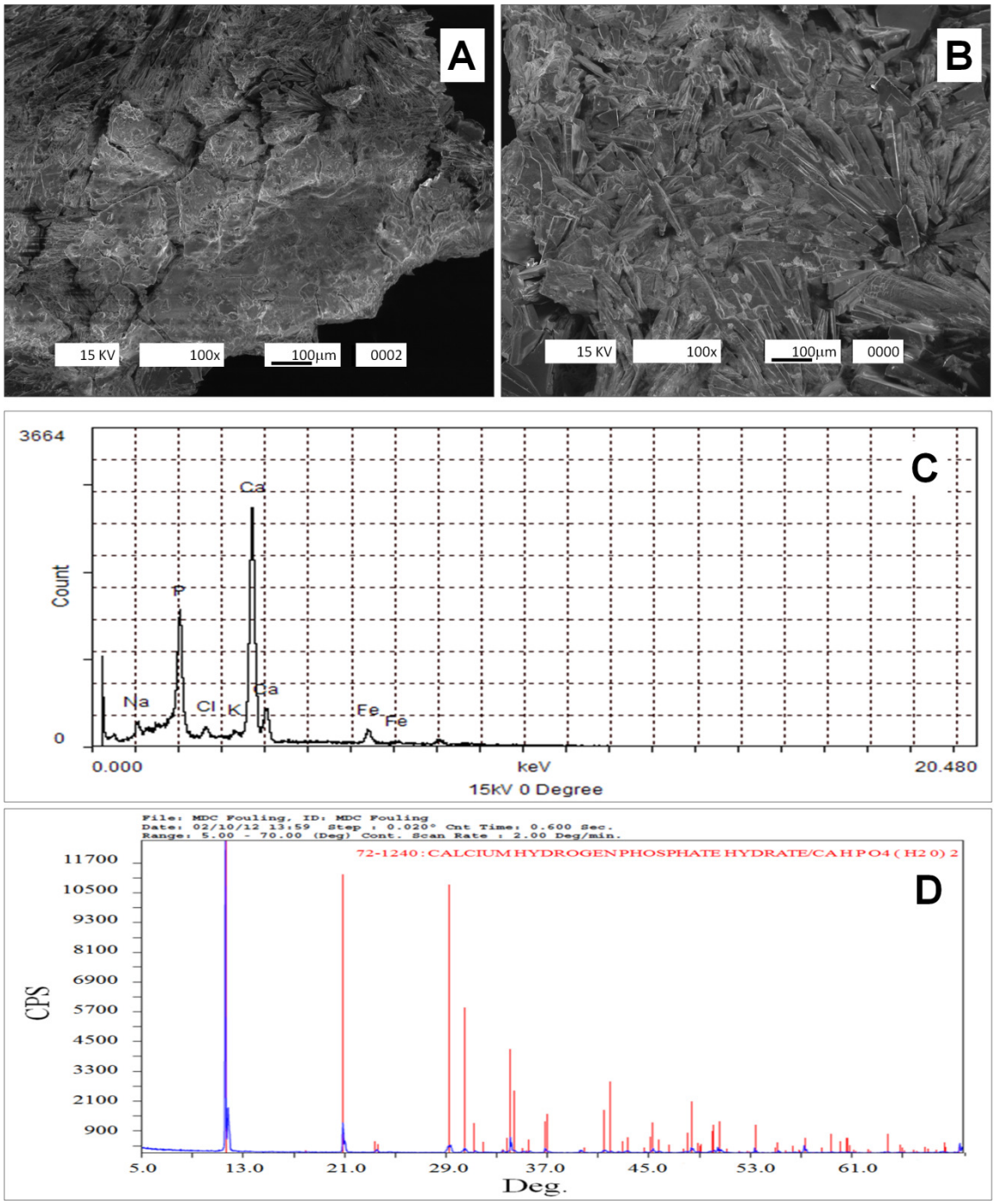

Figure 7: (A) SEM image of CEM at 100x magnification of the cracked mud structure, (B) SEM image of CEM at 100x magnification of crystalline structure, (C) EDS peaks of the membrane scale, and (D) the XRD structure of the membrane scale.

For example, the use of phosphate buffer and potassium ferricynide can increase the precipitation of the scaling, as shown by the results; replacing those solutes with other catholytes, e.g., an oxygen cathode with acidified water, may alleviate the scaling [18].

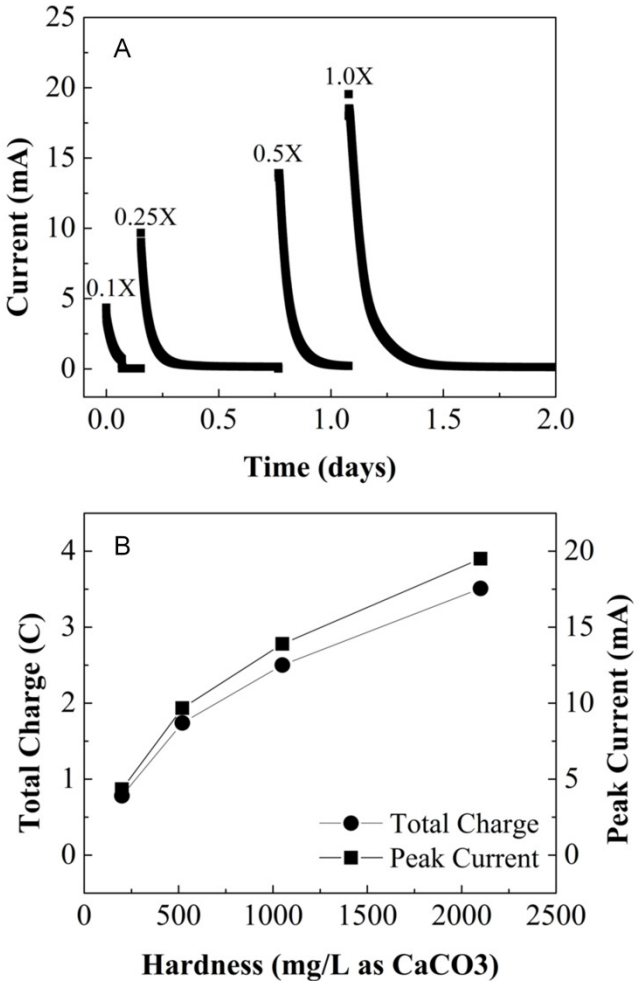

Figure 8: (A) Current variation from the different dilutions of the hard water after the replacement of both the AEM and the CEM, and (B) the relationship between hardness concentration and total charge/peak current.

3.2.2 Removal of Heavy Metals

When the hard water solution was replaced with a heavy metal solution consisting of arsenic, copper, mercury, and nickel, the MDC produced a peak current of 7.67 ± 0.71 mA (Figure 9). Of the heavy metal ions, the MDC removed 89% of the arsenic, 97% of the copper, 95% of the nickel, and 99% of the mercury (Table 2).

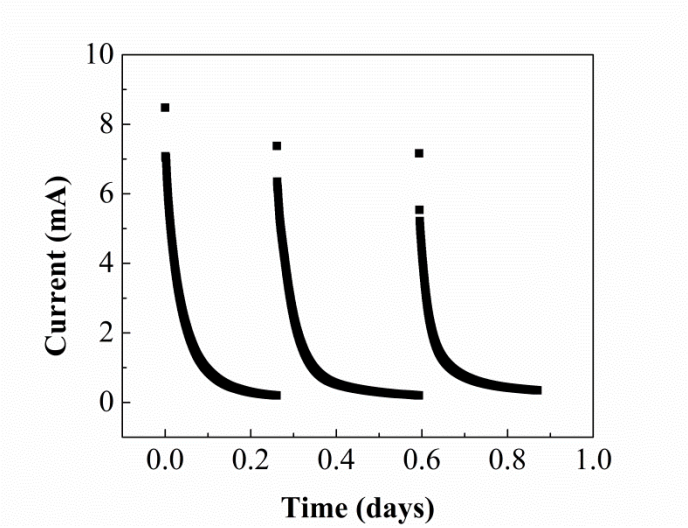

Figure 9: Current variation in the MDC treating a synthetic heavy metal solution consisting of arsenic, copper, nickel, and mercury.

Table 2: Heavy metal removal and energy generation in the MDC.

Heavy Metal	Initial Concentration [ppm]	% Metals Removal	Peak Current [mA]	Total Charge [C]
Arsenic (As(V))	13	89% ± 6%	7.67 ± 0.71	1.38 ± 0.13
Copper (Cu(II))	391	97% ± 0%		
Nickel (Ni(II))	357	95% ± 1%		
Mercury (Hg(II))	11	99% ± 2%		

The removal efficiencies of the metals can be explained by examining their relative affinities for ion exchange resin. Typically, ion exchange prefers cations with

higher valence, and for cations of the same valence, the cation of higher atomic number [66–69]. This preference leads to mercury with the highest valence removed the fastest, and arsenic with the lowest valence removed the slowest.

$$Hg^{2+} > Cu^{2+} > Ni^{2+} > As^{5+}$$

Thus, for the relationship observed during this experiment, metals with a lower valence electron potential faced higher removal efficiency than those with a higher valence electron potential, it is in good agreement with the literature results [70].

3.2.3 Perspective

These results have shown that MDC technology can be effective for softening hard water, and it is potentially advantageous as a low-energy softening technology with the additional benefit of wastewater treatment. The use of ion exchange membrane and a post-disinfection method (such as a UV light) can prevent the potential microbial contamination of softened water. As a proof of concept, the MDC used in this study was not optimized in terms of configuration and operation; bioelectricity generation can be further improved, and thus the efficiency of water softening. MDC technology may not be practical for use in residential applications due to the proximity of (anode) bacterial organisms to people; however, it could be a good candidate to replace lime softening, a pre-treatment mechanism for membrane processes [5,6,71,72]. Lime softening requires the use of chemicals for adjusting the pH and it produces a high-volume lime sludge stream, whereas MDC does neither [6]. Despite the potential advantages of MDC water softening in low-energy consumption, fewer required chemicals, and a combined function of wastewater treatment, one must also note its limitations. For example, a long retention

time is generally required in MDC treatment because of slow biological processes in its anode, which can be compensated either by a larger reactor volume or a lower concentration of hardness, or by increasing MDC electricity generation.

3.3 Conclusion

This study demonstrated that microbial desalination cell (MDC) technology for water softening offers a viable alternative to ion exchange systems and lime softening with advantages in reduced energy consumption, and high rejection of hardness and heavy metals,. The MDC removed 95% of hardness ions from a water stream while producing electricity in batch operation, and current generation was closely related to the concentration of hardness in water. Of the heavy metals tested, the MDC was sufficient for removing 89% of arsenic, 97% of copper, 99% of mercury, and 95% of nickel.

CHAPTER 4: PHOTO-ELECTROCHEMICAL WATER TREATMENT DEVICE FOR DRINKING WATER

This study experimentally demonstrated a photo-electrochemical water treatment device (PEWT) for residential drinking water treatment. The PEWT device was analyzed using design of experiments in order to identify the optimum process parameters for operation to achieve the highest amount of hard water rejection possible. The proposed device was found to soften water at a removal efficiency of 60% and was able to achieve 3.9 logs of bactericidal disinfection.

4.1 Materials and Methods

4.1.1 Photo-electrochemical Setup

The photo-electrochemical reactor used in this study was a tubular reactor with three chambers as shown in Figure 10. The three chambers were separated with heterogeneous ion-exchange membranes: an anion-exchange membrane (AEM; AMI-7001, Membrane International, Inc., Glen Rock, NJ, USA) between the anode chamber and the middle chamber, and a cation-exchange membrane (CEM; CMI-7000, Membrane International, Inc.) between the cathode chamber and the middle chamber. A tubular UV source (11 W, Phillips) was inserted into the middle anode chamber. The titanium electrode was created using titanium mesh (18x18 mesh, 0.01" wire diameter, 67.24% open area, Cleveland Wire Cloth, Cleveland, OH, USA) and spot welded to form a cylinder (Spot Welder Info, Heat Setting 6) and centered between the UV quartz sleeve and the AEM.

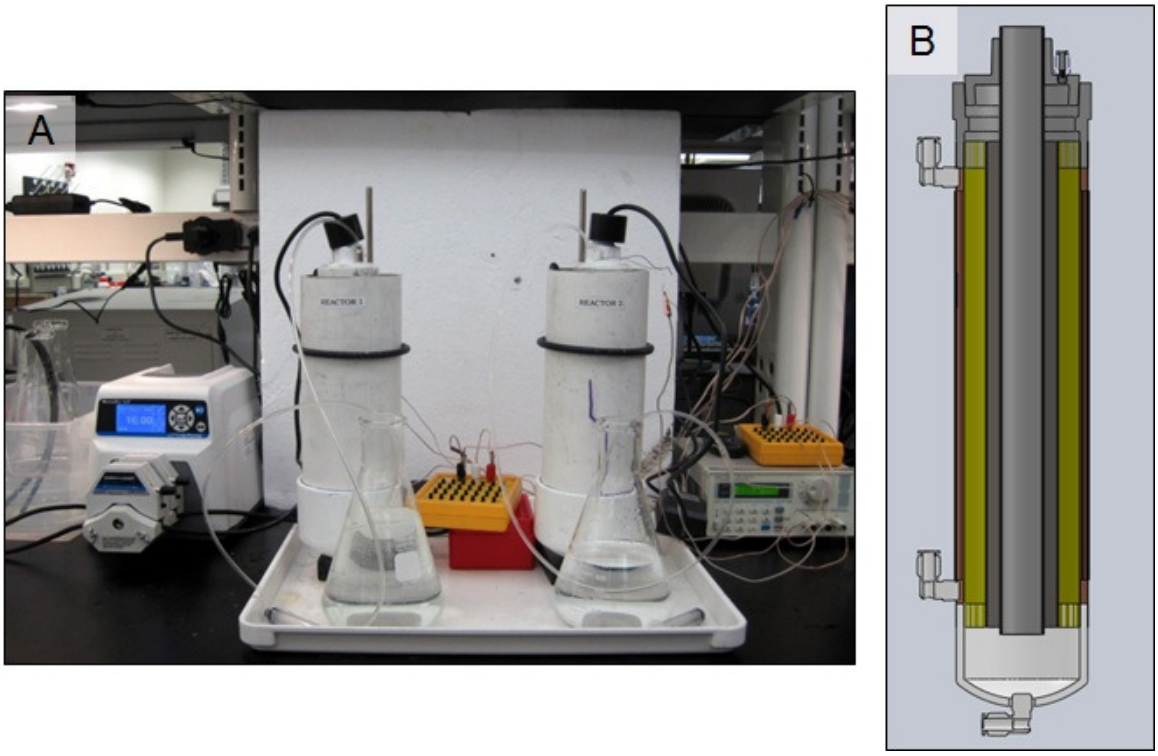

Figure 10: (A) Experimental setup and (B) a cross-section of one of the experimental models.

In this configuration water is first fed into the middle chamber, where hardness ions (e.g. calcium and magnesium) migrate into the cathode chamber driven by electric force, thereby softening the water. The effluent from this process is then supplied to the anode chamber where UV light inactivates any pathogenic bacteria and the photochemical oxidation of any organics in the water is completed by the TiO_2 electrode. The photochemical reactions are intended to oxidize any recalcitrant organics (*e.g.* personal care products and/or pharmaceuticals) and partially provide electrons for hardness removal. In order to accelerate the process, especially when there is a low concentration of organics in the water, an external electric potential can be applied and water electrolysis may occur with the production of hydrogen and oxygen gas in small quantities (Figure 11).

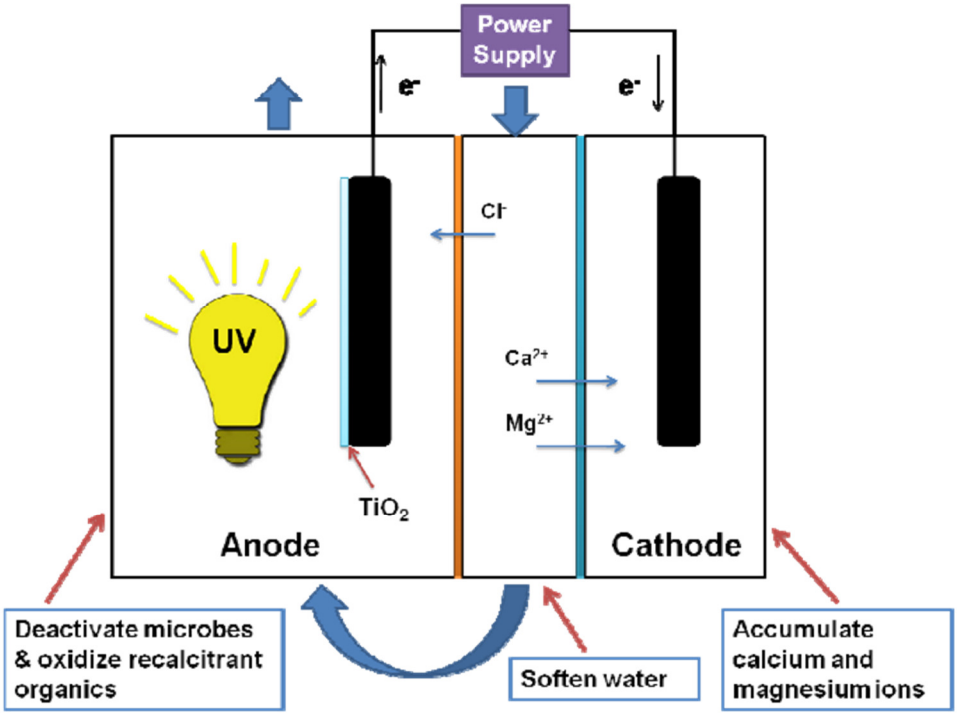

Figure 11: Schematic of a photo-electrochemical water treatment device.

The anode chamber held a liquid volume of 675 mL and the hardwater chamber held a liquid volume of 200 mL. The external resistance was set at 100 Ω to achieve a high current generation. During water softening, the calcium and magnesium ions moved into the cathode chamber through the cation-exchange membrane, and the chloride ions plus other anions moved into the anode chamber through the anion-exchange membrane.

The thermal electrodes were created by heating the titanium mesh cylinder for 30 minutes in a horizontally mounted tube furnace (ThermoFisher, USA) at 700°C with a 1°C/min ramp-up speed. The oxidized electrodes were allowed to cool in the furnace to room temperature.

The sol-gel electrode was prepared in the following manner. While 5000 mL of 0.1 N nitric acid was stirred, 417 mL of titanium isopropoxide was added slowly. The addition immediately gave a cloudy suspension. The suspension was continuously stirred for 3-4 hours to peptize the suspension and formed a slightly cloudy, bluish sol. In order to obtain a coating with high porosity, the sol was dialyzed after peptization. The dialysis process increases the pH of the sol to the desired value, thereby reducing electrostatic repulsion forces between colloidal particles in the sol and allowing the particles to aggregate slightly. Spectra/Por dialysis tubing with a flat width of 54 mm and a molecular weight cutoff of 3,500 was employed. Prior to use, the tubing was washed in an aqueous solution of 0.001 M EDTA and 2% (w/w) sodium bicarbonate. After the sol was created, it was applied to the titanium electrode by dip coating. After coating, the electrode was heated in a furnace for 3 hours at 350°C in order to create the xerogel coating.

4.1.2 Operating Conditions

Most of the studies conducted by researchers and scientists on fuel cell reactor operation involve changing one independent parameter at a time while maintaining the others at a fixed level. Such studies ignore the interaction effects between important parameters affecting the operation of the reactor. One possible solution is to apply statistical tools such as design of experiments (DOE) where all important parameters are varied simultaneously over a set of experimental runs. DOE has proven to be successful for the determination of effective materials, components, and process parameters [73–75].

In this study, two identical photo-electrochemical water treatment devices were created, each having a different anode electrode. The objective of this study was to identify the optimum process parameters using DOE for the highest amount of hard water rejection. The process variables evaluated were hard water concentrations, applied voltage, hydraulic retention time, and titanium dioxide (TiO_2) coating type (Table 3). Eight experiments were run in duplicate and in a randomized order (Table 4) and the hardness rejection results from these experiments were used to form the basis of the most ideal operating condition. Minitab statistical software was used in the evaluation of the process variables.

For these experiments synthetic hard water solutions were created at 50 mg/L as $CaCO_3$ and 500 mg/L as $CaCO_3$ using calcium chloride and fed into the hard water chamber at a flow rate of either 13 mL/min (HRT of 1 hour) or 2.16 mL/min (HRT of 6 hours).

For the experiments using bacteria, a freeze dried stock bacteria, *E. coli* (ATCC® 15597™, Manassas, VA, USA), was prepared in the following manner. Into an autoclavable bottle, 8 grams of LB Broth was combined with 400 mL of Type III deionized water. The broth was then gently heated on a hot plate until it reached a boil. The boiled solution was next autoclaved at 121°C for 60 minutes until it was sterile. After the LB Broth cooled down to room temperature, a loop of freeze dried *E. coli* (ATCC® 15597™) was inoculated into the solution, then placed in an incubated shaker set at 35°C for 18±2 hours at 130 RPM. After shaking overnight, 400 mL is poured off into eight-50 mL sterile centrifuge tubes. The microbial solution is then centrifuged (Sorvall ST16, Thermo Scientific, Pittsburgh, PA, USA) at 6000 x g for 5 min. After

being centrifuged, the supernate was poured off and replaced with 50 mL of Type III or better deionized water.

Table 3: Experimental independent variables.

Variables	Factor Code	Unit	Level and range (coded)	
			-1	1
Hard water Concentration	A	mg/L as $CaCO_3$	50	500
Applied Voltage	B	V	0	3
Hydraulic Retention Time	C	hr	1	6
Coating Type	D	-	TiO_2 Sol-Gel	TiO_2 Thermal Film

Table 4: Experiment runs and responses for the rejection of hard water within the PEWT.

Run	Factor				Response
	A: hard water concentration (mg/L as $CaCO_3$)	B: applied voltage (V)	C: hydraulic retention time (hr)	D: coating type	Hardness Rejection (%)
1	50	0	1	TiO_2 Sol-Gel	17.0 ± 1.4
2	500	0	1	TiO_2 Thermal Film	5.5 ± 2.1
3	50	3	1	TiO_2 Thermal Film	35.5 ± 4.9
4	500	3	1	TiO_2 Sol-Gel	6.5 ± 2.1
5	50	0	6	TiO_2 Thermal Film	60 ± 14.1
6	500	0	6	TiO_2 Sol-Gel	19.5 ± 0.7
7	50	3	6	TiO_2 Sol-Gel	27.0 ± 8.5
8	500	3	6	TiO_2 Thermal Film	60.5 ± 3.5

Table 5: Estimated effects and coefficients for results.

Term	Effect	Coefficient	Standard Error Coefficient	T	P
Constant		28.938	1.582	18.29	0.000
A	-11.875	-5.937	1.582	-3.75	0.006
B	6.875	3.437	1.582	2.17	0.062
C	25.625	12.812	1.582	8.10	0.000
D	22.875	11.437	1.582	7.23	0.000
A*B	14.125	7.062	1.582	4.46	0.002
A*C	8.375	4.187	1.582	2.65	0.029
A*D	-2.875	-1.438	1.582	-0.91	0.390

4.1.3 Measurements and Analysis

The cell voltage was recorded every three minutes by a digital multimeter (2700, Keithley Instruments, Inc., Cleveland, OH, USA). The conductivity of the solutions was measured with a benchtop conductivity meter (Mettler-Toledo, Columbus, OH, USA). The pH was measured with a benchtop pH meter (Oakton Instruments, Vernon Hills, IL, USA). The total hardness was measured with a digital titrator (Hach Company, Loveland, OH, USA).

4.2 Results and Discussion

4.2.1 Removal of Total Hardness

In order to determine if the UV light itself was driving the generation of current within the PEWT system when water softening occurred or if the softening was a result of diffusion, light on and light off experiments were performed at a 1 hour HRT. When the UV light was on, the hardness removal increased to 14% and a current was generated. When the UV light was off, there was no hardness removal and no current was generated (Figure 12). These results illustrate that the UV light is an essential component for the softening of water in the PEWT system.

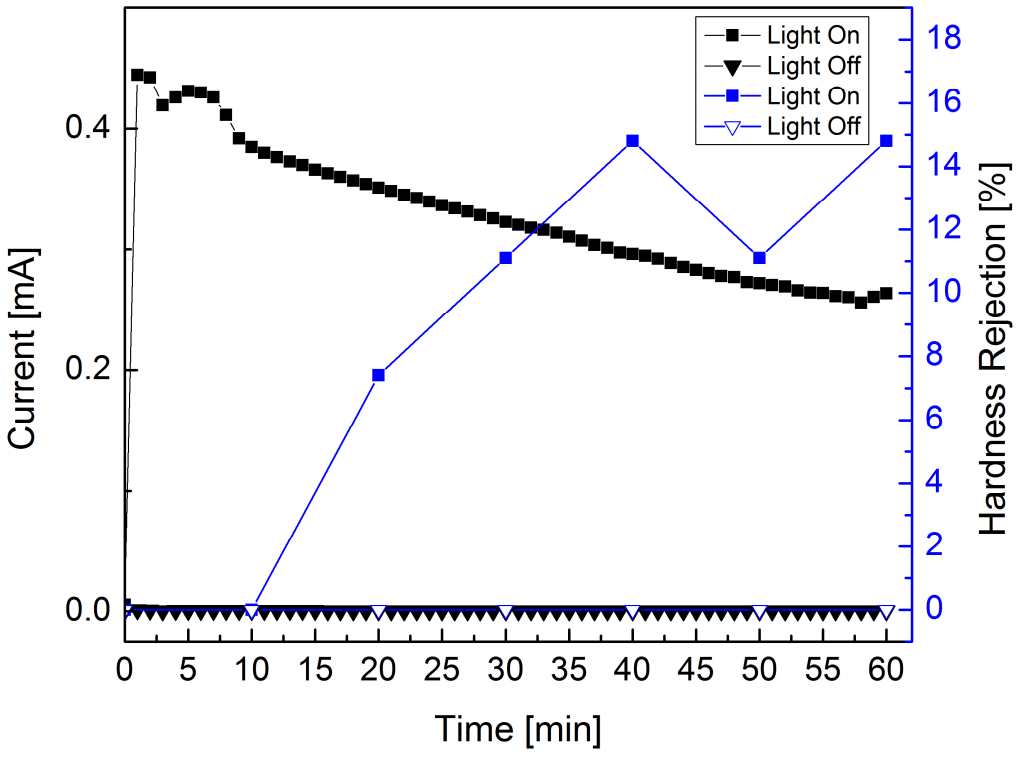

Figure 12: Comparison of the current generation and potential softening effect under light on and light off conditions.

The best set of operating conditions for the PEWT were determined to be a lower hardness level, a longer retention time, and by using the TiO_2 thin film coated electrode. Based upon the effects of the interactions shown in Table 5, the most statistically significant variables are the hardness level, the retention time, and the coating type. In Figure 13, the steeper the line is, the greater the influence the effect has with a larger level value indicating the range had the largest control. The variables with the largest control are the ideal operating conditions for the PEWT.

The long retention combined with the TiO_2 thin film coating yielded the best results. The interaction plot, Figure 14, of coating and retention time indicates that the retention time with the TiO2 sol-gel coating has a minimal effect.

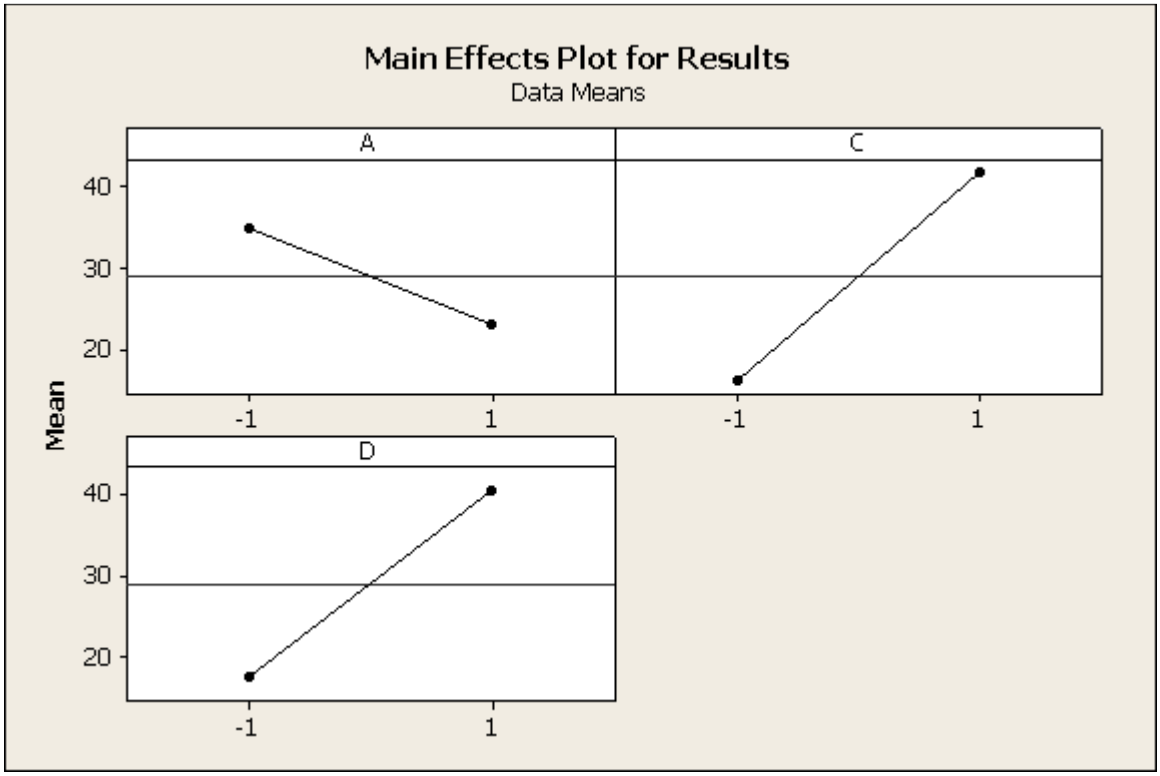

Figure 13: Plot of main effects: hardness concentration (A), hydraulic retention time (C), and TiO_2 coating type (D).

The interaction between hardness concentration and retention time suggests that with a longer retention time it is possible to have the results of a higher hardness concentration water match the results of a lower hardness concentration water. In other words, they likely top out at the same level but after different rates of growth. In Figure 15, the slopes of the interaction lines suggest that further experiments need to be completed in

order to fully understand the effect of hydraulic retention time on hardness concentration. Unlike previous experiments that relied on the movement of electrons to drive water softening where a linear relationship was observed, that may not be the case for photo-electrochemical water treatment systems [76].

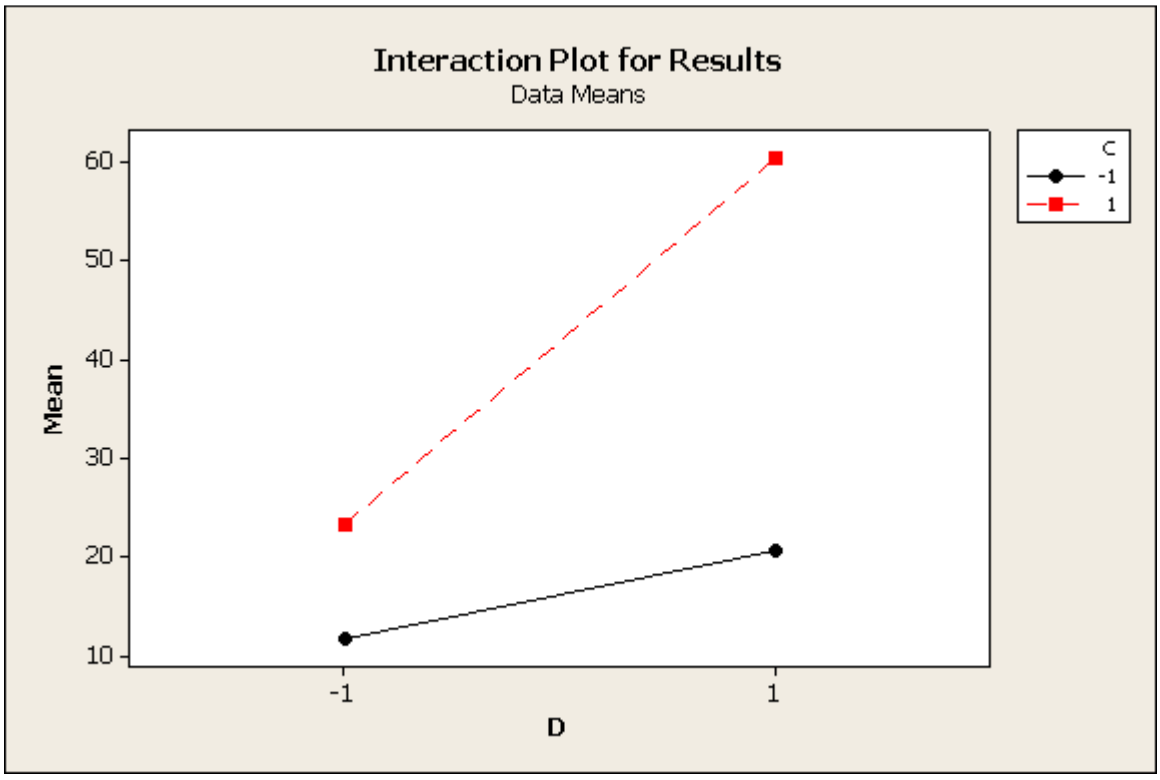

Figure 14: Interaction between hydraulic retention time (C) and TiO_2 coating type (D).

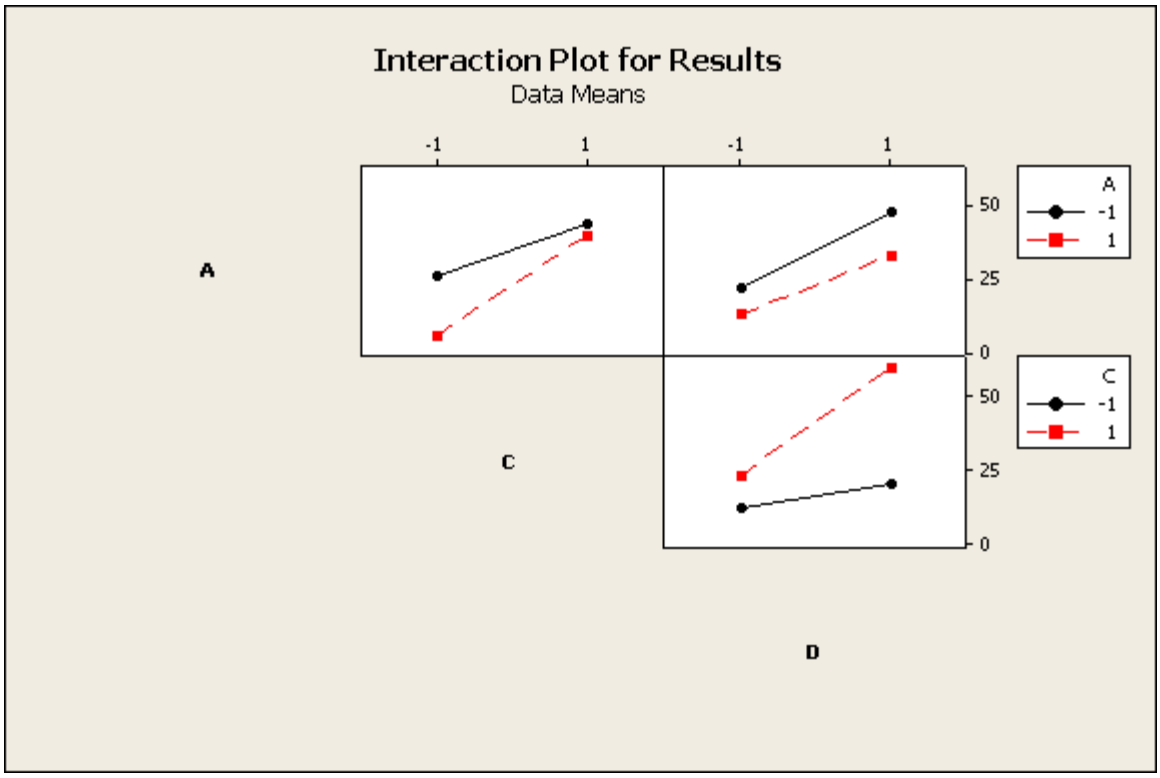

Figure 15: Interaction between hardness concentration (A), hydraulic retention time (C), and TiO_2 coating type (D).

To further explore the relationship between hardness concentration, hydraulic retention time, and hardness rejection, a series of experiments aimed at unveiling the secretes was conducted. Synthetic hard water solutions at concentrations of 50 mg/L as $CaCO_3$, 200 mg/L as $CaCO_3$, 350 mg/L as $CaCO_3$, and 500 mg/L as $CaCO_3$ were created for these experiments. Hydraulic retention times of 1 hour, 2 hours, 4 hours, and 6 hours were used. Based upon the results from these experiments, it appears that the hardness rejection for varying hydraulic retention times and concentration levels is mostly linear (Figure 16).

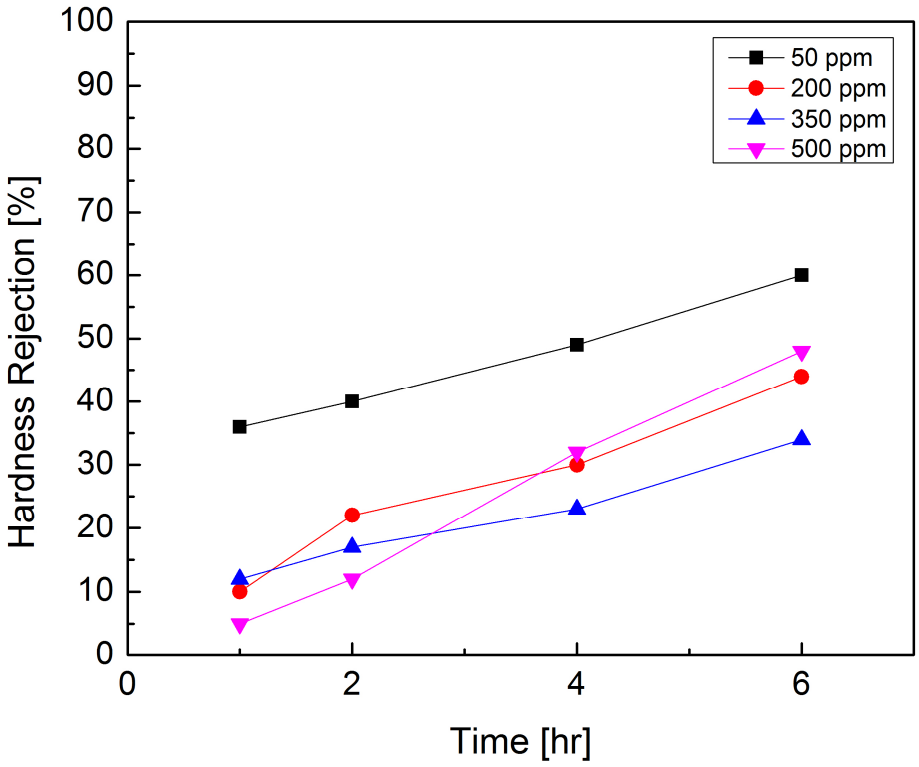

Figure 16: The hardness rejection rates for varying hydraulic retention times and concentrations.

4.2.2 Removal of Bacteria

The disinfection rate of model bacteria *E. coli* was studied for the PEWT system. Using *E. coli* (ATCC#15597™) at a 7.8×10^4 log influent concentration and a one hour hydraulic retention time, the PEWT system was able to remove 3.9 logs of bacteria. This removal rate could be improved by optimizing the reactor configuration for disinfection, but this may mean that the reactor becomes less ideal for hardness rejection.

4.3 Conclusion

This study demonstrated the feasibility of using a photo-electrochemical water treatment device for the softening of hard water and the removal of microorganisms.

Through the results of this study it was determined that it was possible to achieve a 60% removal efficiency for hard water within a six hour time period. This study also recognized that it was possible to obtain a 3.9 log removal of bacteria within a one hour time period with pure water. Further optimization of the PEWT system in terms of the electrode or the reactor design could lead to improvements in the amount of hard water rejected or the amount of disinfection which may occur.

CHAPTER 5: INDIVIDUAL AND COMBINED EFFECTS OF SILVER AND COPPER MODIFIED TIO_2 MEMBRANES ON THE INACTIVATION OF *E. COLI* AND BACTERIOPHAGE MS2

The purpose of this study was to examine the individual and combined effects of silver doped, copper doped, and silver-copper doped titanium dioxide coatings on fiberglass membranes. During batch operation, both *E. coli* and bacteriophage MS2 were examined for their microbial reduction under light and dark conditions. The quantity of free heavy metals ions leaching off of the membranes and their effect on the microbial reduction was also examined.

5.1 Materials and Methods

5.1.1 Preparation of the Photocatalyst

The photocatalytic membranes were created in a two-step procedure: first the titanium dioxide (TiO_2) nanowires were created, then the heavy metals were added through photodeposition for silver and through adsorption for the copper. The TiO_2 nanowires were created by mixing 1 gram of P25 (Sigma-Aldrich, St. Louis, MO, USA) with 65 mL of 10 M NaOH (Sigma-Aldrich, St. Louis, MO, USA) and 65 mL of ethanol (Sigma-Aldrich, St. Louis, MO, USA) together and stirring for one hour. This solution was next processed using hydrothermal treatment in a furnace (Cress C122012/F4H, Carson City, NV, USA) at 160°C for 12 hours. The resulting white gel was gently washed with 0.1 M HCl until the pH dropped below 7, then rinsed with Type 1 deionized water (Synergy UV, EMD Millipore, Darmstadt, Germany) until the pH returned to 7.

After the TiO_2 nanowires were created, they were applied onto a fiberglass substrate through a vacuum filtration method in order to create a uniformly distributed layer. This method consisted of combining 5 mL of TiO_2 nanowires with 47.5 mL of Type 1 deionized water. This solution was sonicated for 15 minutes at 20% amplitude (FB505, Fisher Scientific, Pittsburgh, PA, USA) in order to create a well-ordered layer of TiO_2. After sonication, the nanowires were applied to a 47 mm diameter fiberglass disc via vacuum filtration. To ensure that the nanowires would remain attached, the disc air dried overnight and the following day it was dried in a furnace at 375°C for twelve hours.

A 2% doping of silver onto the titanium dioxide nanowires was selected as the most optimum doping condition due to prior work completed by Li *et. al.*[47]. The photodeposition of silver onto the TiO_2 nanowires was carried out in the following manner. A 3 mol/L solution of HCl was added to a 50 mL solution of TiO_2 nanowires until the pH reached 3. Next, 7 mg of $AgNO_3$ (Sigma-Aldrich, St. Louis, MO, USA) was added to the nanowire suspension. Finally, 2 mL of a 2.5% solution of $HClO_4$ (Sigma-Aldrich, St. Louis, MO, USA) was added to the Ag-TiO_2 mix as a precursor before the solution was placed under a UV light (λ = 365 nm, UVP LLC, Upland, CA, USA) for three hours while stirring continuously. After three hours the solution had turned a dark grey. It was then removed from the UV light and the new silver-titanium dioxide solution was applied onto fiberglass membranes following the same procedure that was used to create titanium dioxide membranes.

The addition of copper onto the TiO_2 and the Ag-TiO_2 membranes was achieved by mixing a 5% copper solution made using $CuNO_3$ (Sigma-Aldrich, St. Louis, MO, USA) into 45 mL of Type 3 deionized water with 5 mL of TiO_2 or Ag-TiO_2. A 5%

solution was selected due to the prior research conducted by Pham *et. al.* who determined that a 5% loading could achieve 0.91 log reduction of bacteria [45]. The resulting solution was allowed to sit overnight on an orbital shaker (KS 130 basic, IKA Works, Staufen, Germany) for 16 hours before it was sonicated for one minute at 20% amplitude and then applied to a fiberglass disc via vacuum filtration. After filtering, the resulting membrane was air dried then fired in a furnace at 375°C for twelve hours.

In order to determine the actual concentrations of heavy metal ions attached to the titanium dioxide nanowires, an acid digestion with high-purity concentrated nitric acid was used. For the digestion, the Ag-TiO_2, Cu-TiO_2, or Ag-Cu-TiO_2 solutions were vacuum filtered onto Pall 0.45 µm GN-6 filter paper to be gently heated in nitric acid and the filtrate was also collected for additional analysis. The heavy-metal loaded photocatalysts immobilized on filter paper were placed into a beaker with about 60 mL of nitric acid and heated to just below a boil. After digestion, the solution was allowed to cool before it was carefully poured into sterile centrifuge tubes. The centrifuge tubes were placed in the centrifuge and centrifuged at 6000 x g for 10 minutes to separate out the TiO_2 from the silver or copper ions now in solution. The heavy metal ions were decanted off and mixed with Type 1 DI water to achieve a 1% nitric acid concentration as per accordance with EPA 200.8 for the Determination of Trace Elements in Waters and Wastes by Inductively Coupled Plasma – Mass Spectrometry. The solutions were then diluted down to a measureable range and measured using ICP-MS.

5.1.2 Photocatalytic Disinfection Test Set-up

The photocatalytic disinfection apparatus used in bench scale testing is shown in Figure 17. The apparatus consisted of the following major component: one UV light source (λ = 254 nm, Phillips), a 500 mL beaker, a stirrer (Corning PC-620, Corning, NY, USA), a peristaltic pump (Masterflex L/S 7523-80, Vernon Hills, IL, USA), an acrylic cell to hold the membrane (Figure 18), Tygon® tubing, and miscellaneous fittings.

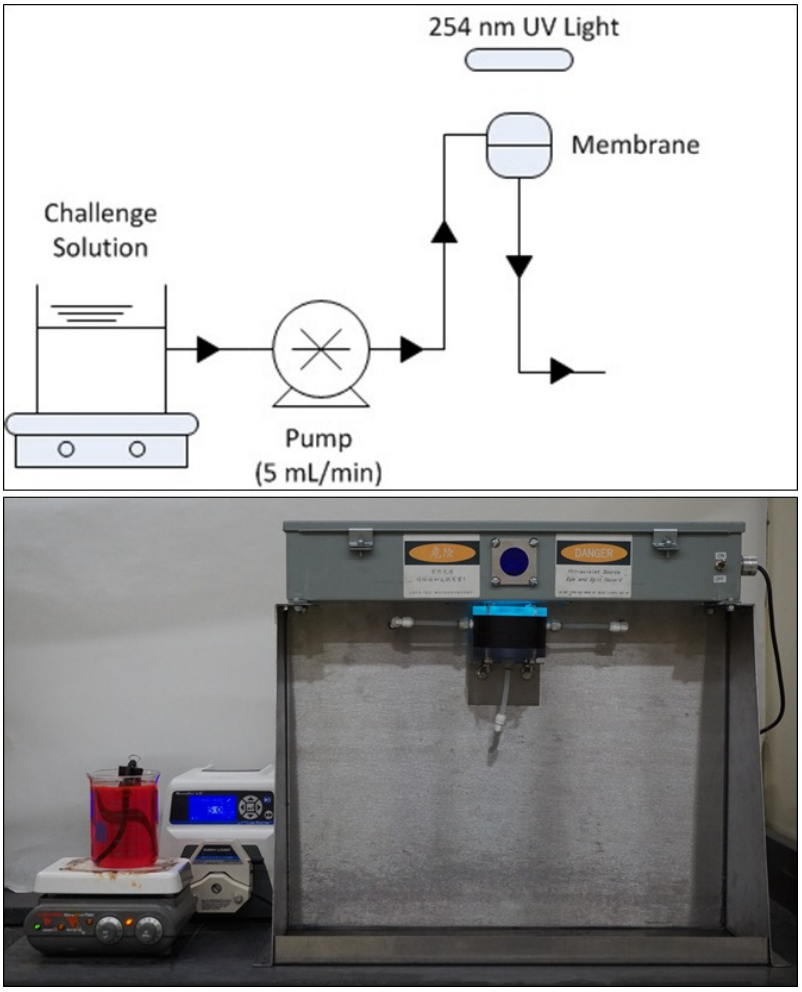

Figure 17: Photocatalytic disinfection test set-up.

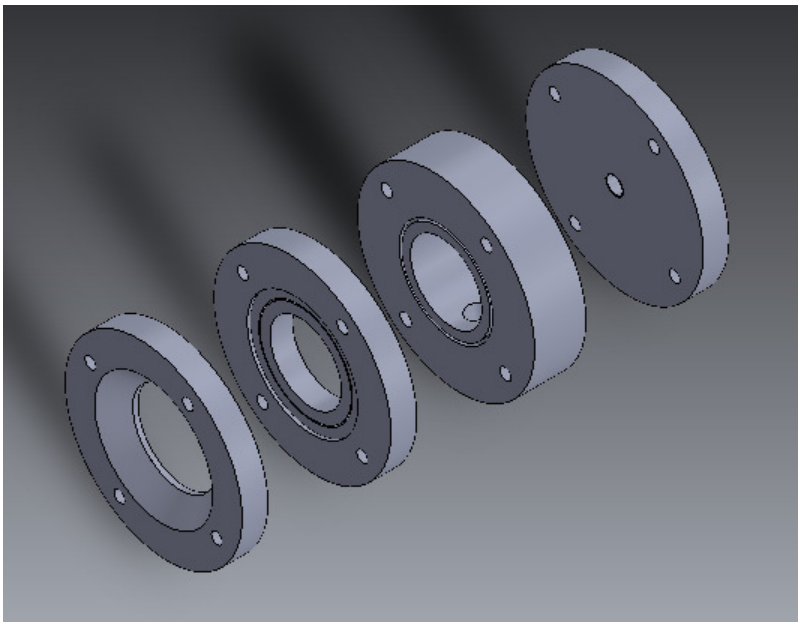

Figure 18: Membrane holder.

The microbial challenge water solution was held in a 500 mL beaker and flowed through the test apparatus via a variable speed peristaltic pump. The challenge solution entered the acrylic membrane holder via two quarter-inch ports on either side of the membrane holder, flowed down through the membrane, and exited out the bottom of the holder through a quarter-inch port. Each experiment lasted for thirty minutes and samples were taken every ten minutes throughout the course of the test. The challenge solution was maintained at a temperature of 22°C (72°F) during all the experiments.

5.1.3 Microbial Challenge Solution

5.1.3.1 Preparation of the bacteria challenge solution

A freeze dried stock bacteria, *E. coli* (Migula) Castellani and Chalmers (ATCC® 11303™, Manassas, VA, USA), was prepared in the following manner. Into an autoclavable bottle, 8 grams of LB Broth was combined with 400 mL of Type III

deionized water. The broth was then gently heated on a hot plate until it reached a boil. The boiled solution was next autoclaved at 121°C for 60 minutes until it was sterile. After the LB Broth cooled down to room temperature, a loop of freeze dried *E. coli* (ATCC® 11303™) was inoculated into the solution, then placed in an incubated shaker set at 35°C for 18±2 hours at 130 RPM. After shaking overnight, 400 mL was poured off into eight-50 mL sterile centrifuge tubes. The microbial solution was then centrifuged (Sorvall ST16, Thermo Scientific, Pittsburgh, PA, USA) at 6000 x g for 5 min. After being centrifuged, the supernate was poured off and replaced with 50 mL of Type III or better deionized water.

5.1.3.2 Preparation of the virus challenge solution

The bacteriophage MS2, the testing virus used in these experiments due to its similar activity of enteric viruses, was prepared in the following manner. MS2 experimental work was completed in a double layer method. To create the top layer of agar, 4 grams of tryptone, 3.2 grams of sea salt, 0.4 grams of yeast extract, and 3.2 grams of agar were weighed out separately then placed into an autoclavable bottle with 400 mL of Type III or better quality deionized water. The bottle was then placed on a hot plate and gently heated while stirring constantly until it came to a boil. After the top layer reached a boil it was autoclaved at 121°C for 60 minutes.

The lower layer was prepared by weighing out 14 grams of LB Broth plus Agar and placing it into an autoclavable bottle fill with Type III or better quality deionized water. The solution was stirred until all the solid media had dissolved. A 10% PBS solution was prepared by pouring 40 mL of PBS stock solution into 360 mL of Type III or better deionized water into an autoclavable bottle. The stock PBS solution was

prepared by dissolving 80 g NaCl, 2 g KH_2PO_4, 29 g Na2HPO4*12H2O and 2 g KCl in Type III deionized water to a final volume of 1 L. The final liquid reagent, LB Broth, was prepared as in section 4.1.3.1 Preparation of the bacteria challenge solution. Before use, all of the liquid reagents were autoclaved at 121°C for 60 min in order to sterilize them completely.

The day before the propagation of the MS2, one inoculation loop of *E. coli* (ATCC® 15597™) was added into the 400 mL bottle of LB Broth. The bottle of broth with *E. coli* was then placed into the incubator shaker overnight at 35°C for 18±2 hours shaking at 130 RPM. After the 18 hours had passed, the bacteria stock solution was poured off into two sterile 50 mL centrifuge tubes and the remainder of the bottle was disposed of.

The day of the MS2 propagation, approximately 5 – 8 mL of lower layer agar was poured onto four petri dishes and allowed to solidify. Next, 5 – 8 mL of LB Broth was poured into a sterile test tube and inoculated with a loopful of freeze-dried bacteriophage MS2 (ATCC® 15597-B1™). Into three separate sterile test tubes 1 mL of the MS2 and LB Broth mixture was pipetted. Into a fourth test tube 1 mL of 10% PBS solution was pipetted. Into each of the four test tubes, 100 µL of the overnight prepared stock *E. coli* solution were pipetted. Next, 5 – 8 mL of the top layer agar was added into each of the four test tubes then each test tube was separately poured out onto one of the four solidified lower layer plates. The plate with the 10% PBS and *E. coli* solution was labeled as the negative blank. After the entire bottle of agar had solidified, all of the plates were inverted and stored in an incubator set to 35°C for 18±2 hours.

The day following the MS2 propagation, the negative blank was checked to ensure that no colonies had formed. If no colonies had appeared, the propagation was allowed to continue. If colonies had appeared on the blank petri dish, the propagation was discontinued. Onto each of the three petri dishes containing bacteriophage MS2, 8 mL of sterile 10% PBS was pipetted. The petri dishes were then placed back into the incubator at 35°C for 20±5 minutes. After the 20 minutes had passed, the PBS solution was carefully poured off into a sterile centrifuge tube and centrifuged at 6000 x g for 5 minutes. Once the solution was centrifuged, a sterile syringe was used to remove the supernatant from the centrifuge tube and it was passed through a 0.45 µm syringe filter into a new centrifuge. This resulting filtered liquid was labeled as the MS2 stock solution and placed in a refrigerator at 4°C for storage.

5.1.4 Experiment Methods

Each membrane was challenged under both light and dark conditions in order to gauge the effectiveness of the photocatalytic activity of the membrane, and to isolate any benefit from mechanical filtration and/or free heavy metal ions in the water. Experiments were conducted using fiberglass membrane without any coating, membranes coated solely with titanium dioxide, membranes coated with silver-titanium dioxide, membranes coated with copper-titanium dioxide, and membranes coated with silver-copper-titanium dioxide. During each experiment samples were collected every ten minutes, generating four samples per experiment in total. For every sample that was completed using a membrane which contained titanium dioxide doped with a heavy metal, extra samples were taken for heavy metal analysis using inductively-coupled plasma mass-spectrometry (ICP-MS). Membranes were challenged with 10^7 CFU/mL of *E. coli* and 10^5 PFU/mL of

bacteriophage MS2, each test being repeated in triplicate. Experiments that were conducted in the dark were used to determine the antimicrobial effect of the UV light and the antimicrobial effect of free heavy metal ions in the water.

Before each test was conducted, the test apparatus was flushed with a 70% isopropyl solution for ten minutes to remove any trace microbial contaminants. After the isopropyl solution had passed through the test apparatus, the system was further flushed with Type III deionized water for 30 minutes. Once the isopropyl solution was completely removed, the water was drained from the system and the challenge microbial stock solution was poured into the 500 mL beaker. The UV light was allowed to warm up for 5 minutes, the intensity of the light was recorded using a UV light meter (ILT77, International Light Technologies, Peabody, MA, USA), and the experiment was allowed to begin.

Each experiment ran for thirty minutes with samples taken every 10 minutes resulting in samples at time 0, 10 minutes, 20 minutes, and 30 minutes. The time 0 sample, noted as sample 1 on the figures, was meant to represent the first flush of water to pass through the membrane. In order to quantitatively evaluate the membrane's performance it was necessary to determine the amount of bacteria rejected by the fiberglass membrane, the TiO_2 membrane, the Ag-TiO_2 membrane, the Cu-TiO_2 membrane, and the Ag-Cu-TiO_2 membrane. The amount of bacteria that was rejected by the filter was determined by serial dilutions and heterotrophic plate counts with a pour plate method using USEPA Method 9215. The reported log reduction was the geometric mean of the bacteria in the effluent solutions. The amount of virus that was rejected by the filter was determined by serial dilutions, a double-layer pour plate method, and the

reported log reduction was the geometric mean of the viruses in the effluent solution. The final log removal of each filter was determined by dividing the concentration of bacteria or viruses in the feed water:

$$\log removal = -log_{10}\left(\frac{N_{out}}{N_{in}}\right)$$

where N_{out} is the concentration of bacteria or viruses in the treated water and N_{in} is the concentration of bacteria or viruses in the influent water. For experiments that used a membrane coated with silver, copper, or both heavy metal ions, extra water was collected for analysis by ICP-MS so that the concentration of heavy metal ions in the water could be determined.

5.2 Results and Discussion

5.2.1 Surface Morphology and Materials Characterization

Prior to evaluating the membranes for their disinfection capabilities, preliminary SEM-EDS was completed to examine the surface morphology of the photocatalysts and to verify the heavy metal loading onto the TiO_2. Membranes coated with TiO_2 as per Section 4.1.1 Preparation of the Photocatalyst had a mostly uniform distribution of TiO_2 nanowires (Figure 19). Membranes that were coated with Ag-TiO_2 showed similar surface morphology to the pure TiO_2 membranes and an even coating of silver (Figure 19); EDS verified the presence of silver (Figure 20). Subsequent digestion of the silver off of the titanium dioxide nanowires with 70% nitric acid as per Section 5.1.1 Preparation of the Photocatalyst and ensuing analysis with ICP-MS confirmed the atomic

ratio was 2%. Membranes that had a coating of Cu-TiO_2 showed an even distribution across the surface of the fiberglass membrane (Figure 19) and EDS confirmed the existence of copper (Figure 21). Again, digestion of the copper off of the titanium dioxide nanowires with 70% nitric acid as per Section 5.1.1 Preparation of the Photocatalyst and ensuing analysis with ICP-MS revealed an atomic ratio of 17% for copper to TiO_2, higher than anticipated. SEM of a Ag-Cu-TiO_2 coated membrane revealed an even coating across the surface of the fiberglass (Figure 19), EDS confirmed the presence of silver and copper (Figure 22), and ICP-MS after digestion of the silver and copper off the nanowires revealed a 2% silver atomic ratio with a 17% copper atomic ratio. The digestion of silver and copper off of the titanium dioxide nanowires was successful at determining not only the actual loading of heavy metals, but also at determining how well the metals were attached onto the TiO_2. When nitric acid was added to the Cu-TiO_2 membrane for example, after heating to just below a boil for six hours the copper appeared to have all dropped out of solution. The Ag-TiO_2 membrane on the other hand went through a 16 hour digestion before all the metals appeared to have been removed from the nanowires.

Following a characterization of the surface of the differently coated membranes, mercury porosimetry was used to determine the pore size of the membranes in order to evaluate if any microorganisms were being removed through a mechanical filtration mechanism instead of through photocatalysis. Through the intrusion of mercury under high pressure into the pores of the various membranes, it was possible to determine that the fiberglass membrane had the largest open pore volume, the TiO_2, Ag-TiO_2, and Cu-

TiO_2 membrane all had similar pore volumes, and that Ag-Cu-TiO_2 had the smallest pore volume (Figure 23).

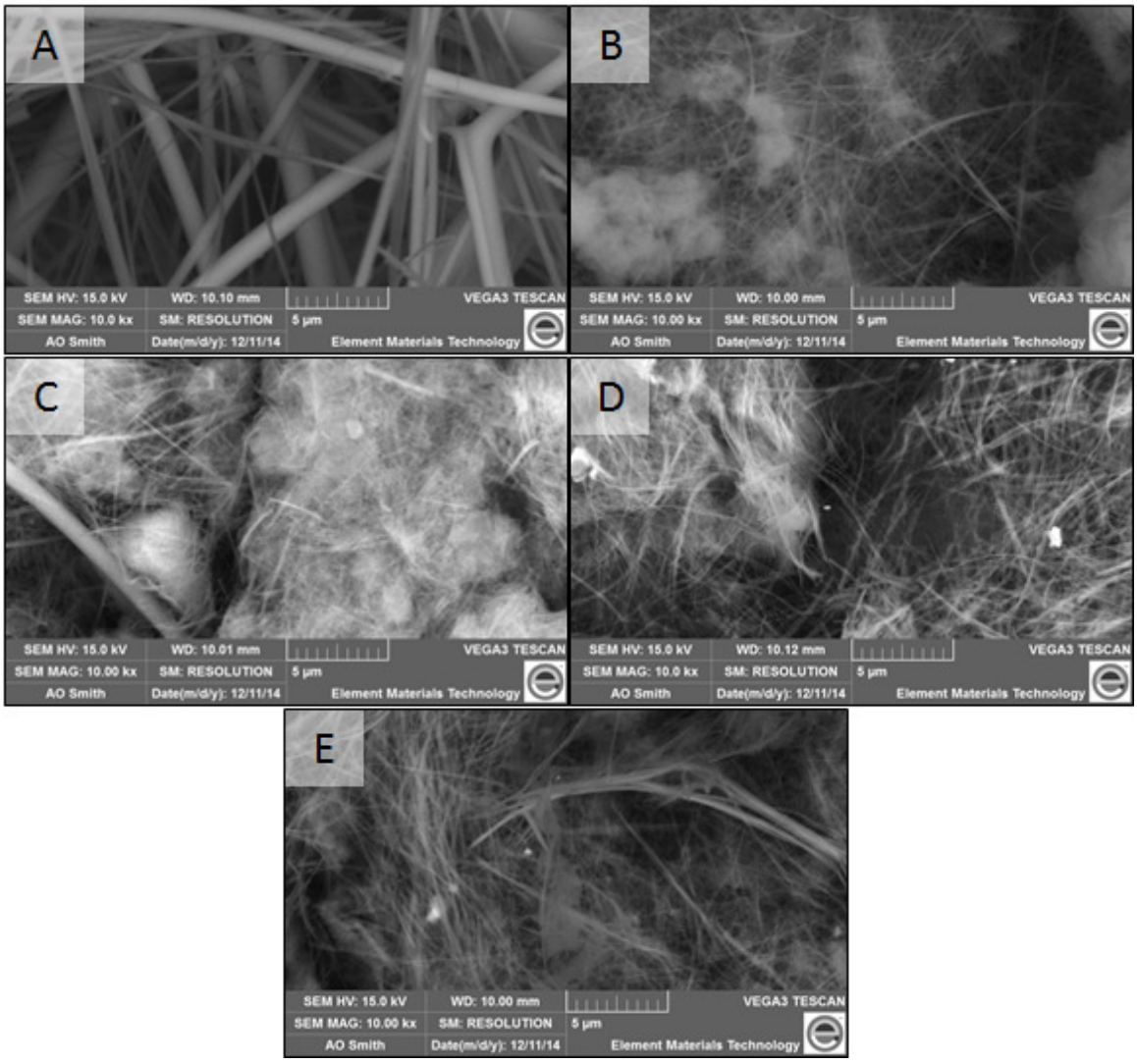

Figure 19: Uncoated fiberglass membrane (A), titanium dioxide coated membrane (B), silver-titanium dioxide coated membrane (C), copper-titanium dioxide coated membrane (D), and a silver-copper-titanium dioxide coated membrane (E) all at 10,000X magnification.

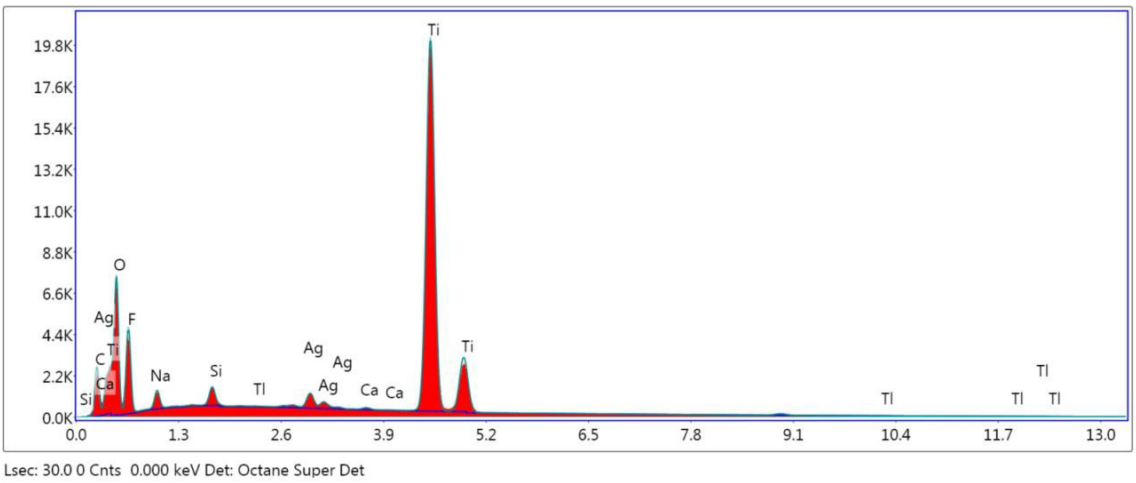

Figure 20: EDS of a Ag-TiO_2 coated membrane.

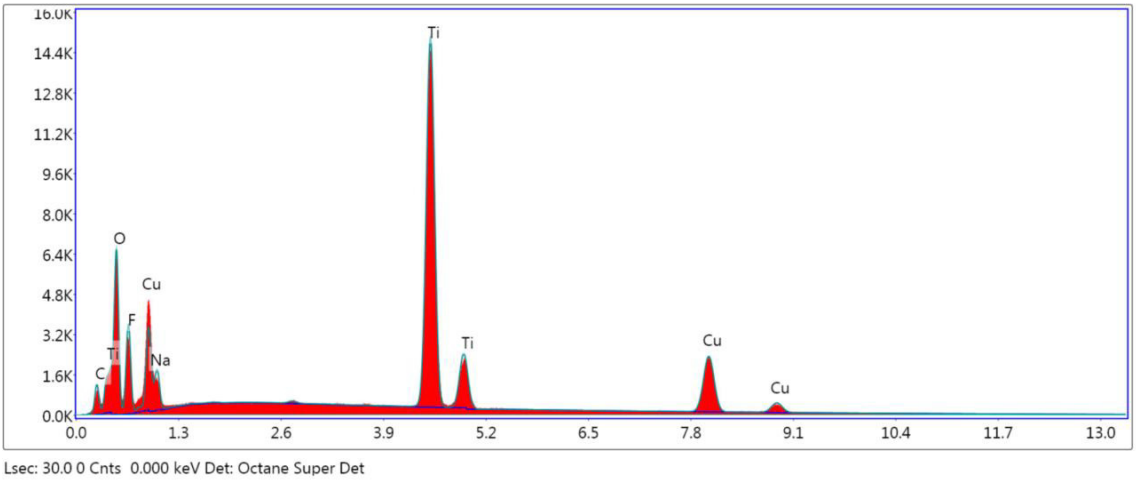

Figure 21: EDS of a Cu-TiO_2 coated membrane

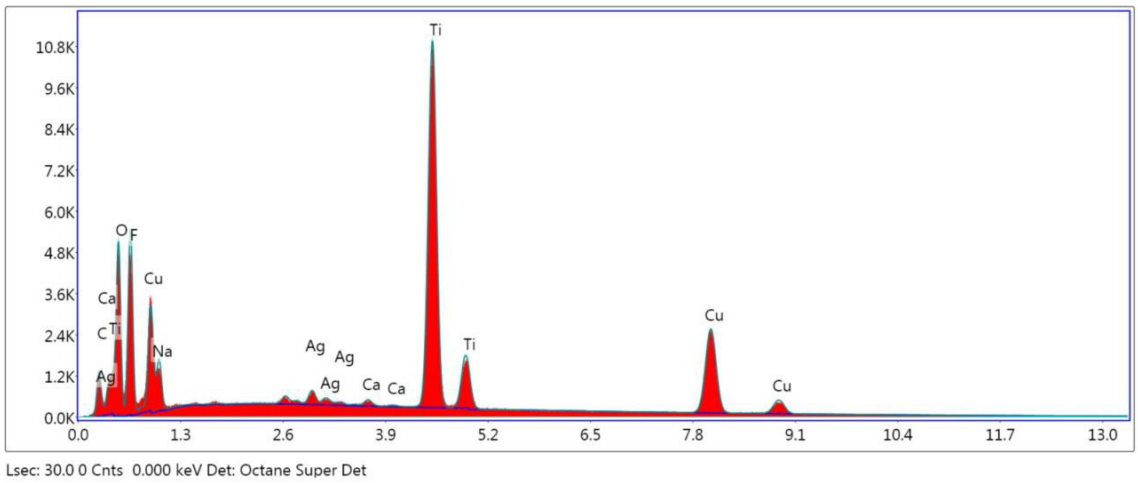

Figure 22: EDS of a Ag-Cu-TiO_2 coated membrane.

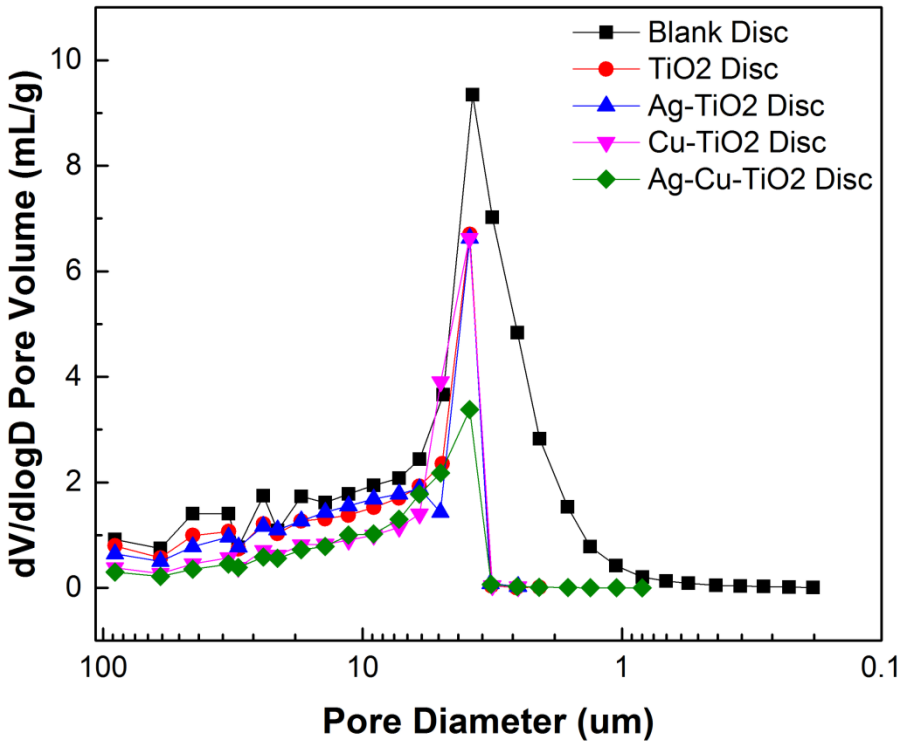

Figure 23: The respective pore size distributions.

5.2.2 Removal of Bacteria and Virus

To evaluate the effectiveness of the UV light, the TiO_2 membranes, the Ag-TiO_2 membranes, the Cu-TiO_2 membranes, and the Ag-Cu-TiO_2 membranes, experiments were conducted using *E. coli* at a 10^7-log influent concentration and a bacteriophage MS2 at a 10^5-log influent concentration. The microorganisms were added into Type III deionized water and allowed to flow through the membrane holder for 30 minutes during each test.

For the bacteria experiments performed with UV light, UV irradiation, TiO_2, and Ag-TiO_2, all exhibited strong bactericidal inactivation while the co-impregnation of Ag-Cu-TiO_2 enhanced the bacteria inactivation significantly (Figure 24). The increased bacterial inactivation by the Ag-Cu-TiO_2 membrane was attributed to an increase in ROS generation due to the synergies of silver and copper working together to increase the photoactivity. An increase in photoactivity due to combining silver and copper together was also recently reported by Behnajady *et. al.* for the removal of C.I. Acid Orange 7 as compared to Ag-TiO_2-P25 or Cu-TiO_2-P25 [39].

The illumination of doped TiO_2 with UV light will cause the formation of various reactive oxygen species (ROS). While bacteria can fight off low-levels of ROS through antioxidant defenses such as glutathione/glutathione disulfide (GSH/GSSG), excess ROS will cause oxidative stress and attack membrane lipids, ultimately leading to membrane and/or DNA damage [77]. The intensified bacterial inactivation of the Ag-Cu-TiO_2 membrane was likely due to increased photoactivity and therefore increased generation of ROS, plus the release of silver and copper ions. As expected, the antibacterial activity between the initial sample and the last sample increased likely due to a slight fouling of

the membrane over time. This also explains why the initial removal rate of bacteria is lower than the subsequent samples. Overall, on average UV illumination was able to inactivate 6.72±0.36 logs of bacteria, TiO_2 was able to inactivate 6.87±0.63 logs of bacteria, Ag-TiO_2 was able to inactivate 6.90±0.70 logs of bacteria, Cu-TiO_2 was able to inactivate 5.36±0.32 logs of bacteria, and Ag-Cu-TiO_2 was able to inactivate 7.66±0.98 logs of bacteria (Figure 25 and Table 6).

The unexpectedly poor performance of the Cu-TiO_2 coated membrane may be explained by copper being an essential trace element vital to the health of microorganisms. Copper has the ability to be incorporated into a variety of essential metabolic proteins and metalloenzymes, stimulating the immune system to fight infections, repair injured tissues, and promote healing [54,78].

In dark conditions, an increase in the amount of bacteria inactivated as time goes on is observed for the Ag-Cu-TiO_2 membrane, whereas a decrease is observed for all the other membranes (Figure 26). Overall, on average the dark condition was able to remove 0.63±0.19 logs of bacteria, TiO_2 was able to remove 0.74±0.25 logs of bacteria, Ag-TiO_2 was able to remove 0.83±0.70 logs of bacteria, Cu-TiO_2 was able to remove 0.37±0.12 logs of bacteria, and Ag-Cu-TiO_2 was able to remove 1.28±0.38 logs of bacteria (Figure 27 and Table 6). This increase in inactivation over time is likely due to the effects of heavy metal ions and is described in more detail in Section 4.2.3 Effects of Free Heavy Metals on Bacteria and Virus Removal.

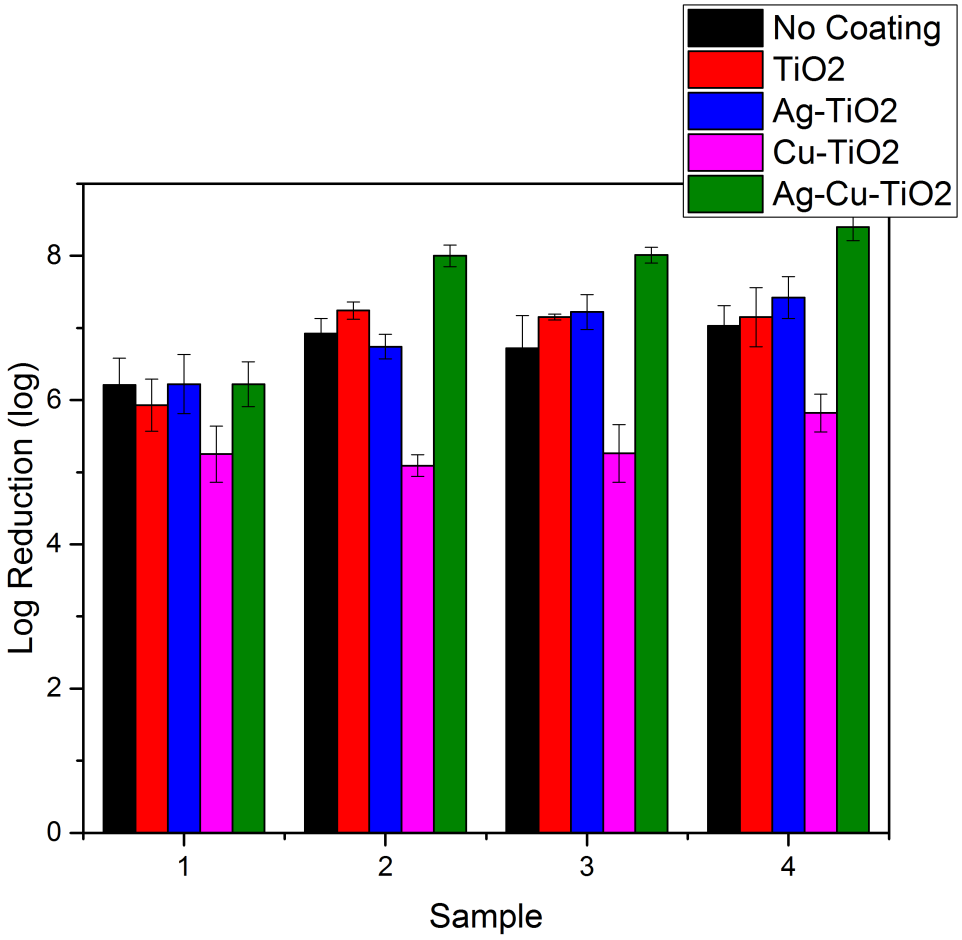

Figure 24: Inactivation of *E. coli* for no coating, TiO_2, Ag-TiO_2, Cu-TiO_2, and Ag-Cu-TiO_2 membranes under light conditions.

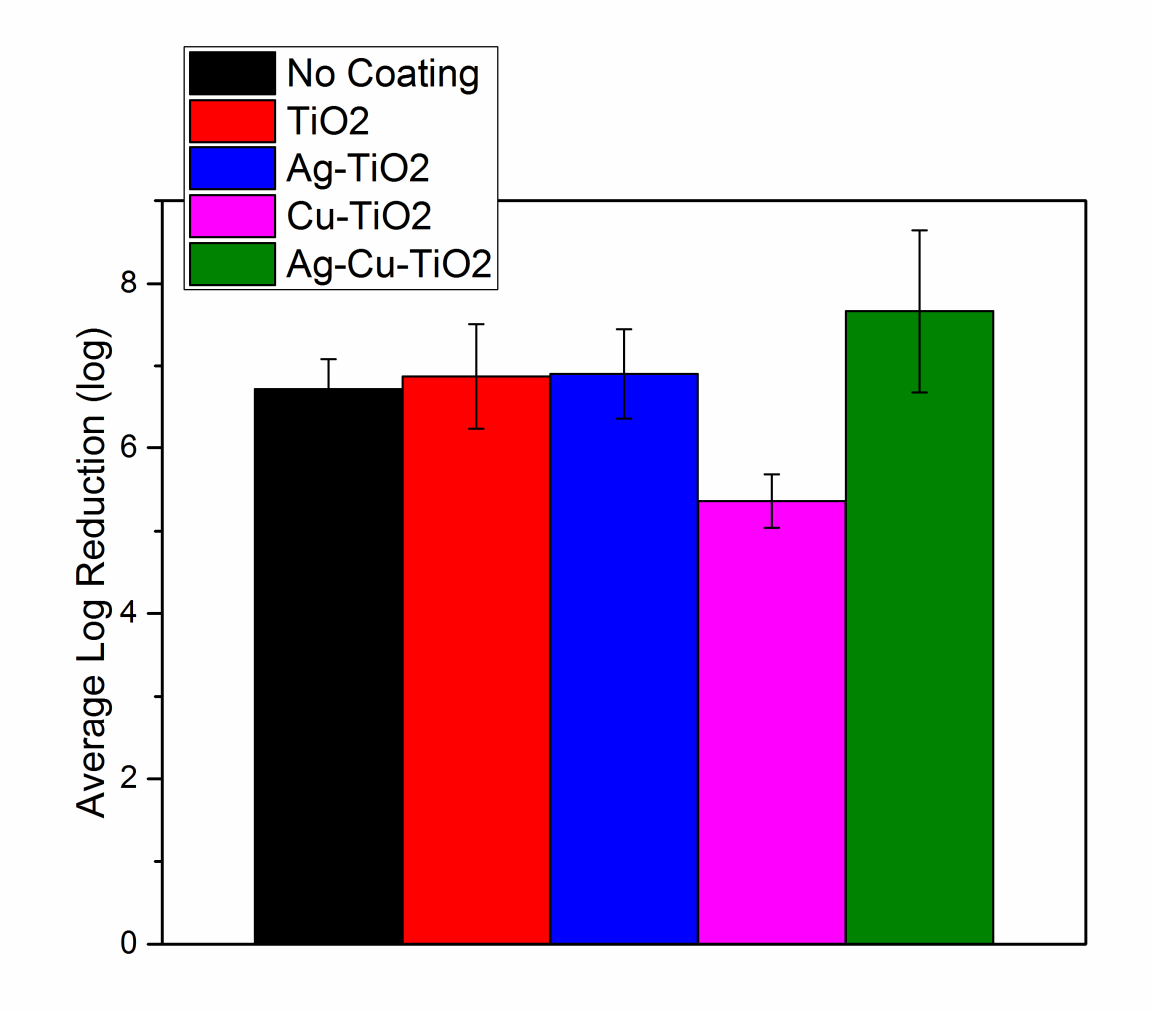

Figure 25: The average inactivation of *E. coli* for no coating, TiO_2, Ag-TiO_2, Cu-TiO_2, and Ag-Cu-TiO_2 membranes under light conditions.

Table 6: The average inactivation of *E. coli* under both light and dark conditions.

Coating Type	Sample				Avg	St Dev
	1	2	3	4		
No Coating, dark	0.87	0.68	0.54	0.42	0.63	0.19
No Coating, light	6.21	6.92	6.72	7.03	6.72	0.36
TiO2, dark	1.00	0.80	0.73	0.41	0.74	0.25
TiO2, light	5.93	7.24	7.15	7.15	6.87	0.63
Ag-TiO2, dark	1.86	0.64	0.47	0.34	0.83	0.70
Ag-TiO2, light	6.22	6.74	7.22	7.42	6.90	0.54
CuTiO2, dark	0.55	0.37	0.30	0.27	0.37	0.12
CuTiO2, light	5.25	5.09	5.26	5.82	5.36	0.32
Ag-Cu-TiO2, dark	1.61	0.90	0.99	1.60	1.28	0.38
Ag-Cu-TiO2, light	6.22	8.00	8.01	8.40	7.66	0.98

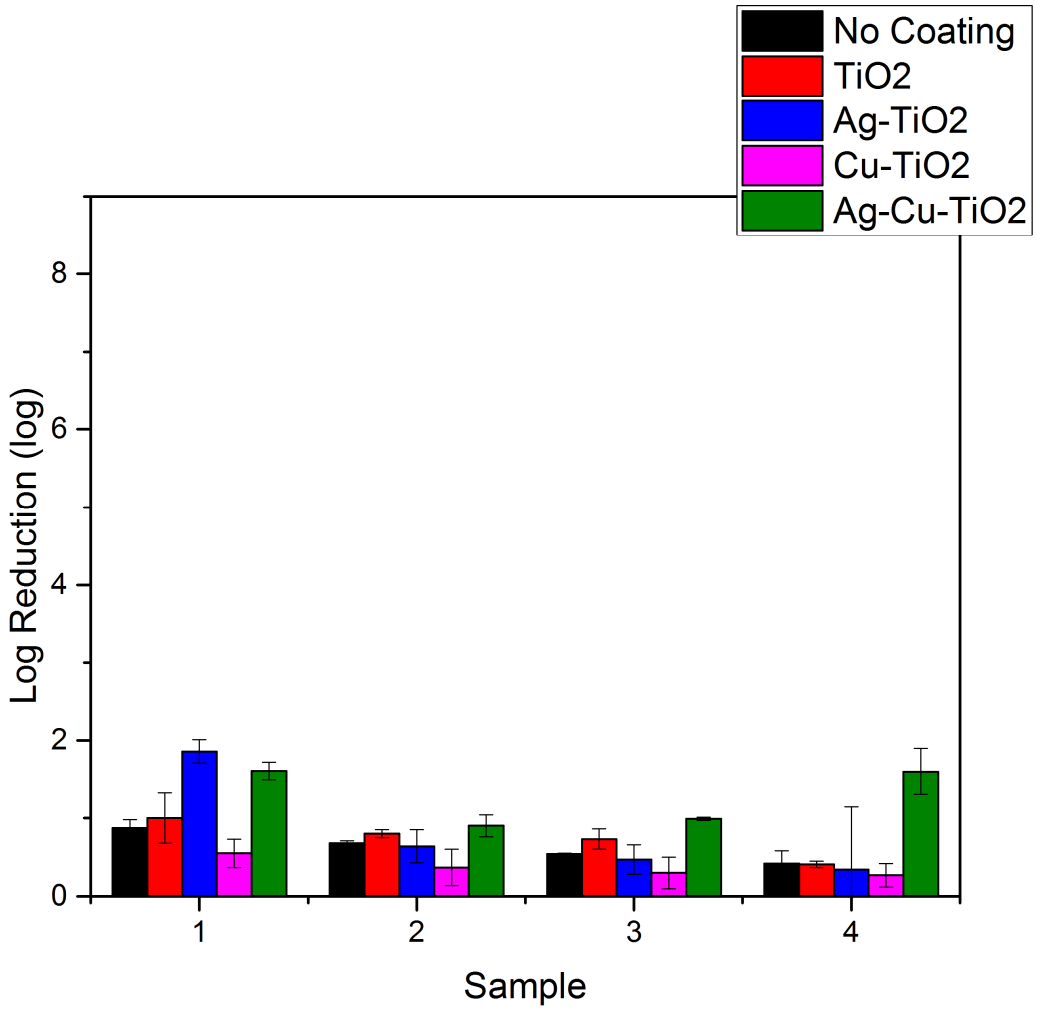

Figure 26: Inactivation of *E. coli* for no coating, TiO_2, Ag-TiO_2, Cu-TiO_2, and Ag-Cu-TiO_2 membranes under dark conditions.

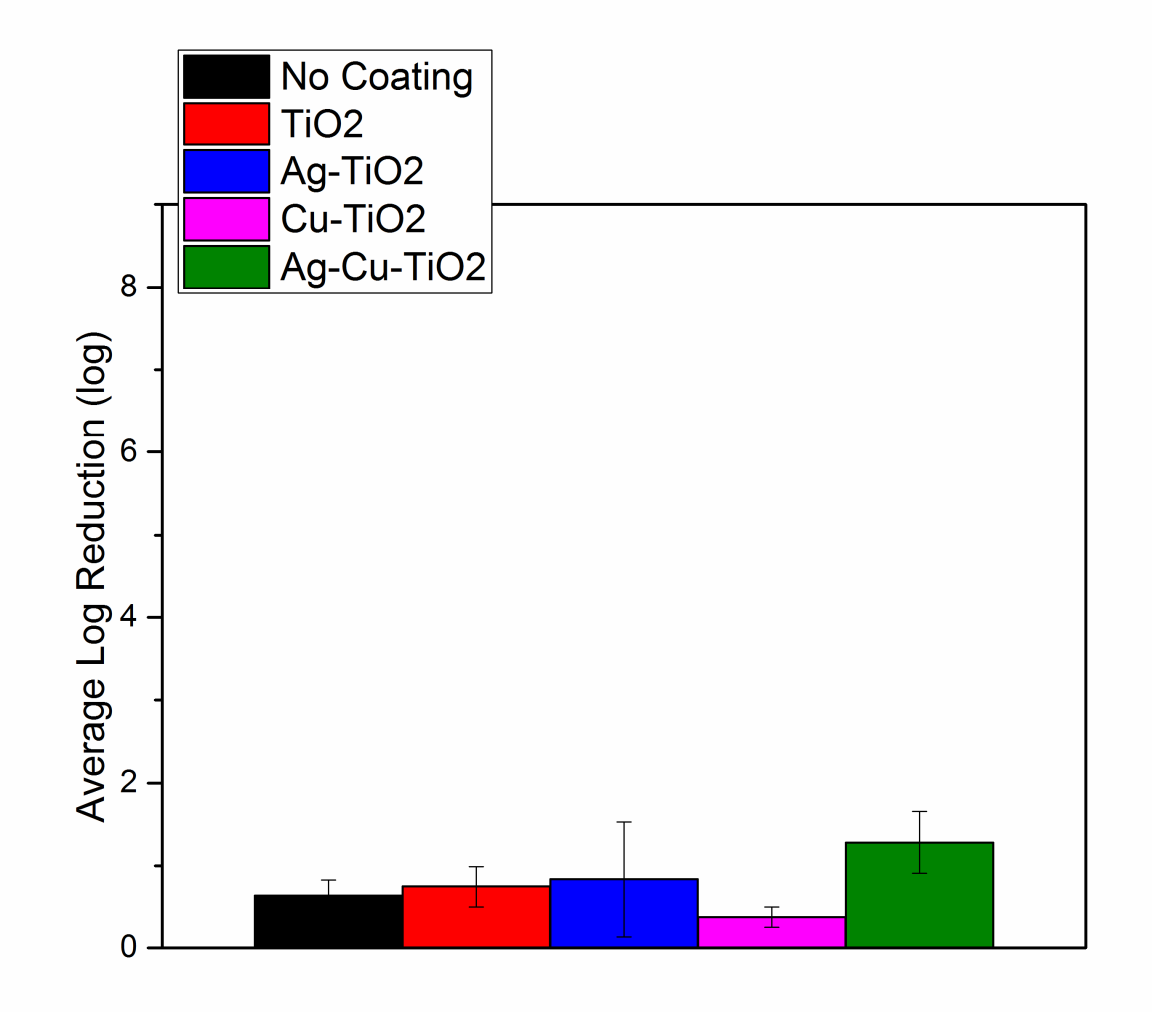

Figure 27: The average inactivation of E. coli for no coating, TiO_2, Ag-TiO_2, Cu-TiO_2, and Ag-Cu-TiO_2 membranes under dark conditions.

The virus experiments performed with UV light, UV irradiation, TiO_2, Ag-TiO_2, and Cu-TiO_2 exhibited decent virucidal inactivation while the co-impregnation of Ag-Cu-TiO_2 enhanced the virus inactivation (Figure 28). The increased virucidal inactivation by the Ag-Cu-TiO_2 membrane was attributed to an increase in ROS generation, and the increase in virucidal inactivation at samples three and four is attributed to death from the antibacterial effects of silver and copper ions. Overall, on average UV illumination was able to inactivate 2.89±0.17 logs of viruses, TiO_2 was able to inactivate 2.98±0.05 logs of

viruses, Ag-TiO_2 was able to inactivate 3.17±0.31 logs of viruses, Cu-TiO_2 was able to inactivate 3.15±0.53 logs of bacteria, and Ag-Cu-TiO_2 was able to inactivate 3.48±0.37 logs of bacteria (Figure 29 and Table 7). The improved log reduction for Cu-TiO_2 of viruses as opposed to bacteria suggests that bacteriophage MS2 may be more susceptible to copper ion inactivation than *E. coli* is.

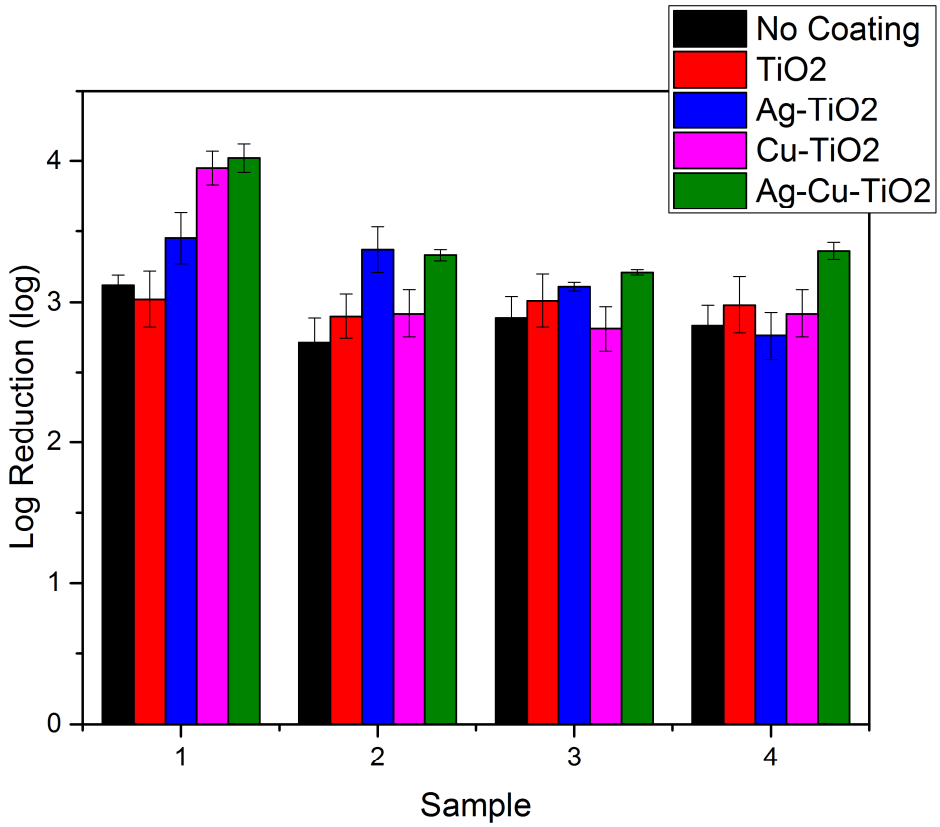

Figure 28: Inactivation of bacteriophage MS2 for no coating, TiO_2, Ag-TiO_2, Cu-TiO_2, and Ag-Cu-TiO_2 membranes under light conditions.

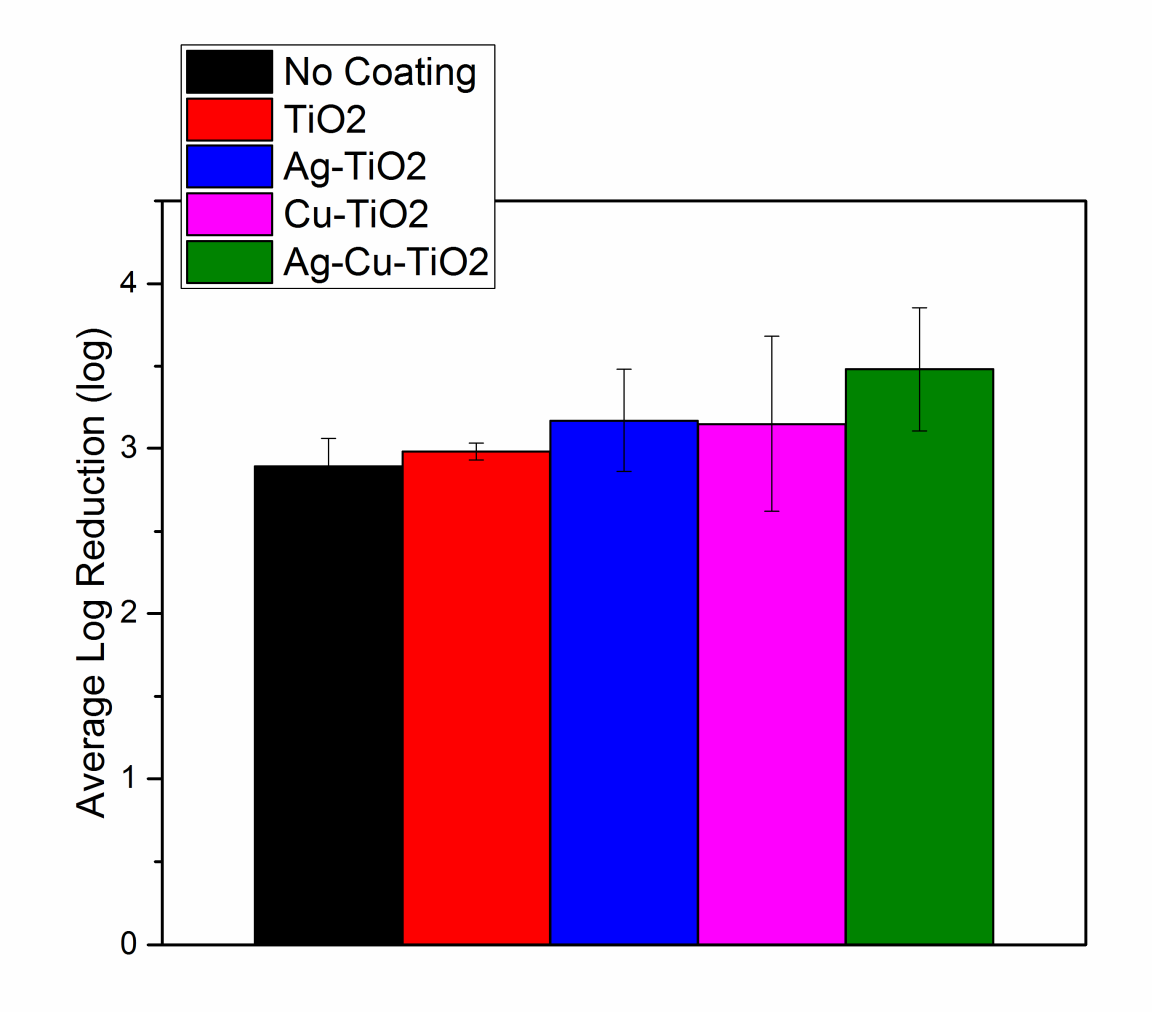

Figure 29: The average inactivation of bacteriophage MS2 for no coating, TiO_2, Ag-TiO_2, Cu-TiO_2, and Ag-Cu-TiO_2 membranes under light conditions.

For the virus experiments performed under dark conditions, very little virucidal inactivation was observed. Ag-Cu-TiO_2 membranes observed the largest inactivation of viruses at 0.48±0.12 log removal, followed by Ag-TiO_2 membranes at 0.25±0.04 log removal (Figure 30). An uncoated membrane, TiO_2, and Cu-TiO_2 all observed similar inactivation results of 0.14±0.08 log, 0.13±0.04 log, and 0.14±0.06 log removal, respectively (Figure 31 and Table 7).

Table 7: The average inactivation of bacteriophage MS2 under both light and dark conditions.

Coating Type	Sample				Avg	St Dev
	1	2	3	4		
No Coating, dark	0.24	0.11	0.15	0.05	0.14	0.08
No Coating, light	3.12	2.71	2.89	2.83	2.89	0.17
TiO2, dark	0.12	0.09	0.12	0.19	0.13	0.04
TiO2, light	3.02	2.90	3.01	2.98	2.98	0.05
Ag-TiO2, dark	0.25	0.29	0.25	0.20	0.25	0.04
Ag-TiO2, light	3.45	3.37	3.11	2.76	3.17	0.31
CuTiO2, dark	0.24	0.10	0.12	0.12	0.14	0.06
CuTiO2, light	3.95	2.92	2.81	2.92	3.15	0.53
Ag-Cu-TiO2, dark	0.43	0.33	0.61	0.53	0.48	0.12
Ag-Cu-TiO2, light	4.02	3.33	3.21	3.36	3.48	0.37

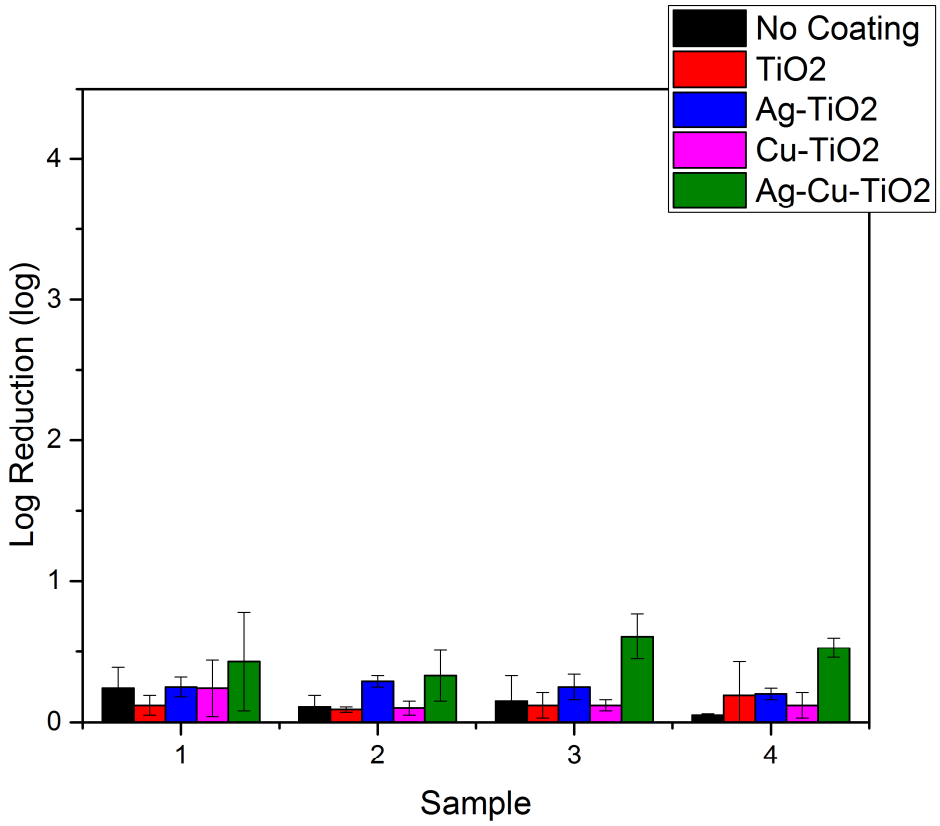

Figure 30: Inactivation of bacteriophage MS2 for no coating, TiO_2, Ag-TiO_2, Cu-TiO_2, and Ag-Cu-TiO_2 membranes under dark conditions.

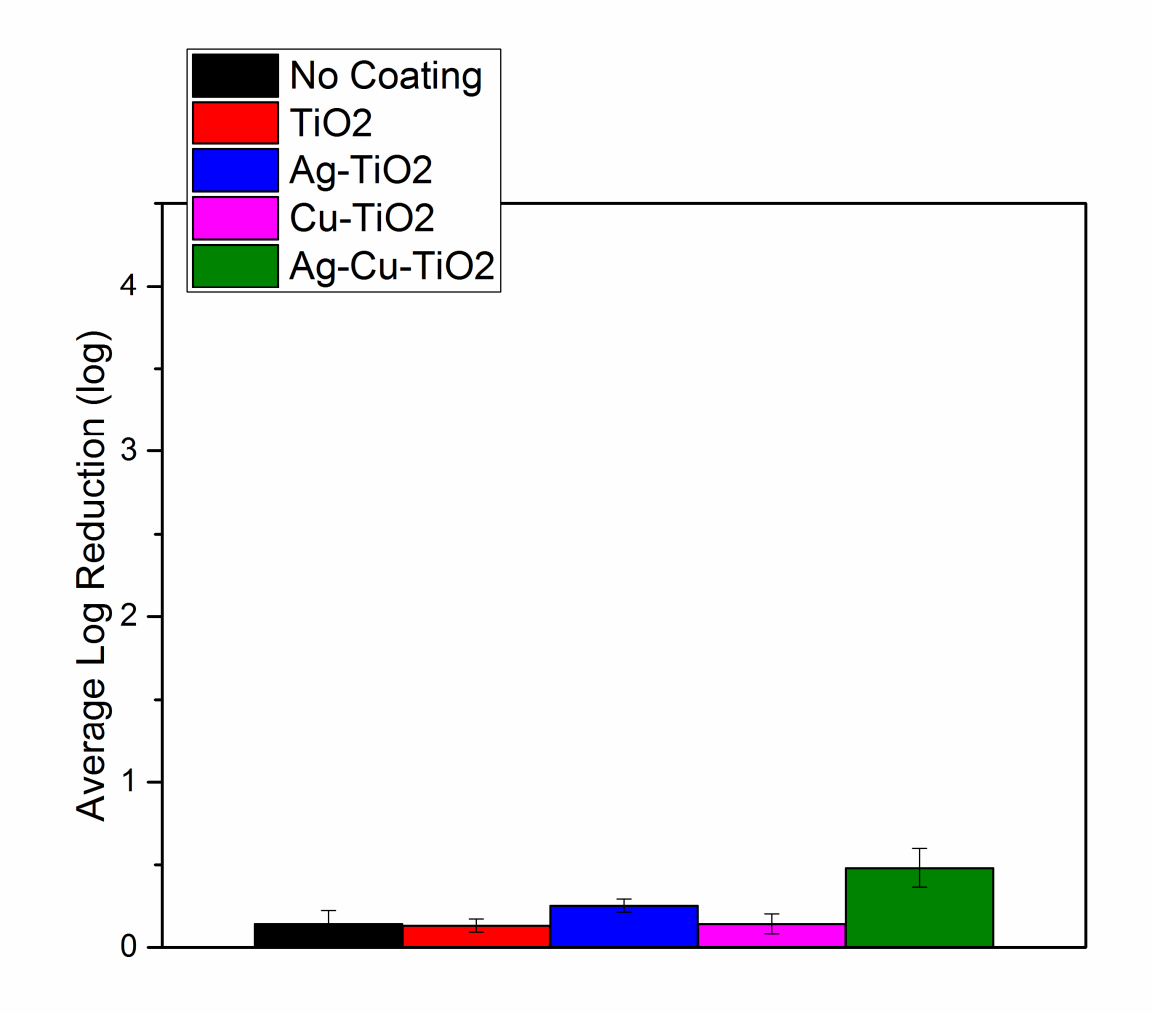

Figure 31: The average inactivation of bacteriophage MS2 for no coating, TiO_2, Ag-TiO_2, Cu-TiO_2, and Ag-Cu-TiO_2 membranes under dark conditions.

The vast majority of studies quoted in literature have been carried out using suspensions of titanium dioxide in water which were irradiated with light in the UV-A region of the electromagnetic spectrum, *i.e.* 320 – 380 nm. In a photocatalytic reactor, UV-A illumination is usually provided by fluorescent low-pressure mercury lamps which emit low-intensity UV-A light. Medium pressure mercury lamps have also been utilized

which emit high intensity UV light in the short, medium, and long UV regions of the electromagnetic spectrum. UV-C radiation in a photocatalytic reactor can be provided either by low-pressure mercury lamps, which emit low-intensity radiation focused at 254 nm, or by medium/high pressure mercury lamps enclosed in quartz tubes which emit high intensity illumination in the UV-A, UV-B, and UV-C regions of the electromagnetic spectrum.

To check the effect of radiation wavelength on the removal rate of bacteriophage MS2, a comparison study between illumination at 254 nm and 365 nm was carried out for an uncoated membrane and a membrane coated with Ag-Cu-TiO_2. Only bacteriophage MS2 was used in these experiments as it is more resistant to UV light than bacteria and is a good indicator microorganism for distinguishing between the effects of UV light and photocatalysis. For the light and dark experiments, the disinfection effect due to photocatalysis is dominated partially by the 254 nm wavelength used. With a 365 nm UV lamp (λ = 365 nm, UVP LLC, Upland, CA, USA), the uncoated membrane removed on average 0.45 log MS2, whereas the Ag-Cu-TiO_2 coated membrane removed 1.19 log MS2.

As one may suspect, it is easier to see the effect of photocatalytic activity on the removal of viruses with the Ag-Cu-TiO_2 coated membrane at 365 nm than at 254 nm. At radiation wavelengths higher than 300 nm, the disinfection of microorganisms is carried out solely by photocatalysis rather than through UV-C disinfection. The difference between the virus removal of the Ag-Cu-TiO_2 membrane and the uncoated membrane is 0.74 logs, similar to the difference between the two membranes under 254 nm light which

would indicate that the removal of viruses reported in Table 7 is achieved primarily through the use of photocatalysis (Figure 32).

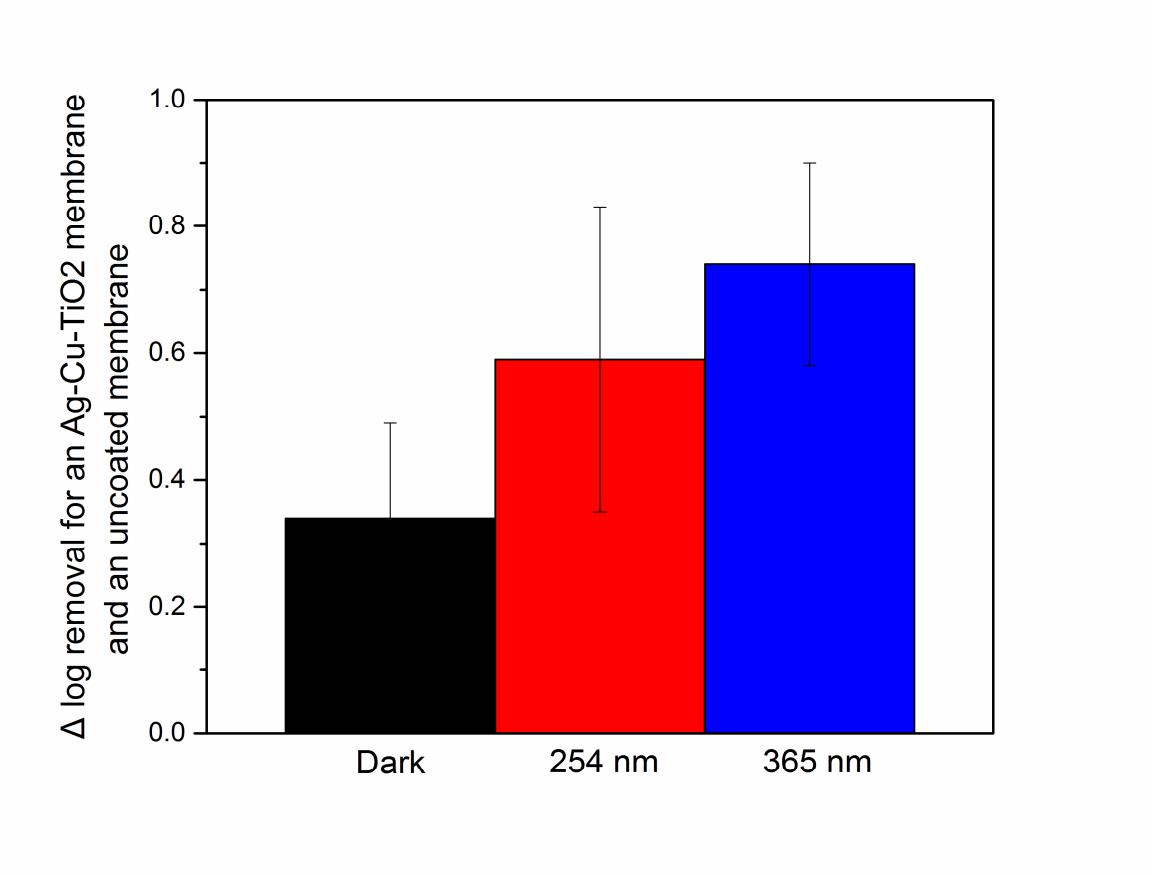

Figure 32: The difference between average log bacteriophage MS2 removal for an uncoated membrane and a Ag-Cu-TiO_2 coated membrane under dark, 254 nm, and 365 nm conditions.

Unfortunately, the photoactivity of the Ag-Cu-TiO_2 membrane is not enough on its own to achieve the level of disinfection required to be considered a microbiological purifier under NSF/ANSI P231, a standard which requires a 4 log removal of viruses. Therefore, it is ideal to pair the Ag-Cu-TiO_2 light with a conventional UV lamp operating at 254 nm (11W, Phillips). The photoactivity of the Ag-Cu-TiO_2 membrane works in

synergy with the 254 nm UV light and the silver copper ions coming off the membrane to achieve a higher log removal of viruses than if one were to rely on UV-C light alone.

5.2.3 Effect of Free Heavy Metals on Bacteria and Virus Removal

In order to isolate the effect of free heavy metal ions in the water on the bacteria and virus removal, the challenge water effluent was saved and tested for its heavy metal content. Water from each Ag-TiO_2 membrane experiment was tested in the dark for its silver ion content using Inductively Coupled Plasma Mass Spectrometry (ICP-MS) (7700ce, Agilent Technologies, Santa Clara, CA, USA) and the amount of free heavy metal ions in the water was compared against the bacteria and virus reduction in the dark (Figure 33).

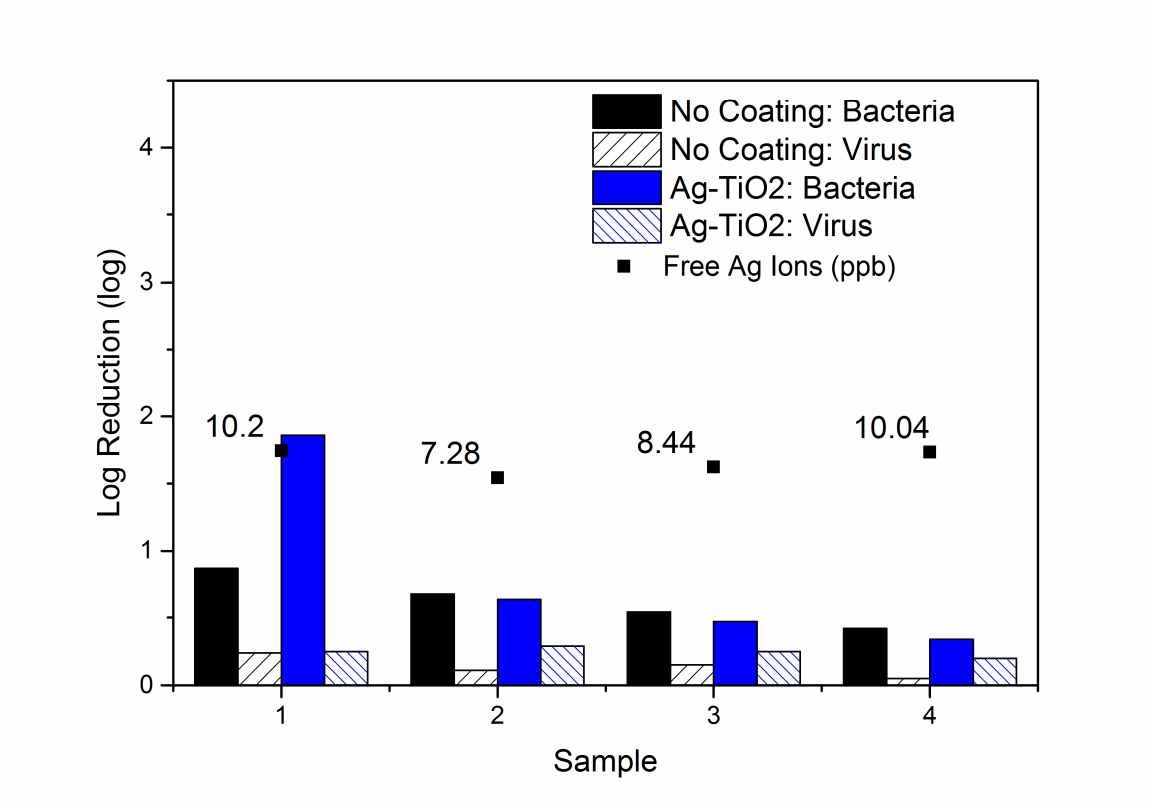

Figure 33: Concentration of free silver ions from the Ag-TiO_2 membranes and the bacteria and virus removal in dark conditions for blank, uncoated discs as well as Ag-TiO_2 discs.

Initially, a 1.86 log reduction of bacteria is observed with the Ag-TiO_2 membrane, versus a 0.87 log reduction of bacteria for an uncoated, or blank, membrane. While a slight increase in the reduction of bacteria for the Ag-TiO_2 membrane could be attributed to a decrease in pore size, the decrease in pore size isn't enough to warrant a 1 log increase in reduction. This reduction of bacteria can therefore likely be attributed to the initial average 10.2 ppb concentration of silver ions found in the effluent of the dark experiments using an Ag-TiO_2 disc. As no increase in reduction was observed for the virus, it's unlikely that the free silver ions in the water had much effect on them.

The membranes coated with Cu-TiO_2 observed no improvement in bactericidal reduction during dark experiments as compared against blank, uncoated fiberglass membranes (Figure 34). The concentration of copper ions coming off of the Cu-TiO_2 membranes at the beginning of dark experiments was 41 ppb and an initial bacteria reduction of 0.55 logs is observed; however, the amount of bacteria inactivated by the Cu-TiO_2 under dark conditions as compared to an uncoated membrane is significantly less which indicates that the copper ions may have been beneficial to the health of the *E. coli*. Copper is an essential trace element necessary to the health of microorganisms. It has the ability to be incorporated into a variety of essential metabolic proteins and metalloenzymes, stimulating the immune system to fight infections, repair injured tissues, and promote healing [54,78]. In the case of the Cu-TiO_2 coated membrane, the free copper ions in the water may have been used to repair any damage caused by ROS. This would seem to indicate that in order to have a significant decrease in the amount of bacteria from free copper ions alone, a larger quantity of copper is required.

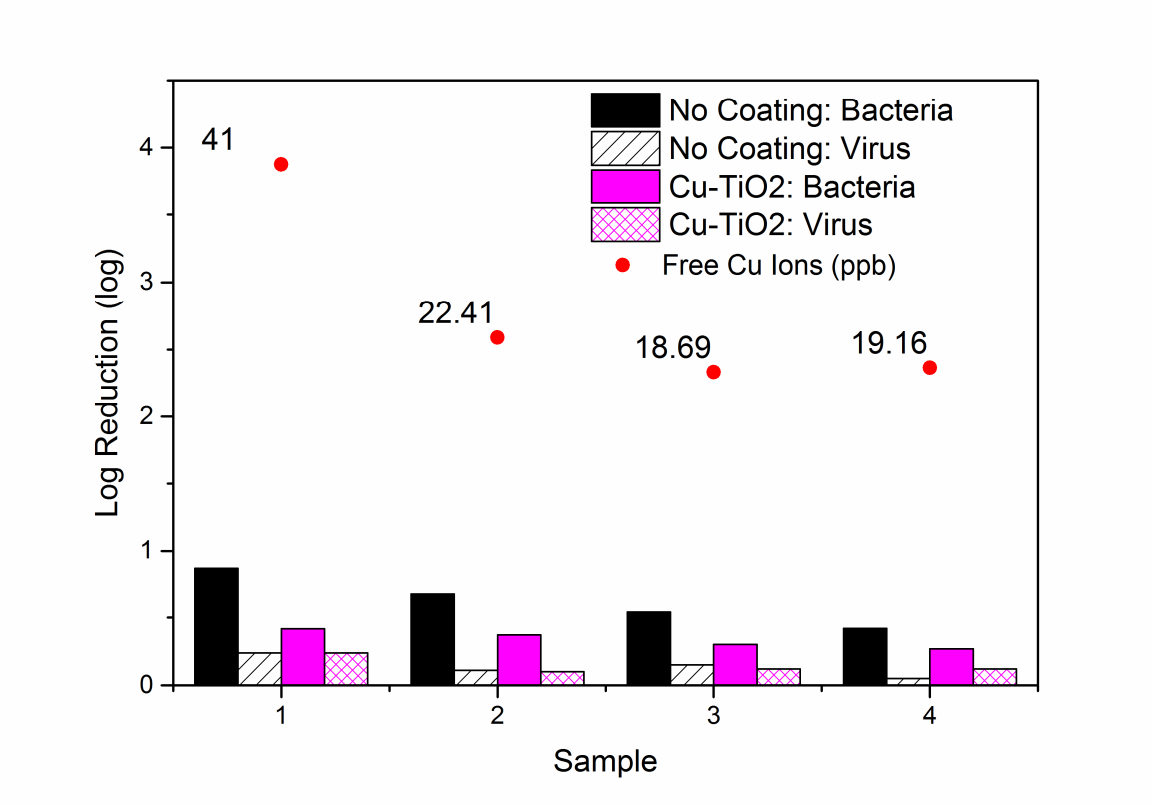

Figure 34: Concentration of free copper ions from the Cu-TiO_2 membranes and the bacteria and virus removal in dark conditions for blank, uncoated discs as well as Cu-TiO_2 discs.

Interestingly, while the concentration of copper coming off of the membrane is higher initially before decreasing over time, the reduction of bacteria over time stays fairly constant. This could indicate that the bacteria were being removed through mechanical filtration and the removal was unrelated to the amount of free copper ions. Similar to the Ag-TiO_2 coated membranes, no improvement in virus reduction is observed for the dark experiments.

In the case of the Ag-Cu-TiO_2 membranes, the bacteria reduction over time slowly trends upwards. Initially, a 1.61 log reduction in bacteria is observed before it drops down to 0.9 logs at the second sample, then up to 0.99 logs at the third sample, before

again reaching a 1.60 log reduction at the fourth sample (Figure 35). This could indicate that the interaction of silver and copper ions together took a little bit of time to reach a steady state of removal.

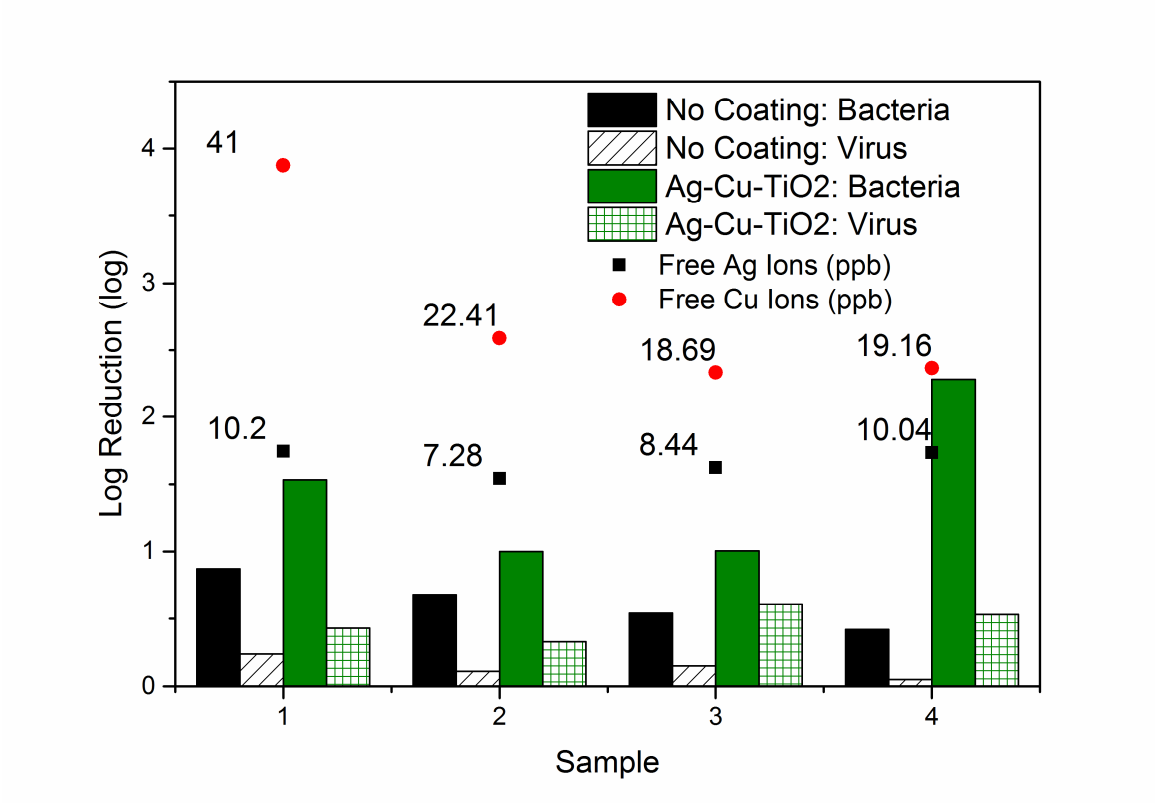

Figure 35: Concentration of free silver and copper ions from the Ag-Cu-TiO_2 membranes and the bacteria and virus removal in dark conditions for blank, uncoated discs as well as Ag-Cu-TiO_2 discs.

For the Ag-Cu-TiO_2 coated membranes, the amount of silver and copper coming off of the membrane is high initially, at 10.2 ppb for silver and 41 ppb for copper, before decreasing over time. This synergistic effect of photocatalysis and free heavy metal ions is augmented further, in the case of the disinfection of *E. coli* and bacteriophage MS2.

In order to check that the amount of free silver and copper ions coming off the membrane would not deleteriously affect the performance of the membrane, the amount

of free ions coming off the membrane was analyzed over a ten hour period. Samples were collected every twenty minutes and analyzed through ICP-MS. Over a ten hour period, the silver ions coming off the membrane decreased the concentration of silver ions by 0.16% and the amount of copper ions coming off the membrane decreased the concentration of copper by 0.02% (Figure 36). At this rate, the membranes would foul prior to the concentration of concentration of silver and copper being completely depleted.

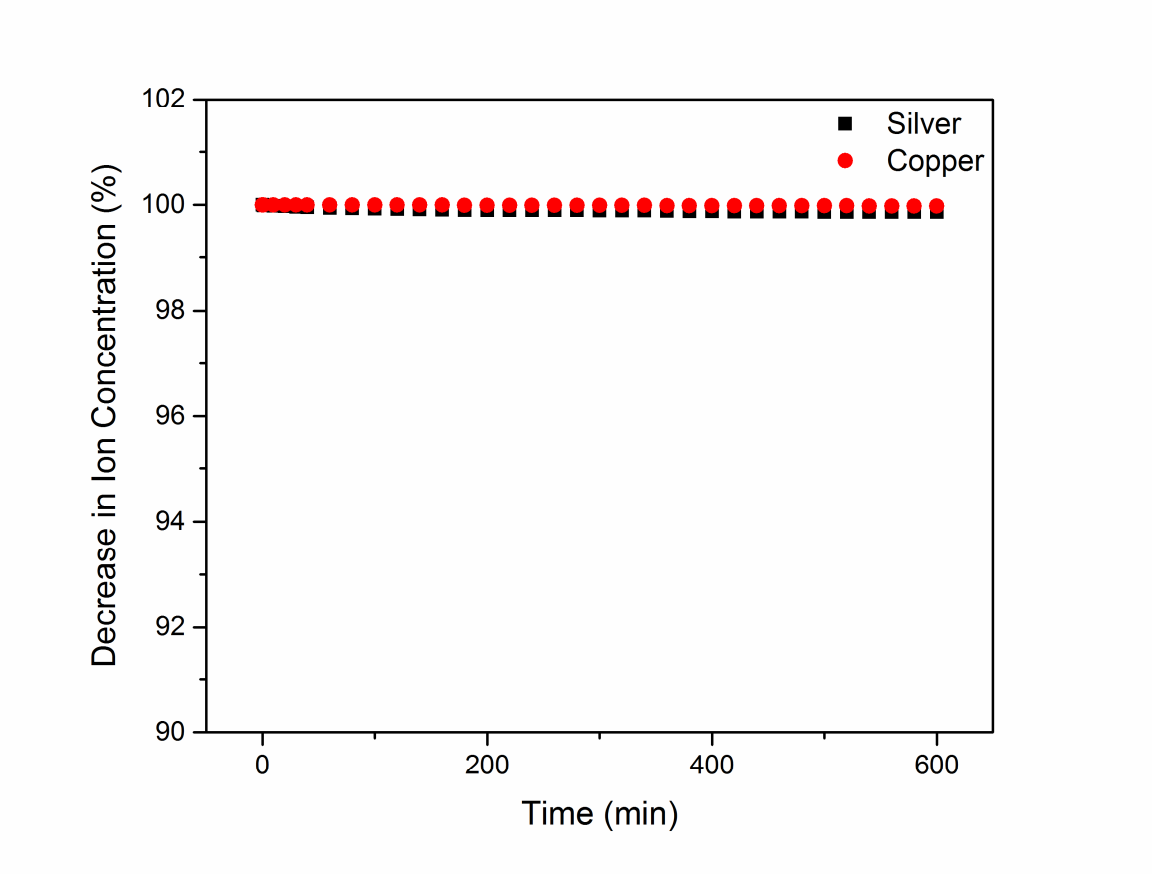

Figure 36: Decrease in ion concentration from an Ag-Cu-TiO_2 membrane over a 10 hour time period.

Due to the results obtained thus far, it is possible to speculate as to the bactericidal process for the inactivation of *E. coli* through Ag-Cu-TiO_2 coated membranes (Figure 37). The first step is a period in which the outer membrane is attacked by the hydroxyl radicals generated by the photocatalytic process and free silver and copper ion species in the water. The cell wall is weakened, and eventually penetrated. As the hydroxyl radicals and free ion species are taken into the cell, oxidative stress begins to occur. The hydroxyl radicals along with the light from UV-C lamp begin to attack the DNA, breaking it apart. The silver and copper ions go after the iron-sulfur protein clusters, with the silver and copper binding to the sulfur displacing the iron into the cell and causing more oxidative stress [59,60]. Eventually, the damage to cell wall and cytoplasmic membrane will cause the cytoplasm to leak out of the bacteria and it will be unable to replicate.

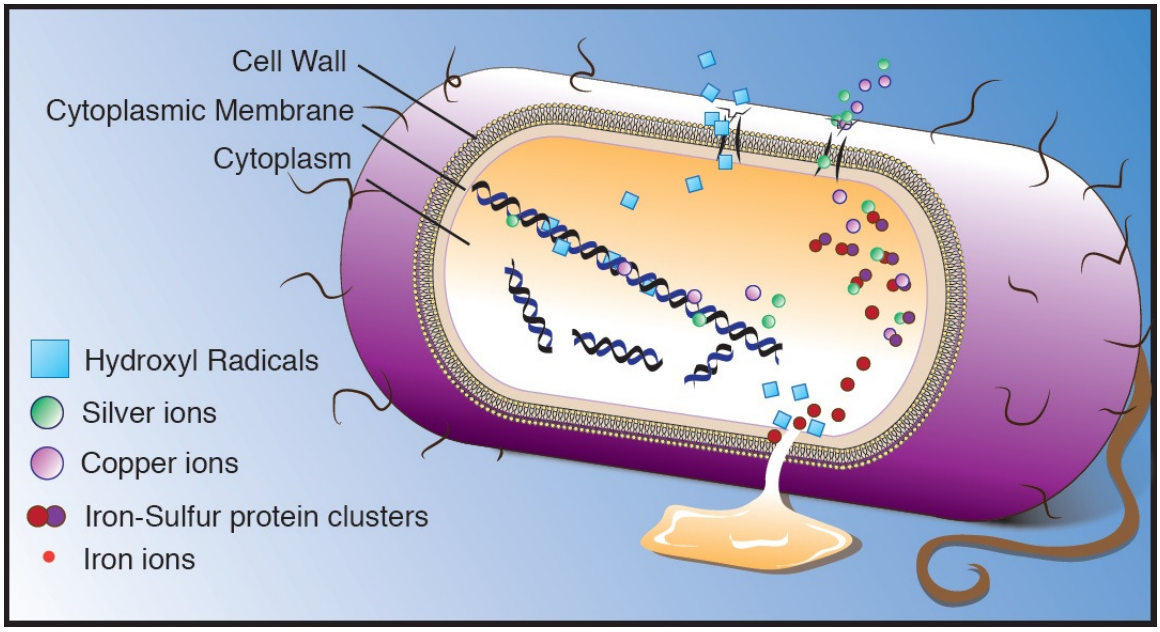

Figure 37: The proposed combined effects of hydroxyl radicals, free copper and silver ions, and UV-C light on bacteria.

Together, the combined effects of the UV-C light, the hydroxyl radicals generated during the photocatalytic process, and the free copper and silver ions in the water cause a trifecta of inactivation methods which are incredibly effecting at disinfecting water of bacteria. These multiple modes of inactivation make it incredibly difficult for the bacteria cell to keep up with the repair, eventually leading to cell death.

5.2.4 Statistical Analysis

Comparisons of the disinfection efficiency induced under both light and dark conditions were analyzed using a *t test* to determine if the Ag-Cu-TiO_2 coated membrane's performance was statistically different from the uncoated membrane.

For bacteria, the proposed statistical hypothesis was:

$$H_0: \mu = 6.72 \; and \; H_1: \mu > 6.72$$

For virus, the proposed statistical hypothesis was:

$$H_0: \mu = 2.89 \; and \; H_1: \mu > 2.89$$

Both of these statistical hypotheses were tested at the 80% level of significance, or $\alpha = 0.10$. The t value was calculated by subtracting the hypothesized population mean from the sample mean and dividing it by the sample standard deviation divided by the square root of the sample size:

$$t = \frac{\bar{X} - \mu}{s/\sqrt{n}}$$

where $\bar{X}$ is the sample mean, μ is the hypothesized population mean, *s* is the sample standard deviation, and *n* is the sample size.

For bacteria the test value was determined to be:

$$t = \frac{\bar{X} - \mu}{s/\sqrt{n}} = \frac{7.66 - 6.72}{0.98/\sqrt{4}} = 1.92$$

The critical value is 1.64 for α = 0.10 and the degrees of freedom = 3. Since 1.92 is greater than 1.62, the null hypothesis for bacteria is rejected. The bacteria inactivation for an Ag-Cu-TiO_2 membrane is statistically different from an uncoated membrane.

For virus the test value was determined to be:

$$t = \frac{\bar{X} - \mu}{s/\sqrt{n}} = \frac{3.48 - 2.89}{0.37/\sqrt{4}} = 3.24$$

The critical value is 1.64 for α = 0.10 and the degrees of freedom = 3. Since 3.24 is greater than 1.62, the null hypothesis for virus is rejected. The virus inactivation for a Ag-Cu-TiO_2 membrane is statistically different from a membrane with no coating.

5.2.5 Increased Flow Rate

In order to verify the performance of the membrane at increased flow rates, experiments were conducted that evaluated the log inactivation at a 2X flow rate increase and a 4X flow rate increase. The performance of an uncoated membrane was evaluated against that of a silver-copper-titanium dioxide membrane under light conditions with both bacteria and virus.

For the experiments conducted using bacteria (Figure 38), the bacteria inactivation decreased as the flow rate increased. This decrease occurred in an almost linear manner for both the uncoated membrane and the silver-copper-titanium dioxide coated membrane. At a 2X flow increase, the bacteria inactivation decreased by 1.5 logs for a Ag-Cu-TiO_2 membrane and with a 4X flow increase the bacteria inactivation decreased further by 1.6 logs as compared to the initial flow rate.

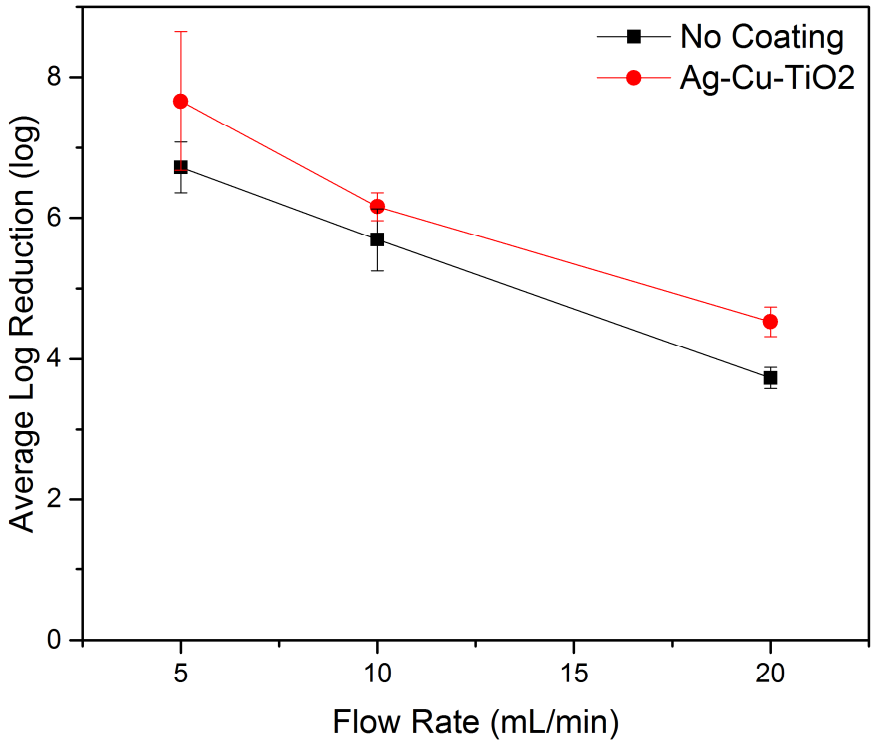

Figure 38: Bacteria inactivation of an uncoated membrane and an Ag-Cu-TiO_2 coated membrane at varying flow rates.

For the experiments conducted using virus (Figure 39), the virus inactivation decreased sharply when the flow rate was increased 2X before slowly tapering off as the

flow rate was increased to 4X the initial flow rate. When the flow rate was doubled, the bacteriophage MS2 inactivation decreased by 1.8 logs for a Ag-Cu-TiO_2 coated membrane and when the flow rate quadrupled the inactivation decreased by another 0.8 logs.

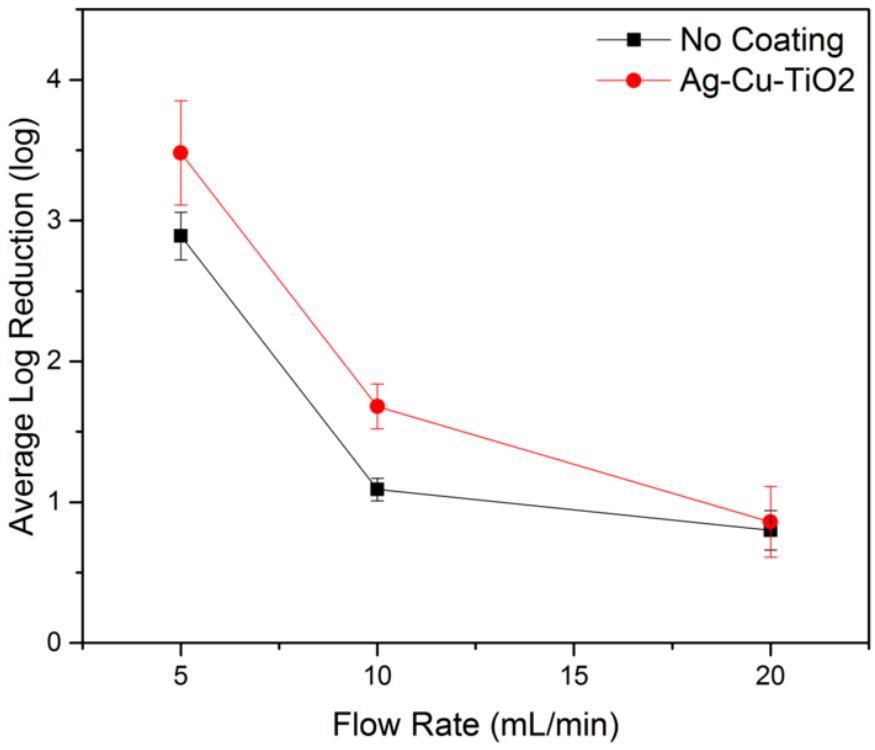

Figure 39: Bacteriophage MS2 inactivation of an uncoated membrane and an Ag-Cu-TiO_2 coated membrane at varying flow rates.

These results demonstrate that while the bacteria are able to withstand an increase in flow rate, significant virus inactivation at increased flow rates is harder to achieve. As the increase in flow rate shortened the contact time of the bacteriophage MS2 with the

photocatalytic coating, it may show that the virus requires a longer contact time to be inactivated through hydroxyl radicals as compared with bacteria.

5.2.6 Decreased Copper to TiO_2 Atomic Ratio

The atomic ratio of copper to TiO_2 was higher than anticipated, nearly four times higher than the targeted 5% solution. As the results reported in Sections 5.2.2 Removal of Bacteria and Virus and Section were completed using a 17% copper to TiO_2 atomic ratio, the experiments were repeated using membranes with a 3% copper to TiO_2 atomic ratio.

When the amount of copper to TiO_2 atomic ratio was decreased and the membranes were challenged with bacteria under light conditions, the 3%Cu-TiO_2 inactivation rate for bacteria also decreased as previously seen with the higher atomic ratio coated membranes (Figure 40). However, the average inactivation for an Ag-3%Cu-TiO_2 coated membrane challenged with bacteria stayed roughly the same as the higher amount, averaging 7.63 ± 0.20 logs.

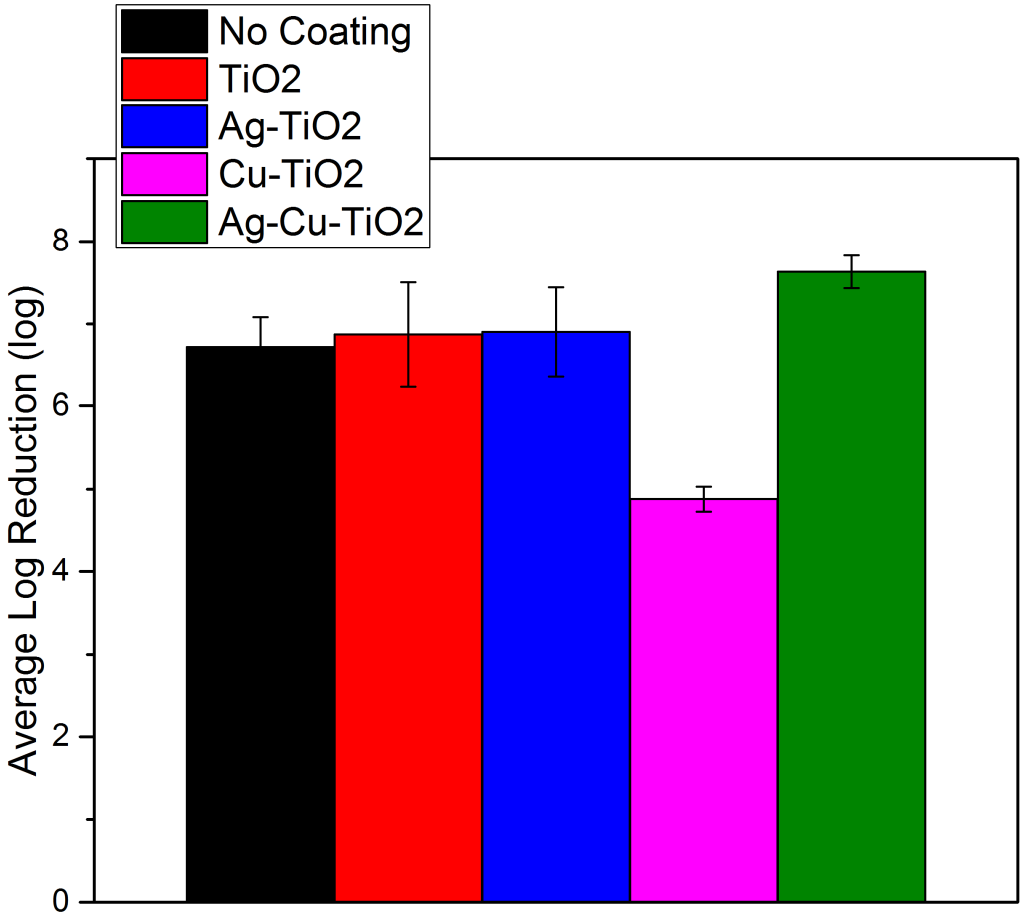

Figure 40: The average inactivation of *E. coli* for no coating, TiO_2, Ag-TiO_2, 3%Cu-TiO_2, and Ag-3%Cu-TiO_2 membranes under light conditions.

When the same membranes were challenged with bacteriophage MS2, there was little discernable difference between the performance of the Cu-TiO_2 membranes from Section 5.2.2 Removal of Bacteria and Viruses, and the new 3%Cu-TiO_2 membranes. However, the performance of the Ag-3%Cu-TiO_2 membranes improved significantly, averaging an inactivation rate of 4.22 ± 0.14 logs (Figure 41). This enhanced inactivation of viruses, microorganisms which are less susceptible to inactivation due to 254 nm UV-

C light, can be attributed to an improvement in photocatalysis with the lower copper to TiO_2 atomic ratio.

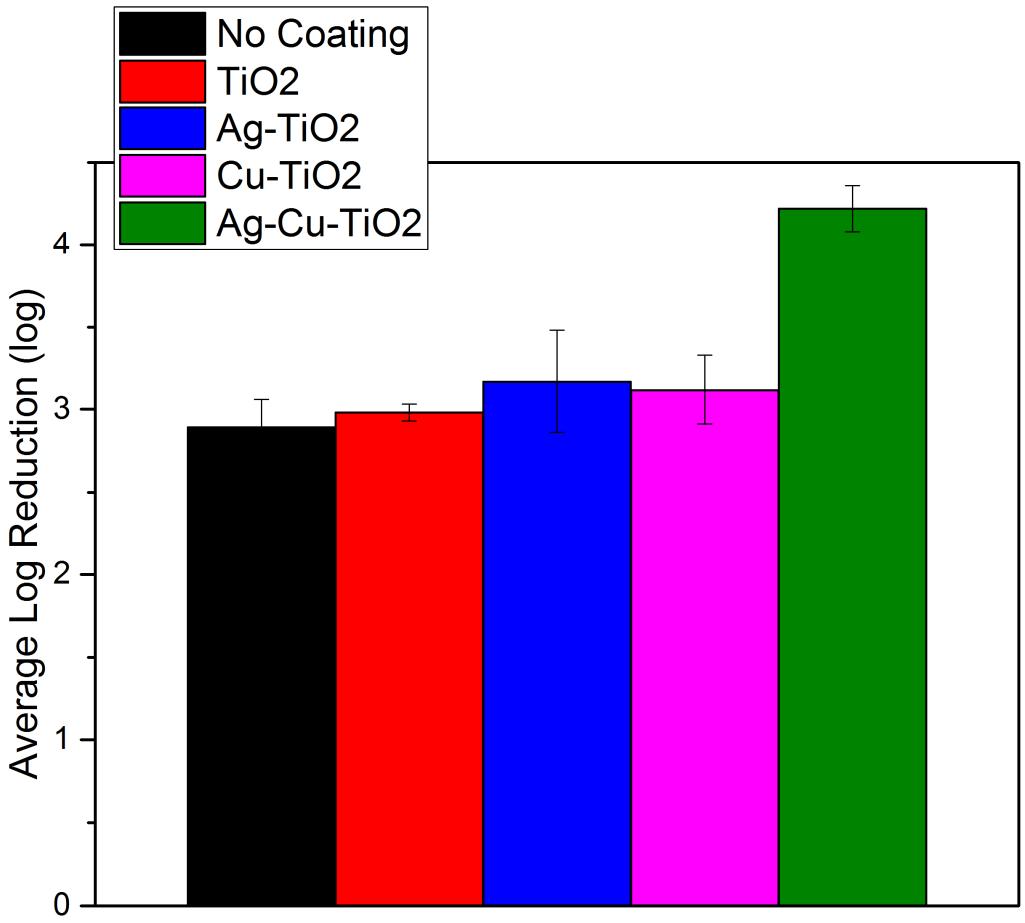

Figure 41: The average inactivation of bacteriophage MS2 for no coating, TiO_2, Ag-TiO_2, 3%Cu-TiO_2, and Ag-3%Cu-TiO_2 membranes under light conditions.

5.2.7 Perspective

These results have shown that a silver-copper doped titanium dioxide membrane can be effective for removing bacteria and viruses from drinking water. The use of a 254 nm light in conjunction with the coated membrane provides the additional benefit of

increased disinfection over a more conventional 365 nm light. As a proof of concept, the membrane used in this study was not optimized in terms of configuration and operation; the photocatalytic coating can be further improved, and thus the efficiency of disinfection at higher flow rates. A flat-sheet membrane may not be practical for use due to the small surface area, however, the Ag-Cu-TiO_2 nanowires can be applied to other substrates which may yield increased disinfection properties and be able to operate at higher flow rates.

As it stands today, there are three primary values of this technology over more conventional UV-C. Primarily, photocatalysis is a product differentiator within the water treatment market. In addition, the photocatalytic membranes will still disinfect the water if the power is off or while the UV-C light is warming up. Lastly, the photocatalytic membrane should reduce bacteria growth on itself due to the use of biostatic silver and copper. There are challenges such as cost, the manufacturing process, and the durability of the membrane but these can be overcome in time.

5.3 Conclusion

This study demonstrated that silver and copper modified titanium dioxide for bacteria and virus removal is a viable technique for meeting drinking water treatment standards of microbiological water purifiers. The Ag-Cu-TiO_2 coated membrane was able to achieve a 7.5 log reduction in bacteria and a 3.5 log reduction in viruses; exceeding the US EPA standard for bacteria inactivation and nearly meeting the standard for virus removal. The heavy metals released from the membrane reached a maximum amount of 10.2 ppb of silver and 41 ppb of copper; far below the US EPA MCL of 100 ppb for silver and 1000 ppb for copper.

CHAPTER 6: PERSPECTIVES

The work in this report has been seeking to address current challenges facing our drinking water supplies around the world. Water is a precious, natural resource that must be protected and once it's contaminated by various contaminants it's important to have remedies in place. Technologies such as microbial desalination cells seek to address the issue of removing cations such as sodium, calcium, and magnesium, and can also be applied to remove heavy metals. Through the development of photocatalysts, new methods of removing viruses and bacteria from drinking water without the creation of disinfection by-products are being explored.

As a proof of concept, the Ag-Cu-TiO_2 membrane used in Chapter 5 was not optimized in terms of configuration and operation; the photocatalytic coating can be further improved, and thus the efficiency of disinfection at higher flow rates. A flat-sheet membrane may not be practical for use due to the small surface area, however, the Ag-Cu-TiO_2 nanowires can be applied to other substrates which may yield increased disinfection properties and be able to operate at higher flow rates. Further scrutiny to the doping of silver and copper into the titanium dioxide lattice can also be completed in order to verify the ions are well integrated and that the right doping level is reached.

Awareness as to the occurrence of pharmaceuticals and personal care products (PPCPs) in drinking water is an emerging area of concern and interest. PPCPs represent a highly diverse collection of chemical substances, including prescription and over-the-counter drugs, veterinary drugs, vitamins, cosmetics, and other consumer products. The current effect of PPCPs on human health and the environment is not well known or

understood at this time, though it's likely that these substances may be regulated by the USEPA in the future. Techniques such as photocatalytic degradation have shown promising in terms of reducing the amount of organic compounds in drinking water and may prove useful for also reducing PPCPs. A membrane coated with Ag-Cu-TiO_2 could potentially achieve combined disinfection of viruses and bacteria from drinking water as well as help to reduce any organics or PPCPs present. Further work will seek to evaluate the use of Ag-Cu-TiO_2 coated membranes for the removal of common organics and pharmaceutical and personal care products present in drinking water.

REFERENCES

[1] F. Fiessinger, G. Thomas, R. King, Advances in Water Treatment and Environmental Management, Oxon: Taylor & Francis, 1990.

[2] L.S. Hager, ed., Water Treatment Membrane Processes, 1st ed., 1996.

[3] M. Christensen, ed., Microfiltration and Ultrafiltration Membranes for Drinking Water, American Water Works Association, Denver, Colorado, 2005.

[4] H. Strathmann, Ion-Exchange Membrane Processes in Water Treatment, Elsevier, 2010. doi:10.1016/S1871-2711(09)00206-2.

[5] R.A. Bergman, Membrane Softening Versus Lime Softening in Florida: A Cost Comparison Update, Desalination. 102 (1995) 11–24. doi:10.1016/0011-9164(95)00036-2.

[6] B. Jurenka, Lime Softening, 2010. http://www.usbr.gov/pmts/water/publications/primer.html.

[7] S. Ghizellaoui, A. Chibani, S. Ghizellaoui, Use of Nanofiltration for Partial Softening of Very Hard Water, Desalination. 179 (2005) 315–322. doi:10.1016/j.desal.2004.11.077.

[8] N. Kabay, M. Demircioglu, E. Ersoz, I. Kurucaovali, Removal of Calcium and Magnesium Hardness by Electrodialysis, Desalination. 149 (2002) 343–349. doi:10.1016/S0011-9164(02)00807-X.

[9] M.A. Tofighy, T. Mohammadi, M. Ahmadzadeh, Permanent Hard Water Softening Using Carbon Nanotube Sheets, Desalination. 268 (2011) 208–213. doi:10.1016/j.desal.2010.10.028.

[10] C. Gabrielli, G. Maurin, H. Francy-Chausson, P. Thery, T.T.M. Tran, M. Tlili, Electrochemical Water Softening: Principle and Application, Desalination. 201 (2006) 150–163. doi:10.1016/j.desal.2006.02.012.

[11] S.-J. Seo, H. Jeon, J.K. Lee, G.-Y. Kim, D. Park, H. Nojima, et al., Investigation on Removal of Hardness Ions by Capacitive Deionization (CDI) for Water Softening Applications., Water Res. 44 (2010) 2267–75. doi:10.1016/j.watres.2009.10.020.

[12] P. Čuda, P. Pospíšil, J. Tenglerová, Reverse osmosis in water treatment for boilers, Desalination. 198 (2006) 41–46. doi:10.1016/j.desal.2006.09.007.

[13] K. Betts, Using Microbes and Wastewater to Desalinate Water, Environ. Sci. Technol. 43 (2009) 6895. doi:10.1021/es901950j.

[14] I. Ieropoulos, J. Greenman, C. Melhuish, J. Hart, Comparative study of three types of microbial fuel cell, Enzyme Microb. Technol. 37 (2005) 238–245. doi:10.1016/j.enzmictec.2005.03.006.

[15] B.E. Logan, B. Hamelers, R. Rozendal, U. Schröder, J. Keller, S. Freguia, et al., Microbial fuel cells: methodology and technology., Environ. Sci. Technol. 40 (2006) 5181–92. http://www.ncbi.nlm.nih.gov/pubmed/16999087.

[16] X. Cao, X. Huang, P. Liang, K. Xiao, Y. Zhou, X. Zhang, et al., A new method for water desalination using microbial desalination cells, Environ. Sci. Technol. 43 (2009) 7148–52. http://www.ncbi.nlm.nih.gov/pubmed/19806756.

[17] K.S. Jacobson, D.M. Drew, Z. He, Efficient salt removal in a continuously operated upflow microbial desalination cell with an air cathode, Bioresour. Technol. 102 (2010) 376–380. doi:10.1016/j.biortech.2010.06.030.

[18] K.S. Jacobson, D.M. Drew, Z. He, Use of a Liter-Scale Microbial Desalination Cell As a Platform to Study Bioelectrochemical Desalination with Salt Solution or Artificial Seawater., Environ. Sci. Technol. (2011). doi:10.1021/es200127p.

[19] F. Zhang, Z. He, Scaling up microbial desalination cell system with a post-aerobic process for simultaneous wastewater treatment and seawater desalination, Desalination. 360 (2015) 28–34. doi:10.1016/j.desal.2015.01.009.

[20] H. Luo, P. Xu, T.M. Roane, P.E. Jenkins, Z. Ren, Microbial desalination cells for improved performance in wastewater treatment, electricity production, and desalination., Bioresour. Technol. 105 (2012) 60–6. doi:10.1016/j.biortech.2011.11.098.

[21] Y. Qu, Y. Feng, X. Wang, J. Liu, J. Lv, W. He, et al., Simultaneous Water Desalination and Electricity Generation in a Microbial Desalination Cell with Electrolyte Recirculation for pH Control, Bioresour. Technol. 106 (2011) 89–94. doi:10.1016/j.biortech.2011.11.045.

[22] M. Mehanna, T. Saito, J. Yan, M. Hickner, X. Cao, X. Huang, et al., Using microbial desalination cells to reduce water salinity prior to reverse osmosis, Energy Environ. Sci. 3 (2010) 1114. doi:10.1039/c002307h.

[23] B.S. Fields, R.F. Benson, R.E. Besser, Legionella and Legionnaires ' Disease : 25 Years of Investigation, 15 (2002) 506–526. doi:10.1128/CMR.15.3.506.

[24] S.D. Richardson, M.J. Plewa, E.D. Wagner, R. Schoeny, D.M. Demarini, Occurrence, genotoxicity, and carcinogenicity of regulated and emerging disinfection by-products in drinking water: a review and roadmap for research., Mutat. Res. 636 (2007) 178–242. doi:10.1016/j.mrrev.2007.09.001.

[25] C. Pablos, J. Marugán, R. van Grieken, E. Serrano, Emerging micropollutant oxidation during disinfection processes using UV-C, UV-C/H2O2, UV-A/TIO2 and UV-A/TiO2/H2O2, Water Res. 47 (2013) 1237–1245.

[26] X. Zhang, S. Echigo, H. Lei, M.E. Smith, R. a. Minear, J.W. Talley, Effects of temperature and chemical addition on the formation of bromoorganic DBPs during ozonation, Water Res. 39 (2005) 423–435. doi:10.1016/j.watres.2004.10.007.

[27] F. Wang, M. Ruan, H. Lin, Y. Zhang, H. Hong, X. Zhou, Effects of ozone pretreatment on the formation of disinfection by-products and its associated bromine substitution factors upon chlorination/chloramination of Tai Lake water, Sci. Total Environ. 475 (2014) 23–28. doi:10.1016/j.scitotenv.2013.12.094.

[28] B.R. Kim, J.E. Anderson, S. a. Mueller, W. a. Gaines, a. M. Kendall, Literature review - Efficacy of various disinfectants against Legionella in water systems, Water Res. 36 (2002) 4433–4444. doi:10.1016/S0043-1354(02)00188-4.

[29] D.F. Ollis, Photocatalytic purification and remediation of contaminated air and water, Comptes Rendus l'Académie Des Sci. - Ser. IIC - Chem. 3 (2000) 405–411. doi:10.1016/S1387-1609(00)01169-5.

[30] X. Chen, S.S. Mao, Titanium dioxide nanomaterials: synthesis, properties, modifications, and applications., Chem. Rev. 107 (2007) 2891–959. doi:10.1021/cr0500535.

[31] D. Wu, H. You, J. Du, C. Chen, D. Jin, Effects of UV/Ag-TiO2/O3 advanced oxidation on unicellular green alga Dunaliella salina: Implications for removal of invasive species from ballast water, J. Environ. Sci. 23 (2011) 513–519. doi:10.1016/S1001-0742(10)60443-3.

[32] H.M. Coleman, C.P. Marquis, J. a. Scott, S.S. Chin, R. Amal, Bactericidal effects of titanium dioxide-based photocatalysts, Chem. Eng. J. 113 (2005) 55–63. doi:10.1016/j.cej.2005.07.015.

[33] A. Hinkova, S. Henke, Z. Bubnik, V. Pour, A. Salova, M. Slukova, et al., Degradation of Food industrial pollutants by photocatalysis with immobilized titanium dioxide, Innov. Food Sci. Emerg. Technol. 27 (2015) 129–135. doi:10.1016/j.ifset.2014.12.006.

[34] J. a. Ibáñez, M.I. Litter, R. a. Pizarro, Photocatalytic bactericidal effect of TiO2 on Enterobacter cloacae. Comparative study with other Gram (-) bacteria, J. Photochem. Photobiol. A Chem. 157 (2003) 81–85. doi:10.1016/S1010-6030(03)00074-1.

[35] M.N. Chong, B. Jin, C.W.K. Chow, C. Saint, Recent developments in photocatalytic water treatment technology: A review, Water Res. 44 (2010) 2997–3027. doi:10.1016/j.watres.2010.02.039.

[36] P.A. Gross, S.N. Pronkin, T. Cottineau, N. Keller, V. Keller, E.R. Savinova, Effect of deposition of Ag nanoparticles on photoelectrocatalytic activity of vertically aligned TiO 2 nanotubes, 189 (2012) 93–100.

[37] Q. Li, S. Mahendra, D.Y. Lyon, L. Brunet, M. V Liga, D. Li, et al., Antimicrobial nanomaterials for water disinfection and microbial control: potential applications and implications., Water Res. 42 (2008) 4591–602. doi:10.1016/j.watres.2008.08.015.

[38] Y. Lin, R. Vidic, J. Stout, V. Yu, Individual and combined effects of copper and silver ions on inactivation of Legionella pneumophila, Water Res. 30 (1996) 1905–1913.

[39] M. a. Behnajady, H. Eskandarloo, Silver and copper co-impregnated onto TiO2-P25 nanoparticles and its photocatalytic activity, Chem. Eng. J. 228 (2013) 1207–1213. doi:10.1016/j.cej.2013.04.110.

[40] S.C. Chan, M. a Barteau, Preparation of highly uniform Ag/TiO2 and Au/TiO2 supported nanoparticle catalysts by photodeposition., Langmuir. 21 (2005) 5588–95. doi:10.1021/la046887k.

[41] A. Zaleska, Doped-TiO2: A Review, Recent Patents Eng. 2 (2008) 157–164.

[42] A. Dawson, P. V Kamat, Semiconductor - Metal Nanocomposites. Photoinduced Fusion and Photocatalysis of Gold-Capped TiO2 (TiO2/Gold) Nanoparticles, J. Phys. Chem. 105 (2001) 960–966.

[43] K. Domen, S. Nalto, T. Onlshl, K. Tamaru, M. Soma, Study of the Photocatalytic Decomposition of Water Vapor over a NiO-SrTiO3 CAtalyst, J. Phys. Chem. 86 (1982) 3657–3661.

[44] A.J. Bard, Photoelectrochemistry and heterogeneous photocatalysis at semiconductors, J. Photochem. 10 (1979) 59–75.

[45] T.D. Pham, B.K. Lee, Cu doped TiO2/GF for photocatalytic disinfection of Escherichia coli in bioaerosols under visible light irradiation: Application and mechanism, Appl. Surf. Sci. 296 (2014) 15–23. doi:10.1016/j.apsusc.2014.01.006.

[46] K. Sunada, T. Watanabe, K. Hashimoto, Bactericidal activity of copper-deposited TiO2 thin film under weak UV light illumination., Environ. Sci. Technol. 37 (2003) 4785–9. http://www.ncbi.nlm.nih.gov/pubmed/14594392.

[47] M. Li, M.E. Noriega-Trevino, N. Nino-Martinez, C. Marambio-Jones, J. Wang, R. Damoiseaux, et al., Synergistic bactericidal activity of Ag-TiO□ nanoparticles in both light and dark conditions., Environ. Sci. Technol. 45 (2011) 8989–95. doi:10.1021/es201675m.

[48] S. States, B. Xin, L. Jing, Z. Ren, B. Wang, H. Fu, Effects of Simultaneously Doped and Deposited Ag on the Photocatalytic Activity and, (2005) 2805–2809.

[49] P. Falaras, I.M. Arabatzis, T. Stergiopoulos, M.C. Bernard, Enhanced activity of silver modified thin-film TiO 2 photocatalysts, 05 (2003).

[50] Y. Liu, J. Hu, J. Li, Synthesis and photoactivity of the highly efficient Ag species/TiO2 nanoflakes photocatalysts, J. Alloys Compd. 509 (2011) 5152–5158. doi:10.1016/j.jallcom.2011.02.020.

[51] H. Cao, Y. Qiao, F. Meng, X. Liu, Spacing-Dependent Antimicrobial Efficacy of Immobilized Silver Nanoparticles, J. Phys. Chemsitry Lett. 5 (2014) 743–748.

[52] D.M. Tobaldi, C. Piccirillo, R.C. Pullar, A.F. Gualtieri, M.P. Seabra, P.M.L. Castro, et al., Silver-Modified Nano-titania as an Antibacterial Agent and Photocatalyst, J. Phys. Chem. C. 118 (2014) 4751–4766.

[53] L. Liu, W. Yang, Q. Li, S. Gao, J.K. Shang, Synthesis of Cu_2O nanospheres decorated with TiO_2 nanoislands, their enhanced photoactivity and stability under visible light illumination, and their post-illumination catalytic memory., ACS Appl. Mater. Interfaces. 6 (2014) 5629–39. doi:10.1021/am500131b.

[54] S. Chen, Y. Guo, H. Zhong, S. Chen, J. Li, Z. Ge, et al., Synergistic antibacterial mechanism and coating application of copper/titanium dioxide nanoparticles, Chem. Eng. J. 256 (2014) 238–246. doi:10.1016/j.cej.2014.07.006.

[55] K. Jomova, M. Valko, Advances in metal-induced oxidative stress and human disease., Toxicology. 283 (2011) 65–87.

[56] L. Macomber, R. Hausinger, Mechanisms of nickel toxicity in microorganisms, Metallomics. 11 (2011) 1153–1162.

[57] S.M. Quintal, Q.A. DePaula, N.P. Farrell, Zinc finger proteins as templates for metal ion exchange and ligand reactivity. Chemical and biological consequences., Metallomics. 3 (2011) 121–139.

[58] B. Rajanna, M. Hobson, L. Harris, L. Ware, C.S. Chetty, Effects of cadmium and mercury on Na(+)-K+, ATPase and uptake of 3H-dopamine in rat brain synaptosomes., Arch. Int. Phys. Biochem. 5 (1990) 291–296.

[59] F.F. Xu, J. a Imlay, Silver(I), mercury(II), cadmium(II), and zinc(II) target exposed enzymic iron-sulfur clusters when they toxify Escherichia coli., Appl. Environ. Microbiol. 78 (2012) 3614–21. doi:10.1128/AEM.07368-11.

[60] J.R. Morones-Ramirez, J. a Winkler, C.S. Spina, J.J. Collins, Silver enhances antibiotic activity against gram-negative bacteria., Sci. Transl. Med. 5 (2013) 190ra81. doi:10.1126/scitranslmed.3006276.

[61] S. Leong, A. Razmjou, K. Wang, K. Hapgood, X. Zhang, H. Wang, TiO2 based photocatalytic membranes : A review, J. Memb. Sci. 472 (2014) 167–184. doi:10.1016/j.memsci.2014.08.016.

[62] S.K. Papageorgiou, F.K. Katsaros, E.P. Favvas, G.E. Romanos, C.P. Athanasekou, K.G. Beltsios, et al., Alginate fibers as photocatalyst immobilizing agents applied in hybrid photocatalytic/ultrafiltration water treatment processes, Water Res. 46 (2012) 1858–1872. doi:10.1016/j.watres.2012.01.005.

[63] X. Zhang, A.J. Du, P. Lee, D.D. Sun, J.O. Leckie, TiO2 nanowire membrane for concurrent filtration and photocatalytic oxidation of humic acid in water, J. Memb. Sci. 313 (2008) 44–51. doi:10.1016/j.memsci.2007.12.045.

[64] X. Zhang, A.J. Du, P. Lee, D.D. Sun, J.O. Leckie, Grafted multifunctional titanium dioxide nanotube membrane: Separation and photodegradation of aquatic pollutant, Appl. Catal. B Environ. 84 (2008) 262–267. doi:10.1016/j.apcatb.2008.04.009.

[65] Z. He, S.D. Minteer, L.T. Angenent, Electricity generation from artificial wastewater using an upflow microbial fuel cell, Environ. Sci. Technol. 39 (2005) 5262–7. http://www.ncbi.nlm.nih.gov/pubmed/16082955.

[66] A. Smara, R. Delimi, E. Chainet, J. Sandeaux, Removal of heavy metals from diluted mixtures by a hybrid ion-exchange/electrodialysis process, Sep. Purif. Technol. 57 (2007) 103–110. doi:10.1016/j.seppur.2007.03.012.

[67] R. Vinodh, R. Padmavathi, D. Sangeetha, Separation of heavy metals from water samples using anion exchange polymers by adsorption process, Desalination. 267 (2011) 267–276. doi:10.1016/j.desal.2010.09.039.

[68] a Dabrowski, Z. Hubicki, P. Podkościelny, E. Robens, A. Da, Selective removal of the heavy metal ions from waters and industrial wastewaters by ion-exchange method., Chemosphere. 56 (2004) 91–106. doi:10.1016/j.chemosphere.2004.03.006.

[69] D. Clifford, T.J. Sorg, G.L. Ghurye, Ion Exchange and Adsorption of Inorganic Contaminants, in: J.K. Edzwald (Ed.), Water Qual. Treat., Sixth Edit, American Water Works Association, Denver, CO, 2011: pp. 12.1–12.97.

[70] A. Zagorodni, Ion Exchange Materials: Properties and Applications, Elsevier Science, Stockholm, 2006.

[71] S.A. Mcclellan, S.S. Beardsley, Membrane Softening : An Emerging Technology Helping Florida Communities Meet the Increased Regulations for Quality Potable Water, Membr. Technol. (1995) 1–5.

[72] D.E. Weiss, The role of ion-exchange desalination in municipal water supplies, Desalination. 1 (1966) 107–128.

[73] W. Yu, S. Wu, S. Shiah, Parametric analysis of the proton exchange membrane fuel cell performance using design of experiments, Int. J. Hydrogen Energy. 33 (2008) 2311–2322. doi:10.1016/j.ijhydene.2008.02.040.

[74] M. Dopar, H. Kusic, N. Koprivanac, Treatment of simulated industrial wastewater by photo-Fenton process. Part I: The optimization of process parameters using design of experiments (DOE), Chem. Eng. J. 173 (2011) 267–279. doi:10.1016/j.cej.2010.09.070.

[75] B. Wahdame, D. Candusso, X. Francois, F. Harel, J. Kauffmann, G. Coquery, Design of experiment techniques for fuel cell characterisation and development, Int. J. Hydrogen Energy. 34 (2009) 967–980. doi:10.1016/j.ijhydene.2008.10.066.

[76] K.S. Brastad, Z. He, Water softening using microbial desalination cell technology, Desalination. 309 (2013) 32–37. doi:10.1016/j.desal.2012.09.015.

[77] C. Marambio-Jones, E.M. V. Hoek, A review of the antibacterial effects of silver nanomaterials and potential implications for human health and the environment, J. Nanoparticle Res. 12 (2010) 1531–1551. doi:10.1007/s11051-010-9900-y.

[78] S. Kaitainen, A.J. Mähönen, R. Lappalainen, H. Kröger, M.J. Lammi, C. Qu, TiO2 coating promotes human mesenchymal stem cell proliferation without the loss of their capacity for chondrogenic differentiation., Biofabrication. 5 (2013) 025009. doi:10.1088/1758-5082/5/2/025009.

CURRICULUM VITAE

Kristen Brastad

EDUCATION

Ph.D. Civil Engineering and Mechanics, expected May 2015
University of Wisconsin - Milwaukee
GPA: 3.2/4.0

M.S. Environmental Engineering, August 2010
Milwaukee School of Engineering
GPA: 3.5/4.0

B.S. Architectural Engineering, August 2010
Milwaukee School of Engineering
GPA: 3.3/4.00

ACADEMIC RESEARCH EXPERIENCE

Photocatalytic Disinfection
University of Wisconsin – Milwaukee, Fall 2013 – May 2015
Research Assistant, Photocatalysis Lab, Adviser: Dr. Ying Li

- Fabricated and tested nanofiber materials and membranes for concurrent micro-pollutant filtration and microbial disinfection.
- Conducted nanomaterial (metal-ion doped TiO_2) synthesis and characterization.

Saltless Water Softening Techniques using Fuel Cell Technology
University of Wisconsin – Milwaukee, Fall 2010 – May 2013
Research Assistant, Environmental Biotechnology & Bioenergy Lab, Adviser: Dr. Zhen He

- Designed and tested a lab-scale photo-electrocatalytic fuel cell for saltless water softening and microbial disinfection.
- Assisted with the design and testing of an enzymatic fuel cell adapted for saltless water softening.
- Designed and tested a lab-scale microbial fuel cell adapted for saltless softening and heavy metal removal.

Water Softening using Forward Osmosis
Milwaukee School of Engineering, Fall 2009 – August 2010
Adviser: Dr. Frank Mahuta

- Designed a bench-scale prototype for testing the ability of forward osmosis membranes to reject hardness ions.
- Investigated the economic and technical feasibility of forward osmosis for residential systems.

MEMBERSHIPS AND ASSOCIATIONS

- American Water Works Association
- American Society of Civil Engineers
- Society of Women Engineers

AWARDS AND HONORS

- Value's Recognition Nominee, A. O. Smith Corporation (2013, 2014)
- Chairman's Award Recipient, A. O. Smith Corporation (2012, 2013)
- P3 Grant Recipient, Environmental Protection Agency (2012)
- Chancellor's Award Recipient, University of Wisconsin – Milwaukee (2010 – 2013)
- Dean's List, Milwaukee School of Engineering (2008 – 2010)
- Student Worker of the Year Nominee (2008)

PUBLICATIONS

[1] **Brastad, K.S.** (2010) *Water softening using forward osmosis: economic and technical feasibility for residential systems*. Milwaukee School of Engineering.

[2] Zhang, F., **Brastad, K.S.** and He, Z. (2011) *Integrating forward osmosis into microbial fuel cells for wastewater treatment, water extraction and bioelectricity generation*. Environmental Science & Technology. Vol 45, pp 6690-6696.

[3] Arugula, M.A., **Brastad, K.S.**, Minteer, S.D. and He, Z. (2012) *Enzyme catalysed-electricity driven water softening system.* Enzyme and Microbial Technology. Vol 51, pp 396-401.

[4] **Brastad, K.S.** and He, Z. (2013) *Water softening using microbial desalination technology.* Desalination. Vol 309, pp 32-37.

[5] **Brastad, K.S.**, Zhang, Q., Robinson, R., Lee, E., He, Z., and Li, Y. *Individual and Combined Effects of Silver and Copper Modified TiO2 Membranes for the Inactivation of E. coli and Bacteriophage MS2*. Working paper.

POSTER PRESENTATIONS

[1] **Brastad, K.S.** and He, Z. (2011) *Water softening using microbial desalination technology*. UW – Milwaukee College of Engineering and Applied Science Student Researcher Poster Competition.

[2] **Brastad, K.S.** and He, Z. (2012) *Water softening using microbial desalination cell technology*. UW – Milwaukee College of Engineering and Applied Science Student Researcher Poster Competition.

[3] Li, X., Jacobson, K., **Brastad, K.S.**, Zheng, G., and He, Z. (2013) *Development of photo-bioelectrochemical systems for wastewater treatment*. US Environmental Protection Agency P3 Competition.

[4] Robinson, R., Zhang, Q., **Brastad, K.S.** (2014) *TiO_2 Photocatalytic Disinfection*. Milwaukee Area Technical College Biochemical Excellence in Science and Technology Student Poster Presentation.

INDUSTRIAL EXPERIENCE

A. O. Smith Corporation, Milwaukee, WI
Water Treatment Engineer & Biological Safety Officer, May 2009 - Present

- Designed, created, and ran experiments to test new and emerging water treatment technologies ranging from novel membranes to photocatalytic oxidation.
- Completed the engineering design of new products from proof of concept to full-scale working prototype for the Asian market. Continued to work directly with manufacturing to ensure the final product met specifications.
- Coordinated samples and products sent to third party test labs for analysis and certification.
- Worked with international teams, academic professionals, and vendors to develop new products for a variety of markets.
- Experienced with residential carbon block technology, ultraviolet disinfection, ultrafiltration, and reverse osmosis systems.
- Conducted technology due diligence for acquisition targets within the water treatment market.
- Biological Safety Officer in charge of supervising a Biosafety Level 1 laboratory.

WMA Consulting Engineers, Chicago, IL
Plumbing Engineering Intern, May 2008 – August 2008

- Assisted with the plumbing design for a variety of projects stretching from office and medical renovations to new construction high-rise condominiums and hotels.
- Developed and applied knowledge of plumbing system design, layout, and calculations for high-rise buildings.

SKILLS

Biological testing: BSL-1 bacteria and viruses, total coliform, and total bacteria
Data analysis: MATLAB, Minitab, and Origin
Drafting: AutoCAD and SolidWorks DraftSight
Inorganic analysis: flame and graphite atomic adsorption (PG Instruments), inductively coupled plasma mass spectrometry (Agilent), ion chromatography (Dionex), and UV-Vis spectrophotometer (Hach)
Materials characterization: scanning electron microscope (Hitachi and Topcon), and X-ray diffraction (Scintag)
Metallography